ISSN: 2146-1414

MIRT

Molecular Imaging and Radionuclide Therapy

February 2017 Volume 26 Issue 1 www.tsnm.org

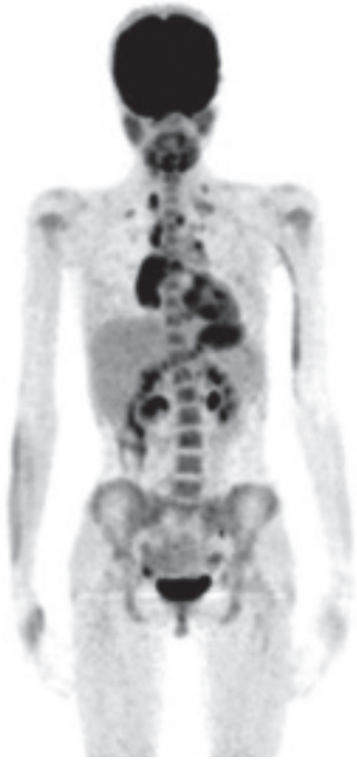

"Official Journal of the Turkish Society of Nuclear Medicine"

galenos yayınevi

TURKISH SOCIETY OF NUCLEAR MEDICINE 1975

MIRT

Molecular Imaging and Radionuclide Therapy

EDITORIAL BOARD

MIRT

Molecular Imaging and Radionuclide Therapy

EDITORIAL BOARD

Turkish Society of Nuclear Medicine
Cinnah Caddesi Pilot Sokak No: 10/12 Çankaya 06650 Ankara, Turkey
Phone: +90 312 441 00 45 **Fax:** +90 312 441 12 95 **Web:** www.tsnm.org **E-mail:** dernekmerkezi@tsnm.org
"Formerly Turkish Journal of Nuclear Medicine"

♾ The paper used to print this journal conforms to ISO 9706: 1994 standard (Requirements for Permanence). The National Library of Medicine suggests that biomedical publications be printed on acid-free paper (alkaline paper). Reviewing the articles' conformity to the publishing standards of the Journal, typesetting, reviewing and editing the manuscripts and abstracts in English, creating links to source data, and publishing process are realized by Galenos.

Publisher
Erkan Mor

Publication Director
Nesrin Çolak

Publication Coordinator
Burak Sever

Web Coordinators
Eren Arsel
Soner Yıldırım
Turgay Akpınar

Research&Development
Büşrah Toparslan

Project Coordinators
Ebru Boz
Eda Kolukısa
Hatice Balta
Melis Kuru
Zeynep Altındağ

Graphics Department
Ayda Alaca
Çiğdem Birinci

Finance Coordinator
Sevinç Çakmak

Publisher Contact
Address: Molla Gürani Mah. Kaçamak Sk. No: 21/1
34093 İstanbul, Turkey
Phone: +90 (212) 621 99 25 **Fax:** +90 (212) 621 99 27
E-mail: info@galenos.com.tr/yayin@galenos.com.tr
Web: www.galenos.com.tr

Printing at: Özgün Ofset Ticaret Ltd. Şti.
Yeşilce Mah. Aytekin Sk. No: 21 34418 4. Levent, İstanbul, Turkey
Phone: +90 (212) 280 00 09
Printing Date: February 2017
ISSN: 2146-1414 **E-ISSN:** 2147-1959
International scientific journal published quarterly.

MIRT

Molecular Imaging and Radionuclide Therapy

ABOUT US

Molecular Imaging and Radionuclide Therapy(formerly Turkish Journal of Nuclear Medicine) is the official publication of Turkish Society of Nuclear Medicine.

Focus and Scope

Molecular Imaging and Radionuclide Therapy (Mol Imaging Radionucl Ther, MIRT) is a double-blind peer-review journal published in English language. It publishes original research articles, reviews, editorials, short communications, letters, consensus statements, guidelines and case reports with a literature review on the topic, in the field of molecular imaging, multimodality imaging, nuclear medicine, radionuclide therapy, radiopharmacy, medical physics, dosimetry and radiobiology. MIRT is published three times a year (February, June, October). Audience: Nuclear medicine physicians, medical physicists, radiopharmaceutical scientists, radiobiologists.

The editorial policies are based on the "Recommendations for the Conduct, Reporting, Editing, and Publication of Scholarly Work in Medical Journals (ICMJE Recommendations)" by the International Committee of Medical Journal Editors (2013, archived at http://www.icmje.org/) rules.

Molecular Imaging and Radionuclide Therapy is indexed in PubMed, PubMed Central (PMC), Emerging Sources Citation Index (ESCI), TUBITAK-ULAKBIM, Gale/ Cengage Learning, EBSCO databases, ProQuest Health & Medical Complete, CINAHL, DOAJ, Türkiye Atıf Dizini (Türkiye Citation Index), Turk Medline.

Open Access Policy

This journal provides immediate open access to its content on the principle that making research freely available to the public supports a greater global exchange of knowledge.

Open Access Policy is based on rules of Budapest Open Access Initiative (BOAI) (http://www.budapestopenaccessinitiative.org/). By "open access" to [peer-reviewed research literature], we mean its free availability on the public internet, permitting any users to read, download, copy, distribute, print, search, or link to the full texts of these articles, crawl them for indexing, pass them as data to software, or use them for any other lawful purpose, without financial, legal, or technical barriers other than those inseparable from gaining access to the internet itself. The only constraint on reproduction and distribution, and the only role for copyright in this domain, should be to give authors control over the integrity of their work and the right to be properly acknowledged and cited.

Subscription Information

Manuscripts can only be submitted electronically through the Journal Agent website (http://www.journalagent.com/mirt/?plng=eng) after creating an account. This system allows online submission and review.

All published volumes in full text can be reached free of charge through the website http://mirt.tsnmjournals.org

Instructions for Authors

Instructions for authors are published in the journal and on the website http://mirt.tsnmjournals.org

Correspondence Address

Editor in Chief, Murat Fani BOZKURT, MD, Associate Professor of Nuclear Medicine
Hacettepe University Faculty of Medicine, Department of Nuclear Medicine,
Ankara, Turkey
Phone : +90 212 621 99 25
Fax : +90 212 621 99 27
e-mail : fanibozkurt@gmail.com
Web : http://mirt.tsnmjournals.org

The journal is printed on an acid-free paper.

MIRT

Molecular Imaging and Radionuclide Therapy

INSTRUCTIONS TO AUTHORS

Molecular Imaging and Radionuclide Therapy (Mol Imaging Radionucl Ther, MIRT) publishes original research articles, reviews, editorials, short communications, letters, consensus statements, guidelines and case reports with a literature review on the topic, in the field of molecular imaging, multimodality imaging, nuclear medicine, radionuclide therapy, radiopharmacy, medical physics, dosimetry and radiobiology. MIRT is published by the Turkish Society of Nuclear Medicine three times a year (February, June, October). The journal is printed on an acid-free paper.

Molecular Imaging and Radionuclide Therapy is indexed in PubMed, PubMed Central (PMC), Emerging Sources Citation Index (ESCI), TUBITAK-ULAKBIM, Gale/ Cengage Learning, EBSCO databases, ProQuest Health & Medical Complete, CINAHL, DOAJ, Türkiye Atıf Dizini (Türkiye Citation Index), Turk Medline.

Molecular Imaging and Radionuclide Therapy does not charge any article submission or processing charges.

GENERAL INFORMATION

MIRT commits to rigorous peer review, and stipulates freedom from commercial influence, and promotion of the highest ethical and scientific standards in published articles. Neither the Editor(s) nor the publisher guarantees, warrants or endorses any product or service advertised in this publication. All articles are subject to review by the editors and peer reviewers. If the article is accepted for publication, it may be subjected to editorial revisions to aid clarity and understanding without changing the data presented.

Manuscripts must be written in English and must meet the requirements of the journal. The journal is in compliance with the uniform requirements for manuscripts submitted to biomedical journals published by the International Committee of Medical Journal Editors (NEJM 1997; 336:309-315, updated 2001). Manuscripts that do not meet these requirements will be returned to the author for necessary revision before the review. Authors of manuscripts requiring modifications have a maximum of two months to resubmit the revised text. Manuscripts returned after this deadline will be treated as new submissions.

It is the authors' responsibility to prepare a manuscript that meets ethical criteria. The Journal adheres to the principles set forth in the Helsinki Declaration October 2008. (http://www.wma.net/en/30publications/10policies/b3/ index.html) and holds that all reported research involving "Human beings" conducted in accordance with such principles. Reports describing data obtained from research conducted in human participants must contain a statement in the MATERIALS AND METHODS section indicating approval by the ethical review board and affirmation that INFORMED CONSENT was obtained from each participant.

- All manuscripts reporting experiments using animals must include a statement in the MATERIALS AND METHODS section giving assurance that all animals have received humane care in compliance with the Guide for the Care and Use of Laboratory Animals (www.nap.edu) and indicating approval by the ethical review board.
- Case reports should be accompanied by INFORMED CONSENT and the identity of the patient should be hidden.
- Subjects must be identified only by number or letter, not by initials or names. Photographs of patients' faces should be included only if scientifically relevant. Authors must obtain written consent from the patient for use of such photographs.
- If the proposed publication concerns any commercial product, the author must include in the cover letter a statement indicating that the author(s) has (have) no financial or other interest with the product or explaining the nature of any relations (including consultancies) between the author(s) and editor the manufacturer or distributor of the product.

MANUSCRIPT CATEGORIES

1. Original Articles

2. Short Communications are short descriptions of focused studies with important, but very straightforward results. These manuscripts should be no longer than 2000 words, and include no more than two figures and tables and 20 references.

3. Reviews address important topics in the field. Authors considering the submission of uninvited reviews should contact the editor in advance to determine if the topic that they propose is of current potential interest to the Journal. Reviews will be considered for publication only if they are written by authors who have at least three published manuscripts in the international peer reviewed journals and these studies should be cited in the review. Otherwise only invited reviews will be considered for peer review from qualified experts in the area.

4. Editorials are usually written by invitation of the editor by the editors on current topics or by the reviewers involved in the evaluation of a submitted manuscript and published concurrently with that manuscript.

5. Case Report and Literature Reviews are descriptions of a case or small number of cases revealing a previously undocumented disease process, a unique unreported manifestation or treatment of a known disease process, unique unreported complications of treatment regimens or novel and important insights into a condition's pathogenesis, presentation, and/or management. The journal's policy is to accept case reports only if accompanied by a review of the literature on the related topic. They should include an adequate number of images and figures.

6. Consensus Statements or Guidelines may be submitted by professional societies. All such submissions will be subjected to peer review, must be modifiable in response to criticisms, and will be published only if they meet the Journal's usual editorial standards. These manuscripts should typically be no longer than 4000 words and include no more than six figures and tables and 120 references.

7. Letters to the Editor may be submitted in response to work that has been published in the Journal. Letters should be short commentaries related to specific points of agreement or disagreement with the published work. Letters should be no longer than 500 words with no more than five complete references, and may not include any figures or tables.

Note on Prior Publication

Articles are accepted for publication on the condition that they are original, are not under consideration by another journal, or have not been previously published. Direct quotations, tables, or illustrations that have appeared in copyrighted material must be accompanied by written permission for their use from the copyright owner and authors. Materials previously published in whole or in part shall not be considered for publication. At the time of submission, authors must report that the manuscript has not been published elsewhere. Abstracts or posters displayed at scientific meetings need not be reported.

MANUSCRIPT SUBMISSION PROCEDURES

MIRT only accepts electronic manuscript submission at the web site www. http://mirt.tsnmjournals.org. After logging on to the website Click the 'online manuscript submission' icon. All corresponding authors should be provided with a password and a username after entering the information required. If you already have an account from a previous submission, enter your username and password to submit a new or revised manuscript. If you have forgotten your username and/or password, please send an e-mail to the editorial office for assistance. After logging on to the article submission system please read carefully the directions of the system to give all needed information and attach the manuscript, tables and figures and additional documents.

MIRT

Molecular Imaging and Radionuclide Therapy

INSTRUCTIONS TO AUTHORS

All Submissions Must Include:

1. Completed Copyright Assignment & Disclosure of Potential Conflict of Interest Form; This form should be downloaded from the website (provided in the author section), filled in thoroughly and uploaded to the website during the submission.

2. Informed consent (for case reports); Authors must complete the online submission forms. If you are unable to successfully upload the files please contact the editorial office by e-mail.

There is no submission fee for MIRT.

MANUSCRIPT PREPARATION

General Format

The Journal requires that all submissions be submitted according to these guidelines:

- Text should be double spaced with 2.5 cm margins on both sides using 12-point type in Times Roman font.
- All tables and figures must be placed after the text and must be labeled.
- Each section (abstract, text, references, tables, figures) should start on a separate page.
- Manuscripts should be prepared as a word document (*.doc) or rich text format (*.rtf).
- Please make the tables using the table function in Word.
- Abbreviations should be defined in parenthesis where the word is first mentioned and used consistently thereafter.
- Results should be expressed in metric units. Statistical analysis should be done accurately and with precision. Please consult a statistician if necessary.

Title Page

The title page should be a separate form from the main text and should include the following:

- Full title (in English and in Turkish) Turkish title will be provided by the editorial office for the authors who are not Turkish speakers.
- Authors' names and institutions.
- Short title of not more than 40 characters for page headings.
- At least three and maximum eight key words. (in English and in Turkish) Do not use abbreviations in the key words. Turkish key words will be provided by the editorial office for the authors who are not Turkish speakers. If you are not a native Turkish speaker, please re enter your English keywords to the area provided for the Turkish keywords. English key words should be provided from http://www.nlm.nih.gov/mesh(Medical Subject Headings) while Turkish key words should be provided from http://www.bilimterimleri.com.
- Word count (excluding abstract, figure legends and references).
- Corresponding author's e-mail and address, telephone and fax numbers.
- Name and address of person to whom reprint requests should be addressed.

Original Articles

Authors are required to state in their manuscripts that ethical approval from an appropriate committeeand informed consents of the patients were obtained. These documents may be asked by the reviewers or the editorial board during the submission process.

- **Abstract:** (in English and in Turkish) Original Articles should be submitted with a structured abstract of no more than 250 words. All information reported in the abstract must appear in the manuscript. The abstract should not include references. Please use complete sentences for all sections of the abstract. Structured abstract should include background, objective, methods, results and conclusions. Turkish abstract will be provided by the editorial office for the authors who are not Turkish speakers. If you are not a native Turkish speaker, please re enter your English abstract to the area provided for the Turkish abstract.
- Introduction
- Materials and Methods
- Results
- Discussion
- Study Limitations
- Conclusion
- **Acknowledgement:** May be given for contributors who are not listed as authors, or for grant support of the research.
- **References:** References should be cited in numerical order (in parentheses) in the text and listed in the same numerical order at the end of the manuscript on a separate page or pages. The author is responsible for the accuracy of references. Examples of the reference style are given below. Further examples will be found in the articles describing the Uniform Requirements for Manuscripts Submitted to Biomedical Journals (Ann Intern Med.1988; 208:258-265, Br Med J. 1988; 296:401-405). The titles of journals should be abbreviated according to the style used in the Index Medicus. Journal Articles and Abstracts: Surnames and initials of author's name, title of the article, journal name, date, volume number, and pages. All authors should be listed regardless of number. The citation of unpublished papers, observations or personal communications is not permitted. Citing an abstract is not recommended. **Books:** Surnames and initials of author's names, chapter title, editor's name, book title, edition, city, publisher, date and pages.

Sample References

Journal Article: Sayit E, Söylev M, Capa G, Durak I, Ada E, Yilmaz M. The role of technetium-99m-HMPAO-labeled WBC scintigraphy in the diagnosis of orbital cellulitis. Ann Nucl Med 2001;15:41-44.

Article with DOI Number: Erselcan T, Hasbek Z, Tandogan I, Gumus C, Akkurt I. Modification of Diet in Renal Disease equation in the risk stratification of contrast induced acute kidney injury in hospital inpatients. Nefrologia 2009 doi: 10.3265/Nefrologia.2009.29.5.5449.en.full.

Article in a journal published ahead of print: Ludbrook J. Musculovenous pumps in the human lower limb. Am Heart J 2009;00:1-6. (accessed 20 February 2009).

Book Chapters: Lang TF, Duryea J. Peripheral Bone Mineral Assessment of the Axial Skeleton: Technical Aspects. In: Orwoll ES, Bliziotes M (eds). Osteoporosis: Pathophsiology and Clinical Management. New Jersey, Humana Pres Inc, 2003;83-104.

Books: Greenspan A. Orthopaedic Radiology a Pratical Approach. 3th ed. Philadelphia, Lippincott Williams Wilkins 2000, 295-330.

Website: Smith JR. 'Choosing Your Reference Style', Online Referencing 2(3), http://orj.sagepub.com (2003, accessed October 2008).

- Tables

Tables must be constructed as simply as possible. Each table must have a concise heading and should be submitted on a separate page. Tables must not simply duplicate the text or figures. Number all tables in the order of their citation in the text. Include a title for each table (a brief phrase, preferably no longer than 10 to 15 words). Include all tables in a single file following the manuscript.

- Figure Legends

Figure legends should be submitted on a separate page and should be clear and informative.

MIRT
Molecular Imaging and Radionuclide Therapy

INSTRUCTIONS TO AUTHORS

- Figures

Number all figures (graphs, charts, photographs, and illustrations) in the order of their citation in the text. At submission, the following file formats are acceptable: AI, EMF, EPS, JPG, PDF, PPT, PSD, TIF. Figures may be embedded at the end of the manuscript text file or loaded as separate files for submission. All images MUST be at or above intended display size, with the following image resolutions: Line Art 800 dpi, Combination (Line Art + Halftone) 600 dpi, Halftone 300 dpi. Image files also must be cropped as close to the actual image as possible.

Review Articles:

- Title page (see above)
- Abstract: Maximum 250 words; without structural divisions; in English and in Turkish . Turkish abstract will be provided by the editorial office for the authors who are not Turkish speakers. If you are not a native Turkish speaker, please re enter your English abstract to the area provided for the Turkish abstract.
- Text
- Conclusion
- Acknowledgements (if any)
- References

Case Report and Literature Review:

- Title page (see above)
- Abstract: Approximately 100-150 words; without structural divisions; in English and in Turkish. Turkish abstract will be provided by the editorial office for the authors who are not Turkish speakers. If you are not a native Turkish speaker, please re-enter your English abstract to the area provided for the Turkish abstract.
- Introduction
- Case report
- Literature Review and Discussion
- References

Editorial:

- Title page (see above)
- Abstract: Maximum 250 words; without structural divisions; in English and in Turkish. Turkish abstract will be provided by the editorial office for the authors who are not Turkish speakers. If you are not a native Turkish speaker, please re enter your English abstract to the area provided for the Turkish abstract.
- Text
- References

Letters to the Editor:

- Title page (see above)
- Short comment to a published work, no longer than 500 words, no figures or tables.
- References no more than five.

Proofs and Reprints

Proofs and a reprint order are sent to the corresponding author. The author should designate by footnote on the title page of the manuscript the name and address of the person to whom reprint requests should be directed. The manuscript when published will become the property of the journal.

Archiving

The editorial office will retain all manuscripts and related documentation (correspondence, reviews, etc.) for 12 months following the date of publication or rejection.

Submission Preparation Checklist

As part of the submission process, authors are required to check off their submission's compliance with all of the following items, and submissions may be returned to authors that do not adhere to these guidelines.

1. The submission has not been previously published, nor is it before another journal for consideration (or an explanation has been provided in Comments to the Editor).
2. The submission file is in Microsoft Word, RTF, or WordPerfect document file format. The text is double-spaced; uses a 12-point font; employs italics, rather than underlining (except with URL addresses); and the location for all illustrations, figures, and tables should be marked within the text at the appropriate points.
3. Where available, URLs for the references will be provided.
4. All authors should be listed in the references, regardless of the number.
5. The text adheres to the stylistic and bibliographic requirements outlined in the Author Guidelines, which is found in About the Journal.
6. English keywords should be provided from http://www.nlm.nih.gov/mesh (Medical Subject Headings), while Turkish key words should be provided from http://www.bilimterimleri.com
7. The title page should be a separate document from the main text and should be uploaded separately.
8. The "Affirmation of Originality and Assignment of Copyright/The Disclosure Form for Potential Conflicts of Interest Form" should be downloaded from the website, filled thoroughly and uploaded during the submission of the manuscript.

TO AUTHORS

Copyright Notice

The author(s) hereby affirms that the manuscript submitted is original, that all statement asserted as facts are based on author(s) careful investigation and research for accuracy, that the manuscript does not, in whole or part, infringe any copyright, that it has not been published in total or in part and is not being submitted or considered for publication in total or in part elsewhere. Completed Copyright Assignment & Affirmation of Originality Form will be uploaded during submission.

By signing this form;

1. Each author acknowledges that he/she participated in the work in a substantive way and is prepared to take public responsibility for the work.
2. Each author further affirms that he or she has read and understands the "Ethical Guidelines for Publication of Research".
3. The author(s), in consideration of the acceptance of the manuscript for publication, does hereby assign and transfer to the Molecular Imaging and Radionuclide Therapy all of the rights and interest in and the copyright of the work in its current form and in any form subsequently revised for publication and/or electronic dissemination.

Privacy Statement

The names and email addresses entered in this journal site will be used exclusively for the stated purposes of this journal and will not be made available for any other purpose or to any other party.

Peer Review Process

1. The manuscript is assigned to an editor, who reviews the manuscript and makes an initial decision based on manuscript quality and editorial priorities.
2. For those manuscripts sent for external peer review, the editor assigns at least two reviewers to the manuscript.
3. The reviewers review the manuscript.
4. The editor makes a final decision based on editorial priorities, manuscript quality, and reviewer recommendations.
5. The decision letter is sent to the author.

TURKISH SOCIETY OF NUCLEAR MEDICINE 1975

MIRT

Molecular Imaging and Radionuclide Therapy

CONTENTS

Review
Mol Imaging Radionucl Ther 2017;26:1-8 DOI:10.4274/mirt.60783

^{18}F-Fluorodeoxyglucose-Positron Emission Tomography/Computed Tomography for Other Thyroid Cancers: Medullary, Anaplastic, Lymphoma and So Forth

Diğer Tiroid Kanserleri için ^{18}F-Fluorodeoksiglukoz-Pozitron Emisyon Tomografisi/Bilgisayarlı Tomografi: Medüller, Anaplastik, Lenfoma ve Fazlası

Mine Araz, Derya Çayır
Dışkapı Yıldırım Beyazıt Training and Research Hospital, Clinic of Nuclear Medicine, Ankara, Turkey

Abstract

Positron emission tomography/computed tomography (PET/CT) with ^{18}F-fluorodeoxyglucose (FDG) is used in staging, restaging, and evaluation of therapy response in many cancers as well as differentiated thyroid carcinomas especially in non-iodine avid variants. Its potential in less frequent thyroid tumors like medullary, anaplastic thyroid cancers, thyroid lymphoma and metastatic tumors of the thyroid however, is not well established yet. The aim of this review is to provide an overview on the recent applications and indications of ^{18}F-FDG PET/CT in these tumors and to focus on the controversies in the clinical setting.
Keywords: Thyroid cancer, positron emission tomography, ^{18}F-fluorodeoxyglucose

Öz

^{18}F-fluorodeoksiglukoz (FDG) pozitron emisyon tomografisi/bilgisayarlı tomografi (PET/BT) pek çok kanserde ve özellikle iyot tutmayan varyant olmak üzere diferansiye tiroid karsinomlarında evreleme, yeniden evreleme ve tedaviye yanıtın değerlendirilmesinde kullanılır. Medüller, anaplastik tiroid kanserleri, tiroid lenfoması ve metastatik tümörler gibi tiroidin daha nadir tümörlerindeki potansiyeli henüz tam olarak belirlenmemiştir. Bu derlemenin amacı, ^{18}F-FDG PET/BT'nin bu tümörlerdeki son uygulamaları ve endikasyonları hakkında genel bir bakış sunmak ve klinik çerçevedeki tartışmalar üzerine yoğunlaşmaktır.
Anahtar kelimeler: Tiroid kanseri, pozitron emisyon tomografisi, ^{18}F-fluorodeoksiglukoz

Introduction

^{18}F-fluorodeoxyglucose (^{18}F-FDG) is a metabolic positron emission tomography/computed tomography (PET/CT) imaging agent. Its uptake depends on the glycolytic rate of the tumor. Differentiated thyroid cancers have a relatively low metabolic rate with better differentiation and radioactive iodine avidity. Dedifferentiated and other types of thyroid cancers however, show a higher glycolytic rate and ^{18}F-FDG uptake. ^{18}F-FDG PET/CT now has a common role in staging and restaging of thyroid cancers other than differentiated subtypes. Although some other ^{18}F and Ga-68 labeled radiopharmaceuticals (FDOPA and Ga-68 labeled peptides) have been introduced for the same indications, ^{18}F-FDG PET/CT is still the PET radiopharmaceutical of choice with its wide availability and lower cost, and other PET tracers now only have a complementary role. This paper aims

Address for Correspondence: Mine Araz MD, Dışkapı Yıldırım Beyazıt Training and Research Hospital, Clinic of Nuclear Medicine, Ankara, Turkey
Phone: +90 532 666 73 13 E-mail: minesoylu@yahoo.com **Received:** 12.07.2016 **Accepted:** 26.08.2016

to focus on the role of ^{18}F-FDG PET/CT in less common tumors of the thyroid.

Medullary Thyroid Cancer

Medullary carcinoma is a neuroendocrine tumor of the thyroid originating from the parafollicular C cells. It is relatively infrequent and accounts for 5% of all thyroid cancers. It can present either as sporadic (75%) or familial (25%) forms. It characteristically secretes calcitonin (1).

Once medullary thyroid carcinoma is diagnosed by fine needle aspiration biopsy, neck ultrasound is recommended for preoperative lymph node assessment (2). For patients with preoperative calcitonin levels >500 pg/mL, additional radiologic imaging for evaluation of possible distant metastasis is indicated. Neck and chest CT, contrast-enhanced liver CT or magnetic resonance imaging (MRI), MRI of the axial skeleton and bone scintigraphy may be performed (3). ^{18}F-FDG PET/CT is not routinely recommended at the staging of the disease (4).

Prognosis of the disease depends on the age and stage of the disease at diagnosis and the extent of the primary surgery performed. Additional factors for a better outcome in medullary thyroid cancer are female gender, well-differentiated histology, small tumor size, intracapsular tumor, lower levels of calcitonin in the postoperative period and absence of lymph node or distant metastasis. Although aggressive treatment strategies are followed in medullary thyroid cancer patients, persistent or recurrent disease is still frequently seen. Being the most sensitive tumor marker, serum calcitonin levels are usually elevated in recurrent cases. In approximately one third of the patients, carcinoembryonic antigen (CEA) is also increased. CEA elevation is also a prognostic determinant of advanced disease and dedifferentiation of the tumor (1,5). Biochemical recurrence leads the clinicians to investigate a tumor focus because tumor markers increase before radiologic examinations become positive. This is why identification of recurrent disease is quite problematic in disease management. In patients with postoperative calcitonin values <150 pg/mL, it is thought that recurrence is mostly related to locoregional disease and neck ultrasound is recommended. Serum calcitonin levels ≥150 pg/mL are more likely to be indicative of extensive disease (1). Functional imaging techniques have been found to be useful in this clinical setting (4,6,7,8). In a series of 55 medullary thyroid cancer patients with elevated calcitonin levels, the role of neck and abdomen USG, neck, chest, and abdomen CT, liver and whole-body MRI, bone scintigraphy, and ^{18}F-FDG PET/CT were investigated comparatively. Conventional radiologic imaging methods were found to be more sensitive than ^{18}F-FDG PET/CT for any site of tumor recurrence. They also found that maximum standardized uptake value (SUV_{max}) levels were higher in patients with progressive disease, but there was a significant overlap with the stable cases. The authors concluded that ^{18}F-FDG PET/CT had a low prognostic value in medullary thyroid cancer (9). However, opposing results have been obtained in some other studies (10,11,12,13,14).

There are several studies reported in this era investigating the role of ^{18}F-FDG PET/CT in recurrent medullary thyroid cancer patients with high levels of tumor markers. The sensitivity and specificity of ^{18}F-FDG PET/CT is reported in a wide range (10,11,12,13,14). In a large series of 100 examinations, Diehl et al. (15) have reported a sensitivity of 78% and specificity of 79%. A recent meta-analysis of the published data by Treglia et al. (7) reviewed 24 major studies. Despite the heterogeneity in the definition of true negative and false negatives, examination techniques and inclusion criteria in these studies, on a per patient pooled analysis, the authors calculated a detection rate of 59% [95% confidence interval (CI): 54-63%] for ^{18}F-FDG PET or PET/CT in patients with suspected recurrent medullary thyroid cancer. The detection rate of ^{18}F-FDG PET/CT was higher in advanced disease (for serum calcitonin levels <150 ng/dL; detection rate: 40%, 95% CI: 29-52%, ≥150 ng/dL; detection rate: 64%, 95% CI: 59-70%, and ≥1000 ng/dL; 75%, 95% CI: 67-81%) (7). Undetectability of recurrent tumors at low levels of calcitonin and CEA was mainly attributed to small tumor size or microscopic disease (16).

Detection rates were also found to be higher in patients with lower calcitonin and CEA doubling time (for calcitonin doubling time <12 months, detection rate: 76%, and for CEA doubling time <24 months, detection rate: 91%) (7). This is reasonable, as the tumors with higher rate of proliferation are expected to have a higher metabolic rate and increased glucose consumption and thus higher detectability with ^{18}F-FDG PET/CT (8). However, aggressive forms of medullary thyroid cancer are not always seen in the clinical setting, more indolent cases are sometimes encountered. Such lesions express lower levels of ^{18}F-FDG uptake with SUV_{max} values, previously reported as a mean (±standard deviation): 3.76±1.79. Skoura et al. (17) also reported an interesting finding that the sensitivity of ^{18}F-FDG PET/CT for medullary cancer recurrence in patients with multiple endocrine neoplasia (MEN) type 2A was significantly lower (23%), and for calcitonin levels <2000 pg/mL sensitivity was calculated as 0% in MEN 2A patients. Excluding the patients with MEN 2A, the overall sensitivity of ^{18}F-FDG PET/CT raised from 44.1% to 50%. Thus, the authors concluded that ^{18}F-FDG PET/CT was more reliable in sporadic or MEN 2B patients (17).

Site of metastasis has also been recently reported to be important for detectability by ^{18}F-FDG PET/CT. De Luca et al. (18) have retrospectively analyzed metastatic medullary thyroid cancer patients who had undergone ^{18}F-FDG PET/CT. They concluded that ^{18}F-FDG PET/CT was primarily useful in lymph node involvement evaluation. Lung, liver or brain metastases could be missed due to the small size

or low metabolic activity and as for skeletal metastases, detectability was limited to lytic metastases (18).

Recently other PET radiopharmaceuticals have been suggested for use in detection of recurrence in medullary thyroid cancer patients. ^{18}F-DOPA is reported to have a higher sensitivity as compared to ^{18}F-FDG PET/CT, especially in more indolent disease (15,19,20,21,22,23,24). A recent study by Archier et al. (25) has also revealed that ^{18}F-DOPA PET/CT was reliable for a compartment based approach in lymph node involvement. Gallium-68 labeled peptides are also under scope for this use, especially to identify patients with tumors positive for somatostatin receptors, and thus candidates for radionuclide therapy (26,27). ^{18}F-FDG PET/CT should not be considered as the first step in the diagnostic algorithm and must be spared for the cases with elevated levels of tumor markers but negative conventional imaging examinations. One must also keep in mind that functional imaging methods are complementary to each other in the way that they all have different routes of radiopharmaceutical uptake and that they work efficiently under different circumstances (7,28,29,30).

Anaplastic Thyroid Cancer

Anaplastic thyroid carcinoma is a rare malignancy constituting less than 2% of all thyroid cancers. It originates from follicular cells but is very poorly differentiated to have histopathologic characteristics of the differentiated tumors of the follicular cells. It shows a rapid growth and local invasion (31). Anaplastic thyroid carcinomas have a highly aggressive behavior with the worst prognosis among all thyroid cancers, given a median estimated survival of 6-8 months (1,32). This is why all anaplastic thyroid carcinomas are classified as Stage IV tumors and imaging methods for primary staging of the tumor includes CT of the head, neck, thorax, abdomen and pelvis as well as a bone scan or ^{18}F-FDG PET/CT for identification of local or distant metastatic disease (1,33).

There is a limited number of studies evaluating ^{18}F-FDG PET/CT in anaplastic thyroid carcinomas. However, ^{18}F-FDG PET/CT may have a role in the follow-up of anaplastic thyroid cancer after primary surgery for detection of residual, recurrent, or metastatic disease (34,35). ^{18}F-FDG PET/CT results are suggested to have an impact on the clinical management of anaplastic thyroid cancer. Anaplastic thyroid cancers have been reported to have a high glucose metabolism and thus, show a high ^{18}F-FDG uptake. American Thyroid Association (ATA) have published a clinical management guideline on anaplastic thyroid cancer patients (4). ^{18}F-FDG PET/CT has been recommended in anaplastic thyroid cancer at many steps in the management. It is recommended in the primary staging both for evaluation of lesion resectability and distant metastasis. Follow-up of anaplastic thyroid cancer patients is also successfully done by ^{18}F-FDG PET/CT. It is recommended to be performed 3-6 months after therapy in patients either with or without persistent disease. ^{18}F-FDG PET/CT is also recommended for distinction of anaplastic and differentiated thyroid cancer metastasis, based on the fact that anaplastic thyroid cancer metastases have a significantly higher SUV_{max} (4).

A few studies have investigated the possible prognostic role of ^{18}F-FDG PET/CT in anaplastic thyroid cancer patients. As well as SUV_{max}, metabolic tumor volume has been introduced as a new index. Because some tumors show non-homogenous uptake, metabolic tumor volume has been shown to be a more valuable parameter in various tumors (36). In a series reported by Bogsrud et al. (37), PET has affected management in about 50% of anaplastic thyroid cancer patients. It was also found that SUV_{max} and metabolic tumor volume had a prognostic significance in these patients (37). Poisson et al. (38) similarly concluded that a SUV_{max} >18 and a ^{18}F-FDG uptake volume >300 mL had a significantly worse 6 month survival.

Thyroid Lymphoma

Thyroid lymphoma is a rare disease with female dominance, mostly seen in the elderly. It constitutes 1-5% of all thyroid malignancies and 1-2.5% of all lymphomas (39).

Primary thyroid lymphoma is most commonly B-cell originated, and 60-80% of all cases have been reported to be diffuse-large B-cell lymphomas. They are considered to arise from follicular cells (40,41). About 30% of the thyroid lymphomas is extranodal marginal zone lymphomas of mucosa-associated lymphoid tissue (MALT). They are usually associated with the existence of Hashimoto's thyroiditis (42). Autoimmune stimulation is thought to be responsible for disease development.

There are only a few reports on the role of ^{18}F-FDG PET/CT in primary thyroid lymphomas, and most of them are case presentations. This is partly due to the infrequency of the disease. In a case report presented by Naswa et al. (43), the authors showed that ^{18}F-FDG PET/CT was useful in staging and detecting therapy response in high-grade primary thyroid lymphoma in a 64-year-old female patient with a history of Hashimoto's thyroiditis.

On ^{18}F-FDG PET/CT, Hashimoto's thyroiditis is a primary problem in the differential diagnosis of lymphomas as both entities may show intense diffuse ^{18}F-FDG uptake. MALT lymphomas have been reported to show false-negative results in ^{18}F-FDG PET imaging (44). However, a recent study in a large patient group revealed that SUV_{max} was significantly higher and CT density was lower in primary thyroid lymphoma as compared to chronic thyroiditis. The authors have thus suggested that ^{18}F-FDG PET/CT may be helpful in distinguishing primary thyroid lymphoma from chronic thyroiditis (45). Similarly, a large series of thyroid lymphoma from a single center have been recently reported. Among the defined radiologic characteristics

in this retrospective analysis, high SUV_{max} levels were remarkable. They reported a median SUV_{max} of 22.7 (range: 10.6-37.6) (46). Riedel's thyroiditis, an IgG4-related disease, also presents with diffuse thyroidal uptake and should be kept in mind in differential diagnosis (47).

Metastatic Thyroid Cancer

Metastatic tumors of the thyroid are not uncommon (48,49). In autopsy series, the overall incidence of thyroid metastasis has been reported as 1.25% and as high as 24% in patients with known extensive disease metastatic to other sites (48,50). In a recent report of a large series, Hegerova et al. (49) listed the most common tumor types metastatic to the thyroid as follows: kidney (22%), lung (22%), and head and neck (12%). The role of ^{18}F-FDG PET/CT in detection of metastatic tumors of thyroid is obscure. There are only a few case reports in the literature demonstrating the ^{18}F-FDG uptake patterns of thyroid metastasis in other primary malignancies. Metastatic tumors of the thyroid are known to represent as thyroid masses, and thus they tend to show focal ^{18}F-FDG uptake (51). However, Agrawal et al. (52) have recently defined heterogeneous thyroidal ^{18}F-FDG uptake in a patient with known non-small cell lung carcinoma and multiple metastasis throughout the body. Any kind of unexpected thyroidal uptake in patients with known malignancies should be carefully evaluated for a possibility of thyroid metastasis.

Poorly Differentiated Thyroid Carcinoma

Poorly differentiated thyroid carcinoma histopathologically and behaviorally stands between differentiated thyroid carcinoma and anaplastic thyroid cancer. It does not appear de novo, differentiated tumors become de-differentiated by previously reported genetic alterations (53). Poorly differentiated thyroid carcinoma carries some characteristics of differentiation like thyroglobulin expression along with some features of anaplastic thyroid carcinoma like loss of iodine concentration ability and increased glucose transporter 1 (GLUT1) expression. The inverse relationship between iodine concentration and glucose uptake was defined as "flip-flop phenomenon" (54). Increased glucose uptake is partly related to the increased metabolic activity in highly proliferated tumor cells and Grabellus et al. (55) have also reported that de-differentiation was also accompanied by GLUT1 up-regulation. Increased glucose demand and GLUT expression provides high ^{18}F-FDG uptake and detectability rates with ^{18}F-FDG PET/CT. Compared to radioiodine scanning, poorly differentiated thyroid carcinoma are rather preferred to be screened by ^{18}F-FDG PET/CT (56). It has a well documented role in all stages of disease evaluation. In preoperative staging, it has been reported to change management in 25% of the cases and that there was an inverse correlation between SUV_{max} levels and survival rates (57). In the postoperative period, Nascimento et al. (58) have recently recommended postoperative ^{18}F-FDG PET/CT to be routinely performed in patients with aggressive histology. Usefulness of ^{18}F-FDG PET/CT in the evaluation of therapy response was investigated. In anaplastic thyroid carcinoma patients who had undergone multimodal therapies, ^{18}F-FDG PET/CT was suggested as a marker for treatment response (59).

Hürthle Cell Cancer

Hürthle cell cancer of the thyroid is a relatively uncommon form accounting for only 3.6% of all thyroid cancers (60). It has a worse prognosis and a higher tendency of metastases compared to other differentiated thyroid cancers (61,62,63). It especially has a more aggressive course when the primary tumor is widely invasive (64,65). It is known to have a lower radioiodine avidity (66,67). Thus, ^{18}F-FDG PET/CT becomes a valuable alternative for imaging Hürthle cell cancer. The number of studies investigating the role of ^{18}F-FDG PET/CT in Hürthle cell cancer is limited. A small report involving 12 patients found that ^{18}F-FDG PET/CT was positive in 12 patients and that ^{18}F-FDG PET/CT was the only positive imaging modality for localizing disease in 7/12 patients. Overall sensitivity was reported to be 92% and the patient management was changed by ^{18}F-FDG PET/CT in 50% of all cases (68). In a heterogeneous group of thyroid cancer patients reported by Wang et al. (69), SUV_{max} and tumor volume were reported to have an important prognostic value in Hürthle cell cancer. Pryma et al. (70) reported 44 patients with Hürthle cell thyroid cancer. ^{18}F-FDG PET/CT was performed for risk assessment after total thyroidectomy in patients with elevated thyroglobulin levels. They calculated the overall sensitivity and specificity of ^{18}F-FDG PET/CT as 95% (70).

Thyroid Incidentaloma

Thyroid incidentalomas are defined as thyroid lesions detected by an imaging study that were not previously suspected or detected in an asymptomatic patient. Incidental thyroidal ^{18}F-FDG uptake is not uncommon in oncological ^{18}F-FDG PET/CT studies performed for any other malignancy. As the use of ^{18}F-FDG PET/CT in staging, restaging of other malignancies and evaluation of therapy response increased, the frequency of incidental ^{18}F-FDG uptake has also increased. The incidence has been reported as 0.2-8.9% (71). There are many studies in the literature investigating the clinical significance of thyroidal ^{18}F-FDG uptake. Overall malignancy rate in an incidentally detected thyroid lesion is in a wide range:13-59% (72) .The pattern of ^{18}F-FDG uptake is important for evaluation of the etiology of the uptake. Diffuse thyroidal ^{18}F-FDG uptake has been generally reported to be related to thyroiditis and autoimmune process, and it is seen in about 0.6-3.3% of all ^{18}F-FDG PET/CT studies (73).

The frequency of focal incidentalomas are 0.2-10%. The risk of malignancy is known to be higher in the focal ^{18}F-FDG uptake group as compared to diffuse thyroidal ^{18}F-FDG uptake. However, the malignancy prevalence in patients who present with focal thyroidal ^{18}F-FDG uptake differs in a wide range in the literature (8-64%) (74).

The most common type of thyroid cancer detected in thyroid incidentalomas on ^{18}F-FDG PET/CT is papillary thyroid cancer and follicular type papillary thyroid cancer (81.1%). Primary thyroid lymphoma and thyroidal metastasis of other malignancies account for 4.1% of these (75). In another series reported by Agrawal et al. (76) however, the percentage of metastatic thyroid cancer or thyroid lymphoma incidentally detected were 44.4%. Some investigators have proposed that incidental thyroid malignancies tend to have a more aggressive histologic subtype and a higher tumor grade, and that they should be evaluated more carefully (77). This can be related with the increased ^{18}F-FDG avidity in de-differentiated cancers, as described above.

First step in the evaluation of incidental thyroid nodules is thyroid ultrasound. But two studies revealed that ^{18}F-FDG avid thyroid nodules are indicative of malignancy regardless of suspicious findings on ultrasound (78,79). Therefore, fine needle aspiration biopsy is strongly recommended in metabolically active thyroid nodules (80). The ATA has recently published a management guideline in thyroid nodules in adult patients. Thyroid incidentalomas detected by ^{18}F-FDG PET/CT was also mentioned, and they recommended fine-needle aspiration biopsy for focal ^{18}F-FDG uptake corresponding to a nodule on thyroid ultrasonography. Diffuse ^{18}F-FDG uptake, accompanied by sonographic and clinical evidence of thyroiditis was not a necessity for histopathologic examination (81).

There have been many efforts to determine a SUV_{max} cut-off for thyroidal ^{18}F-FDG uptake, above which will indicate malignancy. It is obvious that the SUV_{max} is statistically significantly high in malignant lesions but there is no safe cut-off value to guide management. In a study by Stangierski et al. (82), a total of 82 patients with focal ^{18}F-FDG uptake in the thyroid were further investigated by fine needle aspiration biopsy. The mean SUV_{max} for benign lesions was calculated as 3.2 and for malignant lesions as 7.1. Because the range of SUV_{max} was between 1.4-17.5 in benign lesions and between 1.8-33.6 in malignant lesions, there was a wide overlap between the two subsets, and therefore no cut-off was reliable. Investigators also found out that for malignant lesions detected by ^{18}F-FDG PET/CT, there was a significant correlation between the diameter of the nodule and SUV_{max}. The authors have thus suggested a cautious examination in small lesions even if they have low ^{18}F-FDG uptake.

SUV_{max} is not the only parameter to evaluate preoperative risk in incidental thyroid malignancies. Kim et al. (83) have investigated the role of total lesion glycolysis and metabolic tumor volume in the prediction of lateral lymph node metastasis in patients with incidentally detected differentiated thyroid carcinoma. They found out that these volume-based PET functional parameters were significant in predicting lateral lymph node metastasis. Risk stratification with these parameters may be of clinical value if supported by larger studies (83).

Functional imaging provides certain advantages which cannot be obtained by conventional anatomical imaging methods. In nuclear medicine practice, ^{18}F-FDG now has a major place as it is a nonspecific marker of increased metabolism. Differentiated thyroid tumors usually have a silent course, while other tumors of the thyroid show a variable presentation. Dedifferentiation, poor differentiation and anaplastic characters of these tumors lean high ^{18}F-FDG avidity. Considering all the aforementioned data, we recommend ^{18}F-FDG PET/CT in both initial evaluation and follow-up of undifferentiated thyroid cancers. Medullary thyroid carcinoma, the neuroendocrine tumor of the thyroid, has other functional imaging options than ^{18}F-FDG PET/CT like somatostatin receptor imaging. But, in advanced cases, especially with high levels of tumor markers, the tumor is most likely to be dedifferentiated and metabolic imaging, to the best of our experience, is the most accurate way to evaluate these patients. Thyroid lymphoma is a rare clinical condition and we have a limited clinical expertise, but recent publications revealed that this tumor presents with high metabolic rate and ^{18}F-FDG PET/CT has a definitive role for thyroid lymphoma, primarily in cases with unexpected findings like rapidly growing neck mass, compression symptoms and weight loss.

Conclusion

In medullary thyroid carcinoma; ^{18}F-FDG PET/CT is not routinely recommended in the primary staging of the disease, but it has been reported to be useful in the follow-up to evaluate high levels of calcitonin and CEA. Detection rates have been found to be higher in shorter tumor marker doubling times and in sporadic cases as compared to MEN syndromes. Its prognostic significance is still under debate in medullary thyroid cancer. Limited data published on anaplastic thyroid carcinomas revealed that ^{18}F-FDG PET/CT may have a role in both staging and follow-up of these patients. SUV_{max} and metabolic tumor volume values seem to have a prognostic importance. ^{18}F-FDG PET/CT can be of value in the differential diagnosis of primary thyroid lymphoma and thyroiditis. Metastatic tumors of the thyroid are not as uncommon as previously assumed, so special attention should be paid on thyroidal ^{18}F-FDG uptake in patients with known malignancies. In poorly differentiated thyroid cancers, it is reasonable to use ^{18}F-FDG PET/CT for follow-up due to high ^{18}F-FDG uptake and metabolic tumor rate. Hürthle cell cancer is a rather rare histopathologic subtype of thyroid cancer with less iodine avidity. ^{18}F-FDG PET/CT seems to have an important role with high detection rates and sensitivity-specificity in Hürthle cell cancer. Incidental thyroidal ^{18}F-FDG uptake

necessitates further clarification, especially if focal uptake corresponds to a sonographically evident thyroid nodule.

Ethics

Peer-review: Externally peer-reviewed.

Authorship Contributions

Concept: Mine Araz, Design: Mine Araz, Data Collection or Processing: Derya Çayır, Analysis or Interpretation: Mine Araz, Derya Çayır, Literature Search: Derya Çayır, Writing: Mine Araz.

Conflict of Interest: No conflict of interest was declared by the authors.

Financial Disclosure: The authors declared that this study received no financial support.

References

1. Pitt SC, Moley JF. Medullary, Anaplastic, and Metastatic Cancers of the Thyroid. Semin Oncol 2010;37:567-579.
2. Pacini F, Castagna MG, Cipri C, Schlumberger M. Medullary thyroid carcinoma. Clin Oncol (R Coll Radiol) 2010;22:475-485.
3. Machens A, Dralle H. Biomarker-based risk stratification for previously untreated medullary thyroid cancer. J Clin Endocrinol Metab 2010;95:2655-2663.
4. American Thyroid Association Guidelines Task Force, Kloos RT, Eng C, Evans DB, Francis GL, Gagel RF, Gharib H, Moley JF, Pacini F, Ringel MD, Schlumberger M, Wells SA Jr. Medullary Thyroid Cancer: Management Guidelines of the American Thyroid Association. Thyroid 2009;19:565-612.
5. Pacini F, Castagna MG, Brilli L, Pentheroudakis G; ESMO Guidelines Working Group. ESMO Clinical Practice Guidelines for diagnosis, treatment and follow-up. Ann Oncol 2012;23(Suppl 7):110-119.
6. Marcus C, Whitworth PW, Surasi DS, Pai SI, Subramaniam RM. PET/CT in the Management of Thyroid Cancers. AJR Am J Roentgenol 2014;202:1316-1329.
7. Treglia G, Villani MF, Giordano A, Rufini V. Detection rate of recurrent medullary thyroid carcinoma using fluorine-18 fluorodeoxyglucose positron emission tomography: a meta-analysis. Endocrine 2012;42:535-545.
8. Adams S, Baum RP, Hertel A, Schumm-Drager PM, Usadel KH, Hör G. Metabolic (PET) and receptor (SPET) imaging of well and less well-differentiated tumours: comaprison with the expression of the Ki-67 antigen. Nucl Med Commun 1998:19:641-647.
9. Giraudet AL, Vanel D, Leboulleux S, Aupérin A, Dromain C, Chami L, Ny Tovo N, Lumbroso J, Lassau N, Bonniaud G, Hartl D, Travagli JP, Baudin E, Schlumberger M. Imaging medullary thyroid carcinoma with persistent elevated calcitonin levels. J Clin Endocrinol Metab 2007;92:4185-4190.
10. Beheshti M, Pocher S, Vali R, Waldenberger P, Broinger G, Nader M, Kohlfurst S, Pirich C, Dralle H, Langsteger W. The value of 18F-DOPA PET-CT in patients with medullary thyroid carcinoma: comparison with 18F-FDG PET-CT. Eur Radiol 2009;19:1425-1434.
11. Kauhanen S, Schalin-Jantti C, Seppanen M, Kajander S, Virtanen S, Schildt J, Lisinen I, Ahonen A, Heiskanen I, Vaisanen M, Arola J, Korsoff P, Ebeling T, Sane T, Minn H, Valimaki MJ, Nuutila P. Complementary roles of 18F-DOPA PET/CT and 18F-FDG PET/CT in medullary thyroid cancer. J Nucl Med 2011;52:1855-1863.
12. Luster M, Karges W, Zeich K, Pauls S, Verburg FA, Dralle H, Glatting G, Buck AK, Solbach C, Neumaier B, Reske SN, Mottaghy FM. Clinical value of 18-fluorinefluorodihydroxyphenyl alanine positron emission tomography/computed tomography in the follow-up of medullary thyroid carcinoma. Thyroid 2010;20:527-533.
13. Treglia G, Castaldi P, Villani MF, Perotti G, de Waure C, Filice A, Ambrosini V, Cremonini N, Santimaria M, Versari A, Fanti S, Giordano A, Rufini V. Comparison of 18F-DOPA, 18F-FDG and 68Ga-somatostatin analogue PET/CT in patients with recurrent medullary thyroid carcinoma. Eur J Nucl Med Mol Imaging 2012;39:569-580.
14. Verbeek HH, Plukker JT, Koopmans KP, de Groot JW, Hofstra RM, Muller Kobold AC, van der Horst-Schrivers AN, Brouwers AH, Links TP. Clinical relevance of 18F-FDG PET and 18F-DOPA PET in recurrent medullary thyroid carcinoma. J Nucl Med 2012;53:1863-1871.
15. Diehl M, Risse JH, Brandt-Mainz K, Dietlein M, Bohuslavizki KH, Matheja P, Lange H, Bredow J, Körber C, Grünwald F. Fluorine-18 fluorodeoxyglucose positron emission tomography in medullary thyroid cancer: results of a multicentre study. Eur J Nucl Med 2001;28:1671-1676.
16. Ong SC, Schöder H, Patel SG, Tabangay-Lim IM, Doddamane I, Gönen M, Shaha AR, Tuttle RM, Shah JP, Larson SM. Diagnostic accuracy of 18F-FDG PET in restaging patients with medullary thyroid carcinoma and elevated calcitonin levels. J Nucl Med 2007;48:501-507.
17. Skoura E, Datseris IE, Rondogianni P, Tsagarakis S, Tzanela M, Skilakaki M, Exarhos D, Alevizaki M. Correlation between calcitonin levels and [18F] FDGPET/CT in the detection of recurrence in patients with sporadic and hereditary medullary thyroid cancer. ISRN Endocrinol 2012;2012:37523.
18. De Luca S, Fonti R, Camera L, Salvatore B, Faggiano A, Ciarmiello A, Segreto S, Colao A, Salvatore M, Del Vecchio S. Multimodal imaging with 18F-FDG-PET/CT and 111In-Octreotide SPECT in patients with metastatic medullary thyroid carcinoma. Ann Nucl Med 2016;30:234-241.
19. Conry BG, Papathanasiou ND, Prakash V, Kayani I, Caplin M, Mahmood S, Bomanji JB. Comparison of 68Ga-DOTATATE and 18F-fluorodeoxyglucose PET/CT in the detection of recurrent medullary thyroid carcinoma. Eur J Nucl Med Mol Imaging 2010;37:49-57.
20. Oudoux A, Salaun PY, Bournaud C, Campion L, Ansquer C, Rousseau C, Bardet S, Borson-Chazot F, Vuillez JP, Murat A, Mirallié E, Barbet J, Goldenberg DM, Chatal JF, Kraeber-Bodere F. Sensitivity and prognostic value of positron emission tomography with F-18-fluorodeoxyglucose and sensitivity of immunoscintigraphy in patients with medullary thyroid carcinoma treated with anticarcinoembryonic antigen-targeted radioimmunotherapy. J Clin Endocrinol Metab 2007;92:4590-4597.
21. Beuthien-Baumann B, Strumpf A, Zessin J, Bredow J, Kotzerke J. Diagnostic impact of PET with 18F-FDG, 18F-DOPA and 3-O-methyl-6-[18F]fluoro-DOPA in recurrent or metastatic medullary thyroid carcinoma. Eur J Nucl Med Mol Imaging 2007;34:1604-1609.
22. Iagaru A, Masamed R, Singer PA, Conti PS. Detection of occult medullary thyroid cancer recurrence with 2-Deoxy-2-[F-18]fluoro-d-glucose-PET and PET/CT. Mol Imaging Biol 2007;9:72-77.
23. Czepczynski R, Kosowicz J, Ziemnicka K, Mikolajczak R, Gryczynska M, Sowinski J. The role of scintigraphy with the use of 99mTc-HYNIC-TOC in the diagnosis of medullary thyroid carcinoma. Endokrynol Pol 2006;57:431-435.
24. Conti PS, Durski JM, Bacqai F, Grafton ST, Singer PA. Imaging of locally recurrent and metastatic thyroid cancer with positron emission tomography. Thyroid 1999;9:797-804.
25. Archier A, Heimburger C, Guerin C, Morange I, Palazzo FF, Henry JF, Schneegans O, Mundler O, Adbullah AE, Sebag F, Imperiale A, Taieb D. 18F-DOPA PET/CT in the diagnosis and localization of persistent medullary thyroid carcinoma. Eur J Nucl Med Mol Imaging 2016;43:1027-1033.
26. Volkan-Salancı B, Kıratlı PÖ. Nuclear medicine in thyroid diseases in pediatric and adolescent patients. Mol Imaging Radionucl Ther 2015;24:47-59.
27. Ozkan ZG, Kuyumcu S, Uzum AK, Gecer MF, Ozel S, Aral F, Adalet I. Comparison of 68Ga-DOTATATE PET-CT, 18F-FDG PET-CT and 99mTc-(V)DMSA scintigraphy in the detection of recurrent or metastatic medullary thyroid carcinoma. Nucl Med Commun 2015;36:242-250.
28. Czepczynski R, Parisella MG, Kosowicz J, Mikolajczak R, Ziemnicka K, Gryczynska M, Sowinski J, Signore A. Somatostatin receptor scintigraphy using 99mTc-EDDA/HYNIC-TOC in patients with medullary thyroid carcinoma. Eur J Nucl Med Mol Imaging 2007;34:1635-1645.

29. Kauhanen S, Seppänen M, Ovaska J, Minn H, Bergman J, Korsoff P, Salmela P, Saltevo J, Sane T, Valimaki M, Nuutila P. The clinical value of [18F]fluorodihydroxyphenylalanine positron emission tomography in primary diagnosis, staging, and restaging of neuroendocrine tumors. Endocr Relat Cancer 2009;16:255-265.
30. Treglia G, Castaldi P, Rindi G, Giordano A, Rufini V. Diagnostic performance of Gallium-68 somatostatin receptor PET and PET/CT in patients with thoracic and gastroenteropancreatic neuroendocrine tumours: a meta-analysis. Endocrine 2012;42:80-87.
31. Khan N, Oriuchi N, Higuchi T, Endo K. Review of fluorine-18-2-fluoro-2-deoxy-D-glucose positron emission tomography (18F-FDG-PET) in the follow-up of medullary and anaplastic thyroid carcinomas. Cancer Control 2005;12:254-260.
32. Chiacchio S, Lorenzoni A, Boni G, Rubello D, Elisei R, Mariani G. Anaplastic thyroid cancer: prevalence, diagnosis and treatment. Minerva Endocrinol 2008;33:341-357.
33. Edge SB, Byrd DR, Compton CC, Fritz AG, Greene FL, Trotti A: AJCC Cancer Staging Manual. 7th edition. New York, NY: Springer; 2010:87–96.
34. Schmid DT, Stoeckli SJ, Bandhauer F, Huguenin P, Schmid S, von Schulthess GK, Goerres GW. Impact of positron emission tomography on the initial staging and therapy in locoregional advanced squamous cell carcinoma of the head and neck. Laryngoscope 2003;113:888-891.
35. Jadvar H, Fischman AJ. Evaluation of rare tumors with [F-18] fluorodeoxyglucose positron emission tomography. Clin Positron Imaging 1999;2:153-158.
36. Soydal C, Yüksel C, Küçük NÖ, Okten I, Ozkan E, Doğanay Erdoğan B. Prognostic Value of Metabolic Tumor Volume Measured by 18F-FDG PET/CT in Esophageal Cancer Patients. Mol Imaging Radionucl Ther 2014;23:12-15.
37. Bogsrud TV, Karantanis D, Nathan MA, Mullan BP, Wiseman GA, Kasperbauer JL, Reading CC, Hay ID, Lowe VJ. 18F-FDG PET in the management of patients with anaplastic thyroid carcinoma. Thyroid 2008;18:713-719.
38. Poisson T, Deandreis D, Leboulleux S, Bidault F, Bonniaud G, Baillot S, Aupérin A, Al Ghuzlan A, Travagli JP, Lumbroso J, Baudin E, Schlumberger M. 18F-fluorodeoxyglucose positron emission tomography and computed tomography in anaplastic thyroid cancer. Eur J Nucl Med Mol Imaging 2010;37:2277-2285.
39. Ansell SM, Grant CS, HAbermann TM. Primary Thyroid lymphoma. Semin Oncol 1999;26:316-323.
40. Skarsgard ED, Connors JM, Robins RE. A current analysis of primary lymphoma of the thyroid. Arch Surg 1991;126:1199-1203.
41. Junor EJ, Paul J, Reed NS. Primary non-Hodgkin's lymphoma of the thyroid. Eur J Surg Oncol 1992;18:313-321.
42. Burke JS. Are there site-specific differences among the MALT lymphomas–morphologic, clinical? Am J Clin Pathol 1999;111(Suppl 1):133-143.
43. Naswa N, Sharma P, Nazar AH, Mohapatra TK, Bal C, Kumar R. (18)F-FDG PET/CT for initial assessment and response monitoring in a case of high grade primary lymphoma of the thyroid gland: A case report and review of literature. Indian J Nucl Med 2014;29:94-96.
44. Mikosch P, Würtz FG, Gallowitsch HJ, Kresnik E, Lind P. F-18-FDG-PET in a patient with Hashimoto's thyroiditis and MALT lymphoma recurrence of the thyroid. Wien Med Wochenschr 2003;153:89-92.
45. Nakadate M, Yoshida K, Ishii A, Koizumi M, Tochigi N, Suzuki Y, Ryu Y, Nakagawa T, Umehara I, Shibuya H. Is 18F-FDG PET/CT useful for distinguishing between primary thyroid lymphoma and chronic thyroiditis? Clin Nucl Med 2013;38:709-714.
46. Sharma A, Jasim S, Reading CC, Ristow KM, Villasboas BJC, Habermann TM, Fatourechi V, Stan M. Clinical presentation and diagnostic challenges of thyroid lymphoma: a cohort study. Thyroid 2016;26:1061-1067.
47. Mansber R, Bency R, Shen L, Bui C, Park K. Riedel's Thyroiditis With Intense FDG uptake demonstrated on FDG PET/CT. Mol Imaging Radionucl Ther 2015;24:29-31.
48. Nakhjavani MK, Gharib H, Goellner JR, van Heerden JA. Metastasis to the thyroid gland: A report of 43 cases. Cancer 1997;79:574-578.
49. Hegerova L, Griebeler ML, Reynolds JP, Henry MR, Gharib H. Metastasis to the thyroid gland: report of a large series from the Mayo Clinic. Am J Clin Oncol 2015;38:338-342.
50. Berge T, Lundberg S. Cancer in Malmo 1958-1969: an autopsy study. Acta Pathol Microbiol Scand 1977;(Suppl)260:1-235.
51. Treglia G, Bongiovanni M, Paone G, Ceriani L, Giovanella L. Metastatic undifferentiated spindle cell sarcoma of the thyroid gland evaluated by 18F-FDG PET/CT. Clin Nucl Med 2015;40:e208-10.
52. Agrawal K, Weaver J, Mohan HK. Metastasis to the thyroid from non-small cell carcinoma of the lung: findings in (18)F-FDG PET/CT study. Endocrine 2015;48:720-721.
53. Nikiforov YE. Genetic alterations involved in the transition from well-differentiated to poorly differentiated and anaplastic thyroid carcinomas. Endocrine Pathology 2004;15:319-327.
54. Feine U, Lietzenmayer R, Hanke JP, Held J, Wöhrle H, Müller-Schauenburg W. Fluorine-18-FDG and iodine-131-iodide uptake in thyroid cancer. J Nucl Med 1996;37:1468-1472.
55. Grabellus F, Nagarajah J, Bockisch A, Schmid KW, Sheu SY. Glucose transporter 1 expression, tumor proliferation, and iodine/glucose uptake in thyroid cancer with emphasis on poorly differentiated thyroid carcinoma. Clin Nucl Med 2012;37:121-127.
56. Muros de Fuentes MA, Mitjavila Casanovas M, Estorch Cabrera M, Lecumberri Santamaria B, Navarro Gonzalez E. Usefulness of 18F-FDG PET/CT in thyroid carcinoma. Rev Esp Med Nucl Imagen Mol 2016;35:186-192.
57. Palaniswamy SS, Subramanyam P. Diagnostic utility of PETCT in thyroid malignancies: an update. Ann Nucl Med 2013;27:681-693.
58. Nascimento C, Borget I, Al Ghuzlan A, Deandreis D, Hartl D, Lumbroso J, Berdelou A, Lepoutre-Lussey C, Mirghani H, Baudin E, Schlumberger M, Leboulleux S. Postoperative fluorine-18-fluorodeoxyglucose positron emission tomography/computed tomography: an important imaging modality in patients with aggressive histology of differentiated thyroid cancer. Thyroid 2015;25:437-444.
59. Levy A, Leboulleux S, Lepoutre-Lussey C, Baudin E, Ghuzlan AA, Hartl D, Deutsch E, Deandreis D, Lumbroso J, Tao Y, Schlumberger M, Blanchard P. (18)F-fluorodeoxyglucose positron emission tomography to assess response after radiation therapy in anaplasticthyroid cancer. Oral Oncol 2015;51:370-375.
60. Hundahl SA, Cady B, Cunningham MP, Mazzaferri E, McKee RF, Rosai J, Shah JP, Fremgen AM, Stewart AK, Hölzer S. Initial results from a prospective cohort study of 5583 cases of thyroid carcinoma treated in the United States during 1996: U.S. and German Thyroid Cancer Study Group-an American College of Surgeons Commission on Cancer Patient Care Evaluation study. Cancer 2000;89:202-217.
61. Azadian A, Rosen IB, Walfish PG, Asa SL. Management considerations in Hurthle cell carcinoma. Surgery 1995;118:711-714.
62. Shaha AR, Ferlito A, Rinaldo A. Distant metastases from thyroid and parathyroid cancer. ORL J Otorhinolaryngol Relat Spec 2001;63:243-249.
63. Shaha AR, Shah JP, Loree TR. Patterns of nodal and distant metastasis based on histologic varieties in differentiated carcinoma of the thyroid. Am J Surg 1996;172:692-694.
64. Stojadinovic A, Ghossein RA, Hoos A, Urist MJ, Spiro RH, Shah JP, Brennan MF, Shaha AR, Singh B. Hurthle cell carcinoma: a critical histopathologic appraisal. J Clin Oncol 2001;19:2616-2625.
65. Stojadinovic A, Hoos A, Ghossein RA, Urist MJ, Leung DH, Spiro RH, Shah JP, Brennan MF, Singh B, Shaha AR. Hurthle cell carcinoma: a 60-year experience. Ann Surg Oncol 2002;9:197-203.
66. Yutan E, Clark OH. Hurthle cell carcinoma. Curr Treat Options Oncol 2001;2:331-335.
67. Yen TC, Lin HD, Lee CH, Chang SL, Yeh SH. The role of technetium-99m sestamibi whole-body scans in diagnosing metastatic Hurthle cell carcinoma of the thyroid gland after total thyroidectomy: a comparison with iodine-131 and thallium-201 whole-body scans. Eur J Nucl Med 1994;21:980-983.

68. Lowe VJ, Mullan BP, Hay ID, McIver B, Kasperbauer JL. 18F-FDG PET of patients with Hurthle cell carcinoma. J Nucl Med 2003;44:1402-1406.
69. Wang W, Larson SM, Fazzari M, Tickoo SK, Kolbert K, Sgouros G, Yeung H, Macapinlac H, Rosai J, Robbins RJ. Prognostic value of [18F]fluorodeoxyglucose positron emission tomographic scanning in patients with thyroid cancer. J Clin Endocrinol Metab 2000;85:1107-1113.
70. Pryma DA, Schöder H, Gönen M, Robbins RJ, Larson SM, Yeung HW. Diagnostic accuracy and prognostic value of 18F-FDG PET in Hürthle cell thyroid cancer patients. J Nucl Med 2006;47:1260-1266.
71. Bertagna F, Treglia G, Piccardo A, Giubbini R. Diagnostic and clinical significance of F-18-FDG-PET/CT thyroid incidentalomas. J Clin Endocrinol Metab 2012;97:3866-3875.
72. Gavriel H, Tang A, Eviatar E, Chan SW. Unfolding the role of PET FDG scan in the management of thyroid incidentaloma in cancer patients. Eur Arch Otorhinolaryngol 2015;272:1763-1768.
73. Liu Y. Clinical significance of thyroid uptake on F18-fluorodeoxyglucose positron emission tomography. Ann Nucl Med 2009;23:17-23.
74. Bertagna F, Treglia G, Piccardo A, Giovannini E, Bosio G, Biasiotto G, Bahij el K, Maroldi R, Giubbini R. F18-FDG-PET/CT thyroid incidentalomas: a wide retrospective analysis in three Italian centres on the significance of focal uptake and SUV value. Endocrine 2013;43:678-685.
75. Soelberg KK, Bonnema SJ, Brix TH, Hegedüs L. Risk of malignancy in thyroid incidentalomas detected by 18F-fluorodeoxyglucose positron emission tomography: a systematic review. Thyroid 2012;22:918-925.
76. Agrawal K, Weaver J, Ul-Hassan F, Jeannon JP, Simo R, Carroll P, Hubbard JG, Chandra A, Mohan HK. Incidence and Significance of Incidental Focal Thyroid Uptake on (18)F-FDG PET Study in a Large Patient Cohort: Retrospective Single-Centre Experience in the United Kingdom. Eur Thyroid J 2015;4:115-122.
77. Are C, Hsu JF, Ghossein RA, Schoder H, Shah JP, Shaha AR. Histological aggressiveness of fluorodeoxyglucose positron-emission tomogram (FDG-PET)-detected incidental thyroid carcinomas. Ann Surg Oncol 2007;14:3210-3215.
78. Kwak JY, Kim EK, Yun M, Cho A, Kim MJ, Son EJ, Oh KK. Thyroid incidentalomas identified by 18F-FDG PET: sonographic correlation. AJR Am J Roentgenol 2008;191:598-603.
79. Choi JS, Choi Y, Kim EK, Yoon JH, Youk JH, Han KH, Moon HJ, Kang WJ, Kwak JY. A risk-adapted approach using US features and FNA results in the management of thyroid incidentalomas identified by 18F-FDG PET. Ultraschall Med 2014;35:51-58.
80. Hoang JK, Langer JE, Middleton WD, Wu CC, Hammers LW, Cronan JJ, Tessler FN, Grant EG, Berland LL. Managing incidental thyroid nodules detected on imaging: white paper of the ACR Incidental Thyroid Findings Committee. J Am Coll Radiol 2015;12:143-150.
81. Haugen BR, Alexander EK, Bible KC, Doherty GM, Mandel SJ, Nikiforov YE, Pacini F, Randolph GW, Sawka AM, Schlumberger M, Schuff KG, Sherman SI, Sosa JA, Steward DL, Tuttle RM, Wartofsky L. 2015 American Thyroid Association Management Guidelines for Adult Patients with Thyroid Nodules and Differentiated Thyroid Cancer: The American Thyroid Association Guidelines Task Force on Thyroid Nodules and Differentiated Thyroid Cancer. Thyroid 2016;26:1-133.
82. Stangierski A, Woli ski K, Czepczy ski R, Czarnywojtek A, Lodyga M, Wyszomirska A, Janicka-Jedy ska M, B czyk M, Ruchała M. The usefulness of standardized uptake value in differentiation between benign and malignant thyroid lesions detected incidentally in 18F-FDG PET/CT examination. PLoS One 2014;9:e109612.
83. Kim BH, Kim SJ, Kim K, Kim H, Kim SJ, Kim WJ, Jeon YK, Kim SS, Kim YK, Kim IJ. High metabolic tumor volume and total lesion glycolysis are associated with lateral lymph node metastasis in patients with incidentally detected thyroid carcinoma. Ann Nucl Med 2015;29:721-729.

Original Article
Mol Imaging Radionucl Ther 2017;26:9-16 DOI:10.4274/mirt.94914

The Correlation Between Pre-treatment Fluorodeoxyglucose Positron Emission Tomography/Computed Tomography Parameters and Clinical Prognostic Factors in Pediatric Hodgkin Lymphoma

Pediatrik Hodgkin Lenfoma Hastalarında Tedavi Öncesi Florodeoksiglukoz Pozitron Emisyon Tomografi/Bilgisayarlı Tomografi Parametreleri ve Klinik Prognostik Faktörler Arasındaki İlişki

Ebru Tatcı[1], İnci Uslu Biner[1], Suna Emir[2], Hikmet Gülşah Tanyıldız[3], Özlem Özmen[1], Engin Alagöz[4], Atila Gökçek[5], Gürses Şahin[3]

[1]*Atatürk Chest Diseases and Thoracic Surgery Training and Research Hospital, Department of Nuclear Medicine, Ankara, Turkey*
[2]*Ankara Children's Hematology Oncology Training and Research Hospital, Department of Pediatric Hematology Oncology, Ankara, Turkey*
[3]*Dr. Sami Ulus Maternity and Children's Health and Diseases Training and Research Hospital, Department of Pediatric Oncology and Hematology, Ankara, Turkey*
[4]*Gülhane Training and Research Hospital, Department of Nuclear Medicine, Ankara, Turkey*
[5]*Atatürk Chest Diseases and Thoracic Surgery Training and Research Hospital, Department of Radiology, Ankara, Turkey*

Abstract

Objective: To compare standardized uptake values (SUV) derived from pre-treatment ^{18}F-fluorodeoxyglucose (FDG) positron emission tomography/computed tomography (PET/CT) imaging and clinical prognostic factors in pediatric patients with Hodgkin lymphoma (HL).

Methods: Pre-treatment FDG PET/CT findings of 28 children with HL were evaluated in this retrospective study. Metabolic tumor volume (MTV), SUV_{max} normalized by weight (SUV_{weight}), lean body mass (SUV_{lbm}), body surface area (SUV_{bsa}) and plasma glucose levels of tumors ($SUV_{glucose}$) were calculated using pre-treatment FDG PET/CT scan images. These metabolic parameters were correlated with clinical factors [age, sex, number of lymph node groups, presence of splenic involvement, bulky mediastinal disease, Ann Arbor stage, serum white blood cell (WBC) count, erythrocyte sedimentation rate (ESR), serum albumin and hemoglobin levels].

Results: SUV_{bsa}, SUV_{lbm}, SUV_{weight}, $SUV_{glucose}$ and MTV were higher in patients with stage III-IV disease, bulky tumor and ≥3 lymph node groups ($p<0.05$). SUV_{bsa} and $SUV_{glucose}$ were higher in patients with splenic involvement ($p<0.05$). There was no significant correlation between these metabolic parameters and sex, ESR, levels of albumin and WBC ($p>0.05$). SUV_{bsa} and SUV_{lbm} were higher in patients with anemia ($p<0.05$). Additionally, significant increases were detected in SUV_{weight}, MTV, and $SUV_{glucose}$ with increasing age ($p=0.005$, $p=0.027$, and $p=0.009$, respectively). SUV_{bsa} and SUV_{lbm} had no significant correlation with age ($p>0.05$).

Conclusion: Metabolic parameters derived from pre-treatment FDG PET/CT may have an important role in predicting high-risk disease in patients with HL. Also, SUV_{bsa} and SUV_{lbm} may be better markers than SUV_{weight} in the quantitative evaluation of FDG PET/CT scans in pediatric patients.

Keywords: Fluorodeoxyglucose positron emission tomography/computed tomography, Hodgkin lymphoma, standardized uptake value, metabolic tumor volume

Address for Correspondence: Ebru Tatcı MD, Atatürk Chest Diseases and Thoracic Surgery Training and Research Hospital, Department of Nuclear Medicine, Ankara, Turkey
Phone: +90 505 914 53 61 E-mail: ebrualkandr@yahoo.com **Received:** 26.07.2016 **Accepted:** 24.10.2016

Öz

Amaç: Hodgkin lenfoma (HL) tanısı konmuş çocuk hastalarda klinik prognostik faktörler ile tedavi öncesi ^{18}F-florodeoksiglukoz (FDG) pozitron emisyon tomografi/bilgisayarlı tomografi (PET/BT) görüntülemeden elde edilen standart tutulum değerlerini (SUV) karşılaştırmaktır.

Yöntem: Bu retrospektif çalışmada HL tanılı 28 çocuk hastanın FDG PET/BT bulguları değerlendirildi. Metabolik tümör volümü (MTV), kiloya (SUV_{kilo}), yağsız vücut kitlesine (SUV_{lbm}), vücut yüzey alanına (SUV_{bsa}) and plazma glukoz seviyesine (SUV_{glukoz}) göre normalize edilmiş SUV_{maks} değerleri tedavi öncesi FDG PET/CT görüntüleri kullanılarak hesaplandı. Bu metabolik parametrelerin klinik faktörler [yaş, cinsiyet, lenf nodu grup sayısı, dalak tutulumu, büyük mediastinal hastalık, Ann Arbor evreleme, serum lökosit sayımı (WBC), eritrosit sedimentasyon hızı (ESH), serum albumin ve hemoglobin seviyesi] ile ilişkisi araştırıldı.

Bulgular: SUV_{bsa}, SUV_{lbm}, SUV_{kilo}, SUV_{glukoz} ve MTV evre 3-4 hastalığı, büyük tümörü ve ≥3 lenf nodu grubu olan hastalarda daha yüksekti (p<0,05). SUV_{bsa} ve SUV_{glukoz} dalak tutulumu olan hastalarda daha fazlaydı (p<0,05). Bu metabolik parametreler ile cinsiyet, ESR, albumin ve WBC seviyeleri arasında önemli bir ilişki yoktu (p>0,05). SUV_{bsa} ve SUV_{lbm} anemisi olan hastalarda daha yüksekti (p<0,05). Ek olarak yaş arttıkça SUV_{kilo}, MTV ve SUV_{glukoz}'da önemli artış olduğu saptandı (sırasıyla; p=0,005, p=0,027 ve p=0,009). SUV_{bsa} ve SUV_{lbm} ile yaş arasında önemli korelasyon yoktu (p>0,05).

Sonuç: HL tanılı hastalarda tedavi öncesi FDG PET/BT'den elde edilen metabolik parametreler yüksek riskli hastalığı tahmin etmede önemli bir rol oynayabilir. Ayrıca, pediatrik hastalarda FDG PET/BT'nin kantitatif değerlendirilmesinde SUV_{bsa} ve SUV_{lbm}, SUV_{kilo}'dan daha iyi belirteç olabilir.

Anahtar kelimeler: Florodeoksiglukoz pozitron emisyon tomografi/bilgisayarlı tomografi, Hodgkin lenfoma, standart tutulum değeri, metabolik tümör volümü

Introduction

Currently, more than 80% of patients with Hodgkin lymphoma (HL) can be cured by contemporary treatment methods. The present major problem with HL is the long-term complications of treatment. Children who have been treated for HL have a higher risk of developing secondary tumors, cardiac events, and infections (1). Prognostic factors are considered during treatment planning to decrease the side effects and the likelihood of recurrence or treatment resistance (2). The most unfavorable prognostic factors according to the International Prognostic Score are stage 4 disease, age ≥45 years, hemoglobin <10.5 g/dl, albumin <4.0 g/dl, white cell count (WBC) ≥15,000/µl, and lymphocyte level <600/µl or <8%, respectively. Also, presence of B symptoms, high erythrocyte sedimentation rate (ESR), male sex, higher number of involved nodal sites, and bulky-mass tumors are additional factors associated with an increased risk of relapse (3).

It has been reported in many studies that FDG PET-CT is a very useful imaging modality in the primary staging, restaging, assessment of treatment response and evaluation of residual masses of lymphomas (4,5,6,7). Standardized uptake value (SUV) is used traditionally for the definition of metabolic activity in FDG PET imaging. The patient's body weight is usually employed as the body size measurement during the calculation of SUV. However, lean body mass or body surface area may be preferred for body size measurement by some authors. SUV is also affected by blood glucose level, post-injection uptake time, image resolution, image reconstruction parameters, and volume-of-interest-definition (8,9). Additionally, the maximum SUV (SUV_{max}) is only measured by the highest image pixel in the tumor regions and doesn't show the metabolic activity of the entire tumor. Metabolic tumor volume (MTV) is another FDG PET/CT parameter, which is the measurement of the tumor volume with increased metabolism. It has been reported that MTV could play an important role in predicting survival in various malignancies (10,11). The purpose of this study was to evaluate the role of FDG-PET/CT in staging pediatric HL, and to establish if the metabolic parameters of pre-treatment FDG PET/CT correlated with clinical prognostic factors in pediatric HL patients. If so, metabolic parameters of pre-treatment FDG PET/CT might have a role in predicting treatment failure. Additionally, we evaluated the correlation of age and metabolic parameters in pediatric patients.

Materials and Methods

Patients

Twenty-eight HL patients who underwent pre-treatment FDG PET/CT examinations between May 2009 and December 2014 were included in this retrospective study. Informed consent was waived due to the retrospective nature of the study. Patients older than 18 years were excluded. The study was approved by the Institutional Ethics Committee. The histologic classifications were established according to the standard WHO classification scheme (12). Results of bone marrow biopsy (BMB), levels of WBC, albumin and hemoglobin values and ESR were recorded. After completion of therapy, patients were

followed by physical examination, laboratory analyses, chest radiographs, ultrasonography, CT or FDG PET/CT scans.

Fluorodeoxyglucose Positron Emission Tomography/ Computed Tomography Imaging

PET/CT imaging was performed forty-five to sixty minutes after intravenous injection of 87.69-414.77 MBq (2.37-11.21 mCi) of FDG with a Siemens Biograph 6 HI-REZ integrated PET/CT scanner (Siemens Medical Solutions, Knoxville, TN, USA). All patients fasted for at least six hours before PET/CT imaging without water restriction. The blood glucose levels of patients were confirmed to be less than 180 mg/dL before FDG injection. Low-dose whole-body CT was used for attenuation correction. PET/CT data were acquired from the top of the skull to the upper thigh.

Fluorodeoxyglucose Positron Emission Tomography/ Computed Tomography Analysis

Visual Analyses

Pre-treatment PET/CT images were retrospectively evaluated by two experienced nuclear medicine physicians and one radiologist. The number of lymph node groups was determined. A splenic FDG uptake greater than hepatic uptake was considered as splenic involvement. The marrow was considered as abnormal when the uptake was equal to or greater than that of the liver. Bulky disease was defined as presence of a lymph node mass greater than 0.33 of the maximum intrathoracic cavity width. The intensity of FDG activity within the bone marrow (BM) was evaluated visually. BMB results were used as the gold-standard for staging. The stage of lymphoma was assessed according to the Ann-Arbor classification (13).

Semi-quantitative Analyses

SUV_{max} and MTV values were obtained from pre-treatment FDG PET/CT images for semi-quantitative evaluation. The SUV_{max} corrected for body weight (SUV_{weight}) was measured within the hottest tumor lesion according to the formula (14):

$$SUV_{weight} = \frac{\text{Tissue concentration (MBq/ml)}}{\text{Injected dose (MBq)/ weight (g)}}$$

The SUV_{max} normalized for lean body mass (SUV_{lbm}), and body surface area (SUV_{bsa}) were calculated using the following equations (14):

$$SUV_{lbm} = \frac{\text{Tissue concentration (MBq/ml)}}{\text{Injected dose (MBq)/ lbm (kg)}}$$

LBM (male) (kg)=(1.1×weight) (kg)-120 [weight (kg)/ height (cm)]^2

LBM (female) (kg)=(1.07×weight) (kg)-148 [weight (kg)/ height (cm)]^2

$$SUV_{bsa} = \frac{\text{Tissue concentration (MBq/ml)}}{\text{Injected dose (MBq)/ BSA (m}^2\text{)}}$$

BSA (m^2)=0.007184×weight (kg)$^{0.425}$×height (cm)$^{0.725}$

SUV values were also corrected for blood glucose level using an established formula, assuming a normal blood glucose level of 5.55 mmol/L (100 mg/dL) (14):

$$SUV_{glucose} = \frac{SUV_{max} \times \text{blood glucose (mmol/L)}}{\text{5.55 mmol/L}}$$

MTV of each hypermetabolic tumor focus was automatically calculated by the software program and MTV of each tumor was summated. The threshold intensity value used in this study was 40% of maximal SUV of each tumor as validated in several previous studies (15,16).

Statistical Analyses

The SPSS 20 software was used for statistical analysis. Comparisons of SUV levels (SUV_{weight}, SUV_{bsa}, SUV_{lbm}, $SUV_{glucose}$, MTV) and clinical parameters (sex, number of lymph node groups, presence of splenic involvement, bulky disease, Ann Arbor stage, serum levels of albumin, WBC, ESR and hemoglobin) were performed using the independent test or Mann-Whitney U test. All quantitative values are given as mean±standard deviation (SD). Pearson's correlation coefficients were used to evaluate the correlation between PET parameters and age. A statistically significant difference was defined as a p value <0.05.

Results

Patients

The characteristics of the patients are presented in Table 1. A total of 28 patients with a mean age ±SD of 9.39±4.2 y (male/female: 17/11) were enrolled in this study. Eleven (39.3%) patients had nodular sclerosis subtype and 15 (53.6%) had mixed cellularity subtype. Histologic subtype remained unclassified in two patients. Of all 28 patients, 18 (64.2%) had undergone BMB.

The laboratory findings of the patients are summarized in Table 2. Among all 28 patients, hemoglobin was <10.5 g/dl in nine patients (32.1%), WBC was ≥15000/ml in 11 patients (39.3%), albumin was <4 g/dl in 16 patients

(57.1%), and ESR was ≥50 mm/hr in 13 patients (46.4%). All of the patients underwent three to six courses (6-12 cycles) of chemotherapy with or without radiation therapy after the initial PET/CT scanning. The mean±SD clinical follow-up period was 29±14 months. All 28 patients were in remission at the last follow up, but one child died of infection. Recurrence was not detected in the follow-up.

Fluorodeoxyglucose Positron Emission Tomography/ Computed Tomography Analyses

Visual Analyses

Pre-treatment FDG PET/CT findings are summarized in Table 2. Bulky mediastinal disease was detected in 15 of the 28 (53.5%) patients. While there were <3 lymph node groups in 28.6% of the 28 patients (n=8), ≥3 lymph node groups were found in 71.4% (n=20). Splenic involvement was detected in 32.1% patients (n=9). Eight patients had stage 1-2 (28.6%) disease, and 20 patients had stage 3-4 (71.4%) disease.

Increased diffuse BM FDG uptake in the axial skeleton was seen in 12/28 (42.8%) patients. BMB was performed in 10 of these 12 (83.3%) patients. Among ten patients with diffuse BM uptake, nine patients had negative BMB results (Figure 1). Only one patient showed positive lymphoma involvement in BMB. There was no increase in BM FDG uptake in 16 of 28 (57.1%) patients. BMB was performed in seven of 16 (43.7%) whose BMB result was negative. Additionally radioluceny and enlargement at the localizations of ischiopubic synchondrosis (IPS) were detected in 4 of the 28 (14.2%) patients. Intense FDG uptakes were seen in these areas (SUV_{max} range 1.17-3.10). These patients didn't suffer from any symptoms such as groin pain and restriction in the movement of the hip joint.

Table 1. Patient characteristics

Characteristics	n, (%)
Sex M/F	
Male	17 (60.7)
Female	11 (39.2)
Age, y (mean±SD)	9.39±4.2
Histological subtype	
Nodular sclerosis	11/28 (39.3)
Mixed cellularity	15/28 (53.6)
Unclassified	2/28 (7.1)
Bone marrow biopsy	18/28 (64.2)
Therapy	
Chemotherapy	12/28 (42.8)
Chemoradiotherapy	16/28 (57.1)

M: Male, F: Female, SD: Standard deviation

Since these focal FDG uptakes weren't identified in follow-up PET/CT scans, they were evaluated as the asymmetric ossification pattern of the IPS rather than malignant bone infiltration (Figure 2).

Quantitative Analyses

SUV_{bsa}, SUV_{lbm}, SUV_{weight}, $SUV_{glucose}$, and MTV values were higher in patients with stage 3-4 disease, a bulky tumor, and ≥3 lymph node groups ($p<0.05$) (Table 2). SUV_{bsa} and $SUV_{glucose}$ were higher in patients with splenic involvement ($p<0.05$). There was no significant correlation between metabolic parameters and a) sex, b) ESR, c) albumin level, and d) WBC level ($p>0.05$). Hemoglobin level lower than 10.5 g/dL was associated with higher SUV_{bsa} and SUV_{lbm} ($p<0.05$). While SUV_{bsa} and SUV_{lbm} ($p>0.05$) did not relate to age; SUV_{weight}, MTV, and $SUV_{glucose}$ values were found to be significantly correlated with age ($p=0.005$, $p=0.027$, $p=0.009$ and $r=0.519$, $r=0.506$, $r=0.504$, respectively).

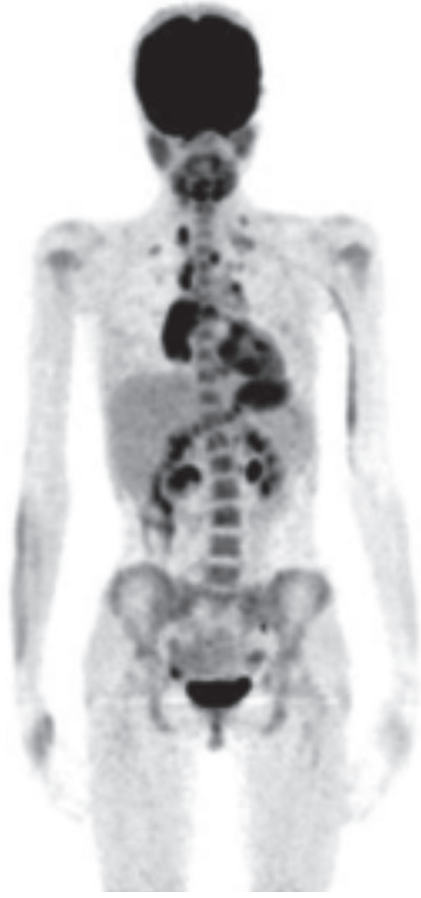

Figure 1. The maximum intensity projection image. Increased diffuse bone marrow fluorodeoxyglucose uptake in the axial system, and fluorodeoxyglucose uptake by supra-diaphragmatic lymph nodes are displayed. Bone marrow biopsy was negative

Table 2. Fluorodeoxyglucose positron emission tomography/computed tomography parameters related to clinical prognostic factors

Parameters	n	SUV_{weight} (mean±SD)	MTV (mean±SD)	SUV_{lbm} (mean±SD)	SUV_{bsa} (mean±SD)	$SUV_{glucose}$ (mean±SD)
Stage						
1-2	8	4.8±2.9	56.2±45.3	1±0.4	2±0.8	5.8±2.1
3-4	20	10.8±4.5	377.7±301.9	2±1.3	3.9±1.3	11.9±4.3
p value		**0.002**	**0.012**	**0.006**	**0.002**	**0.001**
Bulky tumor						
Absent	13	6.2±3.4	162.2±206.4	1.2±0.8	2.4±1.2	6.8±2.8
Present	15	11.6±4.7	417.5±317.6	2.2±1.3	4.2± 1.3	12.7±4.3
p value		**0.002**	**0.032**	**0.034**	**0.001**	**0.001**
NLG*						
<3	8	5.6±3.2	38.7±24.4	1.1±0.4	2.4±0.9	6.3±1.9
≥3	20	10.5±4.8	360.9±299.4	1.9±1.3	3.7±1.5	11.4±4.7
p value		**0.014**	**0.019**	**0.028**	**0.037**	**0.001**
Splenic involvement						
Absent	19	7.9±3.8	225±189.5	1.6±1.2	3±1.3	8.6±3.9
Present	9	11.7±6.1	455.8±403.7	2.1±1.3	4.2±1.6	13.1±5.2
p value		0.054	0.106	0.327	**0.044**	**0.023**
Sex						
Female	11	8.1±3.9	223±212.6	1.6±1	3.2±1.2	8.5±2.9
Male	17	9.7±5.5	341.1±325.4	1.9±1.3	3.4±1.7	11.1±5.5
p value		0.387	0.517	0.639	0.736	0.138
Leukocyte count						
<15000/ml	17	8.4±4.2	194.2±189.7	1.5±1	3±1.5	9.5±4.6
≥15000/ml	11	10.1±5.9	438.7±353.8	2.1±1.5	3.9±1.3	10.7±5
p value		0.4	0.051	0.531	0.159	0.542
Hemoglobin (g/dl)						
≥10.5	19	8.5±5.3	291.5±327.4	1.3±1	2.9±1.4	9.4±4.6
<10.5	9	10.2±3.9	361.8±221.6	2.6±1.2	4.3±1.3	11.4±4.7
p value		0.21	0.165	**0.012**	**0.028**	0.313
ESR (mm/hr)						
<50	15	8.8±5.8	318±344.7	1.5±1.1	3.2±1.4	10±5.1
≥50	13	9.4±3.8	296.3±223.4	1.9±1.3	3.5±1.6	10±4.4
p value		0.779	0.612	0.505	0.632	0.978
Albumin (g/dl)						
≥4	12	9.1±6.5	410.5±398.3	1.3±1	3.1±1.7	9.6±5.5
<4	16	9.1±3.5	236.9±189.4	2±1.3	3.5±1.4	10.3±4
p value		0.991	0.221	0.178	0.463	0.717

*NLG: Number of lymph node groups; SUV_{weight}: Standardized uptake value normalized by weight, SUV_{lbm}: Standardized uptake value normalized by lean body mass, SUV_{bsa}: Standardized uptake value normalized by body surface area, $SUV_{glucose}$: Standardized uptake value normalized by level of glucose, MTV: Metabolic tumor volume, SD: Standard deviation, ESR: Erythrocyte sedimentation rate

Discussion

It was previously demonstrated in some studies in the literature that the amount of FDG accumulation is an important prognostic factor in various malignant tumors (17,18). Ceriani et al. (19) reported that elevated MTV was significantly associated with worse progression-free and overall survival in patients with primary mediastinal (thymic) large B-cell lymphoma. Suh et al. (20) showed that pre-treatment FDG PET could predict treatment response and survival outcomes in patients with extranodal natural killer/T-cell lymphomas of the head and neck. Similarly, we identified a significant association between quantitative FDG uptake and clinical prognostic factors in pediatric patients with HL. The quantitative parameters were higher in patients with stage 3-4 disease, a bulky tumor, and ≥3 lymph node groups ($p<0.05$), which are the clinical parameters that reflect tumor burden. Intensity of tumor cells is one of the most important parameters to determine the efficacy of treatment in HL (21). High SUV_{max} and MTV can indicate poorer survival in patients with HL. Intensive therapy can be administered in these patients. However, in the presence of low FDG uptake, overtreatment can be avoided. The present study has several limitations. Cure was achieved in 27 of the 28 patients at the end of therapy and recurrence was not detected on follow-up. One child died of infection. So, progression-free survival and overall survival couldn't be determined in this study.

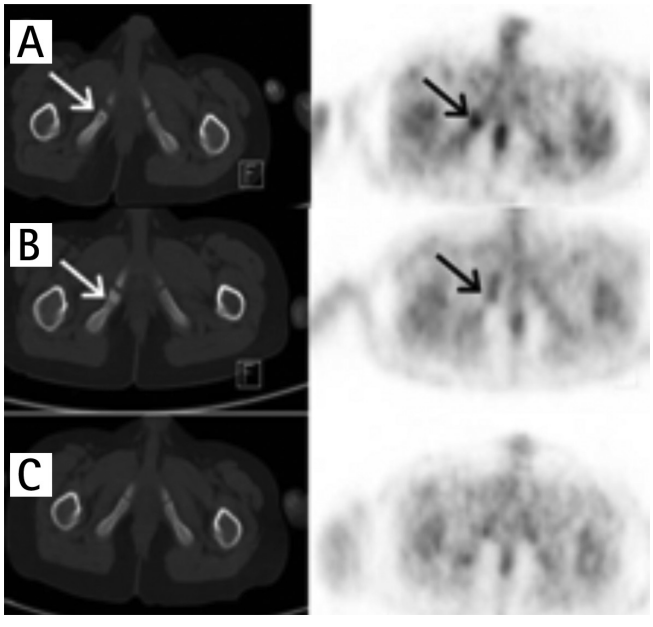

Figure 2. A) Axial positron emission tomography/computed tomography images of the pelvis in the bone window setting showed radiolucency and enlargement at the right ischium and increased focal fluorodeoxyglucose uptake at that area. B) Sclerosis at the same localization and decreased fluorodeoxyglucose uptake four months after therapy were seen. C) After 12 months of therapy no abnormal findings were detected on positron emission tomography/computed tomography scan (arrows)

Anemia, low albumin level, leukocytosis and high ESR level are particularly observed in advanced stage disease (3). HD is characterized by the presence of a low frequency of malignant cells known as Reed-Sternberg cells. The majority of the malignant tissues in HD constitutes a reactive cell infiltrate composed of variable proportions of lymphocytes, histiocytes, eosinophils, and plasma cells. Malignant Reed-Sternberg cells and reactive cells produce different cytokines. Close associations between elevation of cytokine levels in the plasma and presence of B symptoms, anemia, leukocytosis, high ESR and low serum albumin levels has been reported (22,23). Our study results indicate that hemoglobin level lower than 10.5 g/dL was associated with higher SUV_{bsa} and SUV_{lbm} ($p<0.05$). Higher SUV_{bsa} and SUBlbm may be related to higher tumor burden and higher plasma cytokine levels. However, we did not observe significant correlation between metabolic parameters and ESR, levels of albumin and WBC ($p>0.05$). Long-term follow-up studies with a larger group of patients may yield more satisfactory results.

The amountof SUV_{weight} changes was related to patient's body weight. However, some reports show that SUV_{lbm} and SUV_{bsa} are less dependent on body weight than SUV_{weight} (8,9). Concordant with these reports, our study showed that while SUV_{weight}, MTV and $SUV_{glucose}$ increase with age ($p<0.05$), SUV_{bsa} and SUV_{lbm} did not significantly correlate with age ($p>0.05$). Changes with age can reduce the importance of SUV_{weight}, MTV and $SUV_{glucose}$ values as markers to discriminate malignant tumors from benign ones in children. Also, these parameters can be misguiding in evaluating therapy response. SUV_{lbm} and SUV_{bsa} may be preferred in the primary diagnosis, staging and follow up of malignancies in the pediatric population (24).

A diffuse homogeneous BM FDG uptake generally reflects hyperplastic BM caused by severe anemia, use of granulocyte colony stimulating factors, or chemotherapy. However, infiltration of tumor cells can also cause increased diffuse BM FDG uptake. Authors suggest that BMB is the gold standard in the staging of HL (25). However, focal FDG uptake can be adequate in the diagnosis of bone or BM involvement in HL (13). Nevertheless, physiologic FDG uptake patterns mimicking bone metastasis such as IPS should be taken into consideration while evaluating PET/CT scans in the pediatric population (26).

Conclusion

Metabolic parameters derived from pre-treatment FDG PET/CT scanning can be valuable in predicting high-risk disease in pediatric HL. Also, SUV_{bsa} and SUV_{lbm} might be better

markers than SUV_{weight} in the quantitative evaluation of FDG PET/CT scans in pediatric patients. However, prospective studies with a larger group of patients are needed to obtain more reliable results.

Ethics

Ethics Committee Approval: The study were approved by the Atatürk Chest Diseases and Thoracic Surgery Training and Research Hospital of Local Ethics Committee. Informed Consent: Consent form was filled out by all participants. It was taken.

Peer-review: Externally peer-reviewed.

Authorship Contributions

Surgical and Medical Practices: Suna Emir, Hikmet Gülşah Tanyıldız, Gürses Şahin, Concept: Ebru Tatcı, Özlem Özmen,

Design: Ebru Tatcı, Özlem Özmen, Data Collection or Processing: Ebru Tatcı, İnci Uslu Biner, Engin Alagöz, Suna Emir, Hikmet Gülşah Tanyıldız, Atila Gökçek, Analysis or Interpretation: Ebru Tatcı, Özlem Özmen, İnci Uslu Biner, Literature Search: Ebru Tatcı, Writing: Ebru Tatcı.

Conflict of Interest: Authors declared no conflict-of-interest.

Financial Disclosure: The authors declared that this study received no financial support.

References

1. Santoro A, Bonadonna G, Valagussa P, Zucali R, Viviani S, Villani F, Pagnoni AM, Bonfante V, Musumeci R, Crippa F, et al. Long-term results of combined chemotherapy-radiotherapy approach in Hodgkin's disease: superiority of ABVD plus radiotherapy versus MOPP plus radiotherapy. J Clin Oncol 1987;5:27-37.
2. Carde P, Burgers JM, Henry-Amar M, Hayat M, Sizoo W, Van der Schuer en E, Monconduit M, Noordijk EM, Lustman-Marechal J, Tanguy A, et al. Clinical stages I and II Hodgkin's disease: a specifically tailored therapy according to prognostic factors. J Clin Oncol 1988;6:239-252.
3. Hasenclever D, Diehl V. A prognostic score for advanced Hodgkin's disease. International Prognostic Factors Project on Advanced Hodgkin's Disease. N Engl J Med 1998;339:1506-1514.
4. Tatsumi M, Miller JH, Wahl RL. 18F-FDG PET/CT in evaluating non-CNS pediatric malignancies. J Nucl Med 2007;48:1923-1931.
5. Depas G, De Barsy C, Jerusalem G, Hoyoux C, Dresse MF, Fassotte MF, Paquet N, Foidart J, Rigo P, Hustinx R. 18F-FDG PET in children with lymphomas. Eur J Nucl Med Mol Imaging 2005;32:31-38.
6. Newman JS, Francis IR, Kaminski MS, Wahl RL. Imaging of lymphoma with PET with 2-[F-18]-fluoro-2-deoxy-D-glucose: correlation with CT. Radiology 1994;190:111-116.
7. Stauss J, Franzius C, Pfluger T, Juergens KU, Biassoni L, Begent J, Kluge R, Amthauer H, Voelker T, Højgaard L, Barrington S, Hain S, Lynch T, Hahn K. Guidelines for 18F-FDG PET and PET-CT imaging in paediatric oncology. Eur J Nucl Med Mol Imaging 2008;35:1581-1588.
8. Adams MC, Turkington TG, Wilson JM, Wong TZ. A systematic review of the factors affecting accuracy of SUV measurements. AJR Am J Roentgenol 2010;195:310-320.
9. Kim CK, Gupta NC, Chandramouli B, Alavi A. Standardized uptake values of FDG: body surface area correction is preferable to body weight correction. J Nucl Med 1994;35:164-167.
10. Sager S, Asa S, Yilmaz M, Uslu L, Vatankulu B, Halaç M, Sönmezoglu K, Kanmaz B.. Prognostic significance and predictive performance of volume-based parameters of F-18 FDG PET/CT in squamous cell head and neck cancers. J Cancer Res Ther 2014;10:922-926.
11. Park GC, Kim JS, Roh JL, Choi SH, Nam SY, Kim SY. Prognostic value of metabolic tumor volume measured by 18F-FDG PET/CT in advanced-stage squamous cell carcinoma of the larynx and hypopharynx. Ann Oncol 2013;24:208-214.
12. Campo E, Swerdlow SH, Harris NL, Pileri S, Stein H, Jaffe ES. The 2008 WHO classification of lymphoid neoplasms and beyond: evolving concepts and practical applications. Blood 2011;117:5019-5032.
13. Cheson BD. Staging and response assessment in lymphomas: the new Lugano classification. Chin Clin Oncol 2015;4:5.
14. Paquet N, Albert A, Foidart J, Hustinx R. Within-patient variability of (18)F-FDG: standardized uptake values in normal tissues. J Nucl Med 2004;45:784-788.
15. Schwartz DL, Harris J, Yao M, Rosenthal DI, Opanowski A, Levering A, Ang KK, Trotti AM, Garden AS, Jones CU, Harari P, Foote R, Holland J, Zhang Q, Le QT. Metabolic tumor volume as a prognostic imaging-based biomarker for head-and-neck cancer: pilot results from Radiation Therapy Oncology Group protocol 0522. Int J Radiat Oncol Biol Phys 2015;91:721-729.
16. Son SH, Kim DH, Hong CM, Kim CY, Jeong SY, Lee SW, Lee J, Ahn BC. Prognostic implication of intratumoral metabolic heterogeneity in invasive ductal carcinoma of the breast. BMC Cancer 2014;14:585.
17. Berghmans T, Dusart M, Paesmans M, Hossein-Foucher C, Buvat I, Castaigne C, Scherpereel A, Mascaux C, Moreau M, Roelandts M, Alard S, Meert AP, Patz EF Jr, Lafitte JJ, Sculier JP. Primary tumor standardized uptake value (SUVmax) measured on fluorodeoxyglucose positron emission tomography (FDG-PET) is of prognostic value for survival in non-small cell lung cancer (NSCLC): a systematic review and meta-analysis (MA) by the European Lung Cancer Working Party for the IASLC Lung Cancer Staging Project. J Thorac Oncol 2008;3:6-12.
18. Ikenaga N, Otomo N, Toyofuku A, Ueda Y, Toyoda K, Hayashi T, Nishikawa K, Tanaka M. Standardized uptake values for breast carcinomas assessed by fluorodeoxyglucose-positron emission tomography correlate with prognostic factors. Am Surg 2007;73:1151-1157.
19. Ceriani L, Martelli M, Zinzani PL, Ferreri AJ, Botto B, Stelitano C, Gotti M, Cabras MG, Rigacci L, Gargantini L, Merli F, Pinotti G, Mannina D, Luminari S, Stathis A, Russo E, Cavalli F, Giovanella L, Johnson PW, Zucca E. Utility of baseline 18FDG-PET/CT functional parameters in defining prognosis of primary mediastinal (thymic) large B-cell lymphoma. Blood 2015;126:950-956.
20. Suh C, Kang YK, Roh JL, Kim MR, Kim JS, Huh J, Lee JH, Jang YJ, Lee BJ. Prognostic value of tumor 18F-FDG uptake in patients with untreated extranodal natural killer/T-cell lymphomas of the head and neck. J Nucl Med 2008;49:1783-1789.
21. Specht L, Nordentoft AM, Cold S, Clausen NT, Nissen NI. Tumor burden as the most important prognostic factor in early stage Hodgkin's disease. Relations to other prognostic factors and implications for choice of treatment. Cancer 1988;61:1719-1727.
22. Niens M, Visser L, Nolte IM, van der Steege G, Diepstra A, Cordano P, Jarrett RF, Te Meerman GJ, Poppema S, van den Berg A. Serum chemokine levels in Hodgkin lymphoma patients: highly increased levels of CCL17 and CCL22. Br J Haematol 2008;140:527-536.
23. Salgami EV, Efstathiou SP, Vlachakis V, Sekara EV, Syrigos KN, Roussou PP. High pretreatment interleukin-10 is an independent predictor of poor failure-free survival in patients with Hodgkin's lymphoma. Haematologia (Budap). 2002;32:377-387.
24. Meier JM, Alavi A, Iruvuri S, Alzeair S, Parker R, Houseni M, Hernandez-Pampaloni M, Mong A, Torigian DA. Assessment of age-related changes in abdominal organ structure and function with computed tomography and positron emission tomography. Semin Nucl Med 2007;37:154-172.

25. Muzahir S, Mian M, Munir I, Khalid Nawaz M, Salman Faruqui Z, Aftab Mufti K, Bashir H, Uddin N, Siddiqui N, Maaz AU, Mahmood MT. Clinical utility of 18F FDG-PET/CT in the detection of bone marrow disease in Hodgkin's lymphoma. Br J Radiol 2012;85:e490-496.

26. Tsuji K, Tsuchida T, Kosaka N, Tanizawa A, Kimura H. Serial changes of (18)F-FDG PET/CT findings in ischiopubic synchondrosis: comparison with contrast-enhanced MRI. Hell J Nucl Med 2015;18:66-67.

Original Article
Mol Imaging Radionucl Ther 2017;26:17-23 DOI:10.4274/mirt.61587

Assessment of the Prevalence of Diabetic Gastroparesis and Validation of Gastric Emptying Scintigraphy for Diagnosis

Diyabetik Gastroparezi Prevalansı ve Tanısında Mide Boşalma Sintigrafisinin Geçerliliğinin Araştırılması

Zeinab Alipour[1], Foad Khatib[1], Seyed Masoud Tabib[1], Hamid Javadi[2], Esmail Jafari[3], Leila Aghaghazvini[4], Ali Mahmoud-Pashazadeh[3], Iraj Nabipour[5], Majid Assadi[3]

[1]*Bushehr University of Medical Sciences, Bushehr Medical University Hospital, Department of Internal Medicine, Division of Gastroenterology, Bushehr, Iran*

[2]*Golestan University of Medical Sciences, Golestan Research Center of Gastroenterology and Hepatology, Gorgan, Iran*

[3]*Bushehr University of Medical Sciences, The Persian Gulf Nuclear Medicine Research Center, Bushehr, Iran*

[4]*Tehran University of Medical Sciences, Shariati Hospital, Department of Radiology, Tehran, Iran.*

[5]*Bushehr University of Medical Sciences, The Persian Gulf Tropical and Infectious Diseases Research Centre, Bushehr, Iran*

Abstract

Objective: Gastroparesis is defined as delayed gastric emptying and is a common medical condition in diabetic patients. Scintigraphy is commonly used as a standard diagnostic procedure for the quantitative assessment of gastroparesis. The aims of this study were to determine an optimum imaging time for the diagnosis of gastroparesis, to assess the prevalence of gastroparesis, to evaluate the correlation between endoscopy and scintigraphy findings as well as the correlation between gastric emptying with patient genders, blood glucose concentration, and functional dyspepsia.

Methods: Gastric emptying was assessed in 50 diabetic patients with a mean age of 50.16 years. For evaluation of gastric emptying, a test meal containing 2 pieces of toast, 120 cc non-labeled water and fried egg labeled with 1 mCi of ^{99m}Tc was given to each patient. The scintigraphy was performed immediately after ingestion and was repeated at 1, 1.5, 2 and 4 hours after ingestion. In some patients, an additional 90-minute dynamic scan was also acquired.

Results: The prevalence of gastroparesis in this study population was determined as 64%. Also, the results of this study revealed that a 4-hour scan after ingestion is more relevant than a 90-minute dynamic scan for the evaluation of delayed gastric emptying. There was no statistically significant difference between 1-hour and 2-hour scans, 1-hour and 90-minute scans, 2-hour and 90-minute scans, 2-hour and 4-hour scans. Likewise there was no significant correlation between blood glucose levels, gender and calculated values of gastric emptying time in all groups.

Conclusion: According to our findings, it can be suggested that the prevalence of gastroparesis is higher than that mentioned in some previous studies. Also, this study indicates that a gastric emptying scintigraphy at 2 and 4 hours after meal ingestion might provide the anticipated clinical information in diabetic patients with dyspepsia without other evident reasons.

Keywords: Gastroparesis, gastric emptying, diabetes, scintigraphy

Address for Correspondence: Majid Assadi MD, Bushehr University of Medical Sciences, The Persian Gulf Nuclear Medicine Research Center, Bushehr, Iran
Phone: +098-771-2580169 E-mail: assadipoya@yahoo.com **Received:** 27.10.2016 **Accepted:** 13.02.2017

Öz

Amaç: Gastroparezi gecikmiş mide boşalması olarak tanımlanır ve diyabetik hastalarda sık rastlanan bir tıbbi durumdur. Gastroparezinin kantitatif değerlendirmesi için sintigrafi sıklıkla standart bir diagnostik yöntem olarak kullanılmaktadır. Bu çalışmanın amaçları gastroparezi tanısında optimum görüntüleme zamanını belirlemek, gastroparezi prevalansını belirlemek, endoskopi ve sintigrafi bulguları arasındaki uyumu ve mide boşalması ile cinsiyet, kan glukoz düzeyi ve fonksiyonel dispepsi arasındaki ilişkiyi incelemektir.

Yöntem: Ortalama yaşları 50,16 olan 50 diyabetik hastanın mide boşalması değerlendirildi. Mide boşalmasını değerlendirmek için her hastaya 2 dilim tost, 120 cc işaretlenmemiş su ve 1 mCi ^{99m}Tc ile işaretlenmiş kızartılmış yumurtadan oluşan bir öğün verildi. Oral alımın hemen sonrasında 1., 1,5., 2. ve 4. saatlerde sintigrafi yapıldı. Bazı hastalarda ek olarak 90. dakika dinamik görüntülemesi de uygulandı.

Bulgular: Çalışma grubunda gastroparezi prevalansı %64 olarak bulundu. Aynı zamanda oral alımdan sonra 4. saat görüntülemesinin gecikmiş mide boşalmasının değerlendirilmesinde 90. dakika dinamik görüntülemeden daha uygun olduğu bulundu. Birinci saat ve 2. saat, 1. saat ve 90. dakika, 2. saat ve 90. dakika, 2. saat ve 4. saat görüntülemeleri arasında istatistiksel olarak anlamlı fark yoktu. Benzer şekilde, tüm gruplarda kan glukoz düzeyi, cinsiyet ve hesaplanan mide boşalma zamanı arasında anlamlı bir ilişki saptanmadı. Görüntülemeler arasında cinsiyet, kan şekeri düzeyi ve mide boşalma süreleri açısından da fark tespit edilmedi.

Sonuç: Sonuçlarımıza göre gastroparezi prevalansının daha önce bildirilenden daha yüksek olduğu öne sürülebilir. Benzer şekilde, bu çalışma gıda alımından 2 ve 4 saat sonra uygulanan mide boşalma sintigrafisinin dispeptik şikayetleri olan ancak diğer bariz nedenler bulunmayan diyabetik hastalarda gerekli klinik bilgiyi verebileceğini öngörmektedir.

Anahtar kelimeler: Gastroparezi, mide boşalması, diyabet, sintigrafi

Introduction

Gastroparesis is a medical condition that is defined as delayed gastric emptying in the absence of mechanical obstruction, and is known as one of the most common side effects of diabetes mellitus (1,2). Abdominal bloating, satiety and upper abdominal pain symptoms that are associated with delayed gastric emptying in diabetic patients (3,4,5,6).

Amongst all other methods, radionuclide imaging of gastric emptying is accepted as the gold standard to evaluate patients with symptoms related to gastric emptying disorders (7). Since the first use of radionuclide scintigraphy to evaluate gastric emptying in 1966, it has become an acceptable procedure in clinical practice by enabling noninvasive quantitative survey of gastric emptying (8). In this procedure, a solid or liquid meal labeled with radionuclide is used to provide a gastric count as an index of gastric disorder (9).

Based on radionuclide scintigraphy results on gastric emptying in diabetic patients, the prevalence of delayed gastric emptying has been reported as 25-55% and 30% in patients with type 1 and 2 diabetes, respectively (10,11,12). Also, it has been determined that 29% of patients with gastroparesis had diabetes mellitus (13).

The evidence shows that several features of diabetic patients can have an effect on gastric emptying time, thus must be considered during interpretation. For example, acute alterations in blood glucose concentration can change gastric emptying time of both liquid and solid meals (14). Although the pathogenesis of gastroparesis has been attributed to poorly controlled hyperglycemia, some researches did not show a correlation between gastroparesis and autonomic dysfunction (4,12,15). Another study reported a correlation between diabetic gastroparesis and cardiovascular disease and retinopathy (16).

Recently, the Society of Nuclear Medicine and Molecular Imaging and the American Society of Neurogastroenterology and Motility agreed on application of a standard diet and standard imaging protocol for the evaluation of gastric emptying. This procedure has been standardized based on a study on 123 healthy cases, with a standard meal and several imaging times (17). While many studies have been performed on the assessment of gastric emptying by scintigraphy, some issues are still controversial.

In a research study on the diagnosis of gastroparesis, it's mentioned that food remnants were observed within the stomach by endoscopy in patients with normal scintigraphy findings (18,19). Existence of remaining food in the stomach 12 hours after fasting represents gastroparesis in the absence of gastric outflow obstruction. However, the Diabetes Care Standards, published in 2014, did not include endoscopy as a diagnostic method for gastroparesis (18,19).

Nevertheless, it is reported that some patients require scintigraphic evaluation for gastric emptying (20,21,22,23). This may include a group of patients with rapid gastric emptying associated with nausea, bloating and satiety. Similar observations have also been reported in a group of patients with functional dyspepsia. On the other hand, rapid gastric emptying may occur at the beginning of type

2 diabetes in some patients. Many patients present with symptoms that are not distinguishable from gastroparesis. Also, it has been reported that rapid gastric emptying was more common than delayed gastric emptying in patients with autonomic dysfunction.

Further evaluation is needed to assess scintigraphy imaging at the 30- or the 60-minute and the 2- or the 4-hour scans for the diagnosis of rapid gastric emptying (8).

Therefore, the aim of the current study was to find the optimum imaging times for diagnosis of gastroparesis and rapid gastric emptying, and to assess the prevalence of gastroparesis in diabetic patients with dyspepsia. The relations between endoscopy and scintigraphy results for the diagnosis of gastroparesis were also evaluated. We also assessed the correlation between gastric emptying and gender and blood glucose concentration, as well as that between functional dyspepsia and gastric emptying disorders.

Materials and Methods

Fifty diabetic patients (34 men and 16 women) with an age range of 24 to 65 years (mean of 50.16±12.11 years) who have been referred to the Gastroenterology Clinic at our hospital were included in this study. Patients with normal endoscopy who did not have any exclusion criteria were referred to nuclear medicine center for evaluation of gastric emptying. The study was approved by the Bushehr University of Medical Sciences (protocol number: 2345)

Exclusion criteria in this study included heart disease (MI, heart failure and heart valve problems), metabolic disorders (hypothyroidism, kidney failure and liver failure), rheumatic diseases (lupus and scleroderma), history of peptide ulcer disease, history of surgery affecting gastric emptying (vagotomy, gastric bypass), and use of drugs affecting gastric emptying (anticholinergics, prokinetic drugs and opioids).

Before initiation of the study, all study stages were explained to the patients and consent form was obtained. They also had an option to withdraw from study participation at any time.

In case of medications that could affect gastric emptying, all patients were asked to discontinue them for 48 hours before the study, with the supervision of a physician. Patients were also asked to stop using tobacco at least at the morning of the study and were explained that they would not be allowed to smoke until the end of the study. Patients were allowed to take medications which do not affect gastric emptying as well as insulin as prescribed dosages.

In order to decrease the influence of daily activities on gastric emptying, the study was performed in the morning after at least 6 hours of fasting before the study. On the day of the study, blood glucose concentration of each patient was checked and if it was less than 275 mg/dL, the study was continued. Then each patient was given a test meal containing 2 pieces of toast, 120 cc non labeled water and fried egg labeled with 1 mCi of ^{99m}Tc-sulfur colloid.

For evaluation of gastric emptying by scintigraphy, scanning was started in a static acquisition mode immediately after ingestion for each patient (time 0). Then, the study was repeated at post-ingestion times of 30 minutes in 29 patients, 60 minutes in 28 patients, 90 minutes in 27 patients, 2 hours in 48 patients, and also 4 hours in 24 patients. In addition, the study was performed with the 90-minute dynamic mode in 13 patients. The study period was also increased so as to improve the accuracy of the obtained results. Patients who had not taken the labeled meal completely or had vomited before the 2-hour scan were excluded from the study. Also, if there was no possibility of a 4-hour scan (such as vomiting), scanning data of other times was used. The scan was acquired in the anterior and posterior projections in a fixed supine position. Data was acquired with a gamma camera (Pegsys, ADAC Lab, USA) equipped by a low-energy high-resolution collimator. Region of interest of the stomach was initially drawn manually, then with the corresponding software. All measured activities were corrected using the decay factor (DF) expressed as:

$$DF=\exp(-\ln 2\times t/361)$$

Where t refers to the time (minutes) elapsed after the first measurement.

Delayed gastric emptying or gastric retention was defined as 90% retention at the 1-hour, more than 60% at the 2-hour, and more than 10% at the 4-hour scans. Retention less than 30% at the 1-hour or less than 70% at 30-minute scans were considered as rapid gastric emptying (3,17,24). Retention more than 65% in the 90-minute scan was considered as delayed gastric emptying.

Statistical Analysis

Continuous variables were compared with unpaired t-test and categorical variables were compared with chi-square analysis. A p-value less than 0.05 were considered as statistically significant. For statistical analysis, SPSS for Windows software package (Release 18, SPSS Inc., Chicago, Illinois) was used.

Results

According to the analysis of the obtained data, the mean fasting blood sugar (FBS) was determined as 165.63±50.42 mmol/L. Scintigraphy test was done at 30 minutes, 1, 1.5, 2 and 4 hours after eating radioactivity labeled meal thus creating 5 groups of patients. Within the first group of patients (29 patients), eight patients (27.6%) had rapid gastric emptying while others were normal (Table 1, Figure 1). In the second group of 28 patients, 14 patients (50%) had delayed gastric emptying and others were normal (Table

2, Figure 2). In the third group of patients (27 patients), delayed gastric emptying was observed in 3 (11.1%) with 24 (88.9%) normal results (Table 2, Figure 2). Within the fourth group in the 2-hour post ingestion evaluation, 13 (27.7%) and 34 (72.3%) patients showed delayed and normal gastric emptying, respectively (Table 2, Figure 2). Finally, within the fifth group in the 4-hour post ingestion, delayed and normal gastric emptying were observed in 19 (72.9%) and five (20.8%) patients, respectively (Table 2, Figure 2).

Among 13 patients who underwent dynamic scanning of gastric emptying, nine (69.2%) cases showed delayed gastric emptying while four (30.8%) patients were normal (Table 2, Figure 2). In none of the patients, evidence of gastroparesis was detected on endoscopy.

It was observed that patient gender did not have an effect on gastric emptying.

Based on the statistical analysis of the data, a significant correlation between FBS level and gastric emptying score was only detected at the 30-minute scan (p=0.04). Rapid gastric emptying at the 30-minute scan was associated with delayed gastric emptying at 1 hour (p value <0.001).

Because of limited number of cases who completed both tests, the correlation between the 1 and 4 hours scanning results could not be evaluated. However, the reported abnormality rate was significant in both time points (50% and 79%, respectively for 1 and 4 hours).

According to the available data, there was no statistical correlation between the 1-hour scan and the 90-minute static scan (p=0.82). Also, there was no statistically significant difference between the 2-hour scan and the 90-minute dynamic scan (p=0.109).

In comparison of the results of the 2- and 4-hour scans in 24 patients, 12 and 19 cases had delayed gastric emptying, respectively, but there was no statistically significant difference between these two groups (p=0.32).

In the evaluation of the 90-minute dynamic scan and 4-hour scan, nine cases out of 11 patients and 11 cases out of 11 patients showed delayed gastric emptying, respectively, confirming a clear advantage of the 4 hour scan in the evaluation of gastric emptying (p=0.021).

Table 1. Patient data at 30 minute gastric emptying scintigraphy

Time of scan	Number of patients	Normal emptying	Rapid emptying
30 minutes	29	21 (72.4%)	8 (27.6%)

Table 2. Patient data at five time points of gastric emptying scintigraphy

Time of scan	Number of patients	Normal emptying	Delayed emptying
60-minutes	28	14 (50%)	14 (50%)
90-minutes (static)	27	24 (88.9%)	3 (11.1%)
2-hours	47	34 (72.3%)	13 (27.7%)
4-hours	24	5 (20.8%)	19 (79.2%)
90 minutes dynamic scan	13	4 (30.8%)	9 (69.2%)

Discussion

Based on the results of the 30-minute gastric emptying scan performed on 29 patients, eight cases (27.6%) showed rapid gastric emptying. This finding was in accordance with the results of a similar study published in 2009, in which 28 cases of 129 patients (22%) showed rapid emptying of solid materials. The prevalence of rapid gastric emptying in type 2 diabetes was slightly higher in the mentioned study. This discrepancy could be related to the different procedures

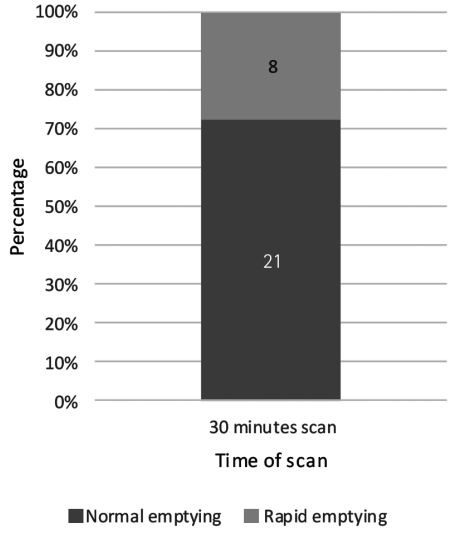

Figure 1. Rapid gastric emptying based on 30-minute gastric emptying scintigraphy

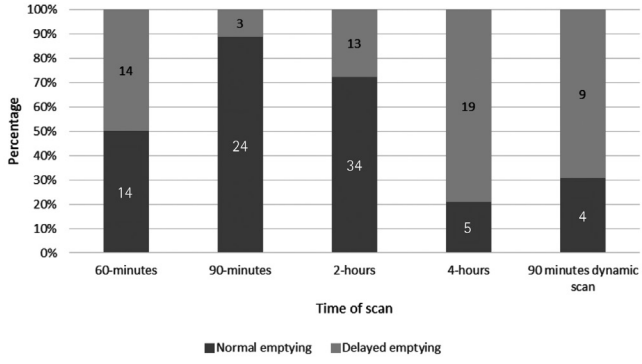

Figure 2. Rapid gastric emptying based on five time points of gastric emptying scintigraphy

used in the two studies. In their study, a 1-hour scan has been used for evaluation of gastric emptying while we used a 30-minute scan (25).

It was previously shown that rapid gastric emptying occurs in both diabetic and functional dyspepsia (26), however, exactly how many patients have rapid gastric emptying is not clear because of complications of or accompaniment with diabetes. Therefore, a clinical trial is required to compare rapid gastric emptying in diabetic patients with dyspepsia and in non-diabetic patients with functional dyspepsia. Unfortunately, in most studies, the control group was selected from healthy people without symptoms of dyspepsia.

According to the statistical analysis of our data, there was a positive correlation between rapid gastric emptying in the 30-minute scan and FBS levels (p=0.048). This finding confirms the finding of a previous study showing that a higher FBS was associated with rapid gastric emptying (27).

In a previous study, C breath test-octanoic acid and T1/2 were used to assess gastric emptying (28). The prevalence of delayed gastric emptying in patients with type 1 diabetes has been reported as 33.7% in that study (28), which is different from our results. This difference could be related to the different procedures applied in the two studies.

In another comprehensive study, the prevalence of gastroparesis was reported as 24.2 in 100000, and the cumulative incidence of gastroparesis in a 10-year period was reported as 5.2% and 1% in type 1 and 2 diabetes respectively, that seems to be very low. However, patients with gastrointestinal symptoms included in that study were not assessed for gastric emptying with scintigraphy, which could have affected their findings (29,30).

In two other studies published in 1983 and 2001, it was determined that 60% of patients with long-lasting type 1 diabetes had suffered from gastrointestinal symptoms of gastroparesis. Although the method of patient selection was different from our study, their results were close to that of ours. It should be noted that these studies were conducted before the routine use of insulin for intensive treatment of type 1 diabetes (4,31,32).

In another study, delayed gastric emptying of solid materials had been discovered in 56% of patients (10). Although this amount was less than our results, it should be considered that in their study gastric emptying half time has been used for the evaluation of gastroparesis (10). Anudeep et al. (12) evaluated the prevalence and predictors of delayed gastric emptying among 140 patients with type 2 diabetes mellitus in which delayed gastric emptying was detected in about 29 % (40/140) of type 2 diabetes patients.

The higher prevalence of gastroparesis in our study can be due to the strict inclusion criteria of our study. On the other hand, gastroparesis was accepted as delayed gastric emptying in the 1-hour scan in our study while in several other studies the 2- or 4-hour scans were taken into consideration.

Gastric emptying study using a 90-minute dynamic scan is usually associated with increased costs and may lead to increased work for both the patient and the staff.

Based on the findings of the current attempt that showed the superiority of the static scan over the dynamic scan, a 2- and/or 4-hour scan instead of a 90-minute scan is recommended in diabetic patients who undergo scintigraphic studies. This is mainly because more cases have been diagnosed with delayed gastric emptying with the 4-hour scan who had initially been recognized as normal with the 90-minute dynamic scan. Therefore, based on the current study results, the most appropriate time for gastric emptying study seems to be either 2 or 4 hours both post meal ingestion to detect as much cases as possible. This could lead to a significantly better management of diabetic patients. While this is a significant advantage, it is not the only superiority of the static scan over dynamic scanning for detecting gastric emptying. Using the static scan, both the patients and the staff who are involved in the scintigraphy exam would spent less time to perform the test as compared to the 90-minute continuous scan. Therefore, it is easier for both groups, patients and staff, to perform the static scan. Additionally, a dynamic scan might exert higher workload to the single-photon emission computed tomography system in comparison to the static one, which is another positive aspect of the static scan.

Regarding the follow-up study, the finding of our survey highlighted the importance of gastric emptying study in diabetic patients. Our results showed that the prevalence of gastroparesis in diabetic patients is more than what it was originally thought. The high rate of patients with delayed gastric emptying indicates that testing should be considered to enable a tailored management of diabetic patients.

Although we tried to keep patient groups homogeneous with applying different scan times and including as much eligible patients as possible to reinforce the validity of our findings, we experienced some limitations in this regard, which is in fact the main drawback of the current survey. Future studies assessing the optimum scanning time of diabetic patients with more uniform groups and higher number of patients should be conducted both to obtain more solid data and to verify our findings.

Conclusion

Based on the study findings, it can be suggested that the prevalence of gastroparesis is higher than the previously reported rates. Although a larger population is needed for overall conclusion, this study can provide context for further studies, which would have been otherwise impossible due to ethical considerations.

According to our findings, it seems that in diabetic patients suffering from dyspepsia without other evident reasons, 2 and/or 4 hours after meal ingestion is an appropriate time to conduct a gastric emptying scintigraphy. Furthermore, we conclude that the prevalence of gastroparesis is higher than the previously reported rates.

Ethics

Ethics Committee Approval: The study was approved by the Bushehr University of Medical Sciences (protocol number: 2345), Informed Consent: Consent form was filled out by all participants.

Peer-review: Externally peer-reviewed.

Authorship Contributions

Surgical and Medical Practices: Zeinab Alipour, Foad Khatib, Seyed Masoud Tabib, Hamid Javadi, Majid Assadi, Concept: Zeinab Alipour, Foad Khatib, Hamid Javadi, Iraj Nabipour, Majid Assadi Design: Zeinab Alipour, Foad Khatib, Seyed Masoud Tabib, Hamid Javadi, Iraj Nabipour, Majid Assadi, Data Collection or Processing: Zeinab Alipour, Foad Khatib, Seyed Masoud Tabib, Hamid Javadi, Majid Assadi, Analysis or Interpretation: Hamid Javadi, Majid Assadi, Literature Search: Zeinab Alipour, Foad Khatib, Esmail Jafari, Leila Aghaghazvini, Ali Mahmoud-Pashazadeh, Writing: Esmail Jafari, Ali Mahmoud-Pashazadeh, Majid Assadi.

Conflict of Interest: No conflict of interest was declared by the authors.

Financial Disclosure: The authors declared that this study has received no financial support.

References

1. Abrahamsson H. Treatment options for patients with severe gastroparesis. Gut 2007;56:877-883.
2. Olausson EA, Brock C, Drewes AM, Grundin H, Isaksson M, Stotzer P, Abrahamsson H, Attvall S, Simren M. Measurement of gastric emptying by radiopaque markers in patients with diabetes: correlation with scintigraphy and upper gastrointestinal symptoms. Neurogastroenterol Motil 2013;25:e224-232.
3. Abell TL, Camilleri M, Donohoe K, Hasler WL, Lin HC, Maurer AH, McCallum RW, Nowak T, Nusynowitz ML, Parkman HP, Shreve P, Szarka LA, Snape WJ Jr, Ziessman HA; American Neurogastroenterology and Motility Society and the Society of Nuclear Medicine. Consensus recommendations for gastric emptying scintigraphy: a joint report of the American Neurogastroenterology and Motility Society and the Society of Nuclear Medicine. Am J Gastroenterol 2008;103:753-763.
4. Jones KL, Russo A, Stevens JE, Wishart JM, Berry MK, Horowitz M. Predictors of delayed gastric emptying in diabetes. Diabetes Care 2001;24:1264-1269.
5. Samsom M, Vermeijden JR, Smout AJ, Van Doorn E, Roelofs J, Van Dam PS, Martens EP, Eelkman-Rooda SJ, Van Berge-Henegouwen GP. Prevalence of delayed gastric emptying in diabetic patients and relationship to dyspeptic symptoms a prospective study in unselected diabetic patients. Diabetes Care 2003;26:3116-3122.
6. Koch KL, Hasler WL, Yates KP, Parkman HP, Pasricha PJ, Calles-Escandon J, Snape WJ, Abell TL, McCallum RW, Nguyen LA, Sarosiek I, Farrugia G, Tonascia J, Lee L, Miriel L, Hamilton F; NIDDK Gastroparesis Clinical Research Consortium (GpCRC). Baseline features and differences in 48 week clinical outcomes in patients with gastroparesis and type 1 vs type 2 diabetes. Neurogastroenterol Motil 2016;28:1001-1015.
7. Talley NJ, Vakil NB, Moayyedi P. American gastroenterological association technical review on the evaluation of dyspepsia. Gastroenterology 2005;129:1756-1780.
8. Griffith G, Owen G, Kirkman S, Shields R. Measurement of rate of gastric emptying using chromium-51. Lancet 1966;1:1244-1245.
9. Javadi H, Bayani H, Mogharrabi M, Pashazadeh AM, Semnani S, Semnani S, Nabipour I, Assadi M. Relation between clinical features and gastric emptying time in diabetic patients. Nucl Med Rev Cent East Eur 2015;18:3-6.
10. Kong M-F, Horowitz M, Jones KL, Wishart JM, Harding PE. Natural history of diabetic gastroparesis. Diabetes Care 1999;22:503-507.
11. Nowak TV, Johnson C, Kalbfleisch J, Roza A, Wood C, Weisbruch J, Soergel KH. Highly variable gastric emptying in patients with insulin dependent diabetes mellitus. Gut 1995;37:23-29.
12. Anudeep V, Vinod KV, Pandit N, Sharma VK, Dhanapathi H, Dutta TK, Sujiv A. Prevalence and predictors of delayed gastric emptying among Indian patients with long-standing type 2 diabetes mellitus. Indian J Gastroenterol 2016;35:385-392.
13. Soykan I, Sivri B, Sarosiek I, Kiernan B, Mccallum RW. Demography, clinical characteristics, psychological and abuse profiles, treatment, and long-term follow-up of patients with gastroparesis. Dig Dis Sci 1998;43:2398-2404.
14. Samsom M, Akkermans LM, Jebbink RJ, van Isselt H, vanBerge-Henegouwen GP, Smout AJ. Gastrointestinal motor mechanisms in hyperglycaemia induced delayed gastric emptying in type I diabetes mellitus. Gut 1997;40:641-646.
15. Annese V, Bassotti G, Caruso N, De Cosmo S, Gabbrielli A, Modoni S, Frusciante V, Andriulli A. Gastrointestinal motor dysfunction, symptoms, and neuropathy in noninsulin-dependent (type 2) diabetes mellitus. J Clin Gastroenterol 1999;29:171-177.
16. Hyett B, Martinez FJ, Gill BM, Mehra S, Lembo A, Kelly CP, Leffler DA. Delayed radionucleotide gastric emptying studies predict morbidity in diabetics with symptoms of gastroparesis. Gastroenterology 2009;137:445-452.
17. Tougas G, Eaker EY, Abell TL, Abrahamsson H, Boivin M, Chen J, Hocking MP, Quigley EM, Koch KL, Tokayer AZ, Stanghellini V, Chen Y, Huizinga JD, Rydén J, Bourgeois I, McCallum RW. Assessment of gastric emptying using a low fat meal: establishment of international control values. Am J Gastroenterol 2000;95:1456-1462.
18. Krishnan B, Babu S, Walker J, Walker AB, Pappachan JM. Gastrointestinal complications of diabetes mellitus. World J Diabetes 2013;4:51-63.
19. American Diabetes Association. Standards of medical care in diabetes-2014. Diabetes Care 2014;37(Suppl 1):S14-80.
20. Delgado-Aros S, Camilleri M, Cremonini F, Ferber I, Stephens D, Burton DD. Contributions of gastric volumes and gastric emptying to meal size and postmeal symptoms in functional dyspepsia. Gastroenterology 2004;127:1685-1694.
21. Lawal A, Barboi A, Krasnow A, Hellman R, Jaradeh S, Massey BT. Rapid gastric emptying is more common than gastroparesis in patients with autonomic dysfunction. Am J Gastroenterol 2007;102:618-623.
22. Lin HC, Van Citters GW, Zhao X-T, Waxman A. Fat intolerance depends on rapid gastric emptying. Dig Dis Sci 1999;44:330-335.
23. Schwartz JG, Green GM, Guan D, McMahan CA, Phillips WT. Rapid gastric emptying of a solid pancake meal in type II diabetic patients. Diabetes Care 1996;19:468-471.
24. Abell T, Starkebaum W, Abidi N. 32 How common is rapid gastric emptying in gastroparesis? Comparison of area under the curve, total gastric emptying and 1-hour values in patients and normal volunteers. Neurogastroenterol Motil 2006;18:490.

25. Bharucha AE, Camilleri M, Forstrom LA, Zinsmeister AR. Relationship between clinical features and gastric emptying disturbances in diabetes mellitus. Clin Endocrinol (Oxf) 2009;70:415-420.
26. Camilleri M, Bharucha AE, Farrugia G. Epidemiology, mechanisms, and management of diabetic gastroparesis. Clin Gastroenterol Hepatol 2011;9:5-12.
27. Bharucha AE, Kudva Y, Basu A, Camilleri M, Low PA, Vella A, Zinsmeister AR. Relationship between glycemic control and gastric emptying in poorly controlled type 2 diabetes. Clin Gastroenterol Hepatol 2015;13:466-476.e1
28. Sfarti C, Trifan A, Hutanasu C, Cojocariu C, Singeap A-M, Stanciu C. Prevalence of gastroparesis in type 1 diabetes mellitus and its relationship to dyspeptic symptoms. J Gastrointestin Liver Dis 2010;19:279-284.
29. Jung HK, Locke GR, Schleck CD, Zinsmeister AR, Szarka LA, Mullan B, Talley NJ. The incidence, prevalence, and outcomes of patients with gastroparesis in Olmsted County, Minnesota, from 1996 to 2006. Gastroenterology 2009;136:1225-1233.
30. Gustafsson RJ, Littorin B, Berntorp K, Frid A, Thorsson O, Olsson R, Ekberg O, Ohlsson B. Esophageal dysmotility is more common than gastroparesis in diabetes mellitus and is associated with retinopathy. Rev Diabet Stud 2011;8:268-275.
31. Feldman M, Schiller LR. Disorders of gastrointestinal motility associated with diabetes mellitus. Ann Intern Med 1983;98:378-384.
32. Bharucha AE. Epidemiology and natural history of gastroparesis. Gastroenterol Clin North Am 2015;44:9-19.

Original Article
Mol Imaging Radionucl Ther 2017;26:24-32 DOI:10.4274/mirt.30306

Correlation of Minimum Apparent Diffusion Coefficient and Maximum Standardized Uptake Value of the Primary Tumor with Clinicopathologic Characteristics in Endometrial Cancer

Endometrium Kanserinde Primer Tümöre Ait Minimum Görünen Difüzyon Katsayısı ve Maksimum Standardize Tutulum Değerleri ile Klinikopatolojik Özelliklerin İlişkisi

Evrim Sürer Budak[1], Tayfun Toptaş[2], Funda Aydın[3], Ali Ozan Öner[4], Can Çevikol[5], Tayup Şimşek[2]
[1]*Antalya Training and Research Hospital, Clinic of Nuclear Medicine, Antalya, Turkey*
[2]*Akdeniz University Faculty of Medicine, Department of Gynecologic Oncological Surgery, Antalya, Turkey*
[3]*Akdeniz University Faculty of Medicine, Department of Nuclear Medicine, Antalya, Turkey*
[4]*Afyon Kocatepe University Faculty of Medicine, Department of Nuclear Medicine, Afyonkarahisar, Turkey*
[5]*Akdeniz University Faculty of Medicine, Department of Radiology, Antalya, Turkey*

Abstract

Objective: To explore the correlation of the primary tumor's maximum standardized uptake value (SUV_{max}) and minimum apparent diffusion coefficient (ADC_{min}) with clinicopathologic features, and to determine their predictive power in endometrial cancer (EC).

Methods: A total of 45 patients who had undergone staging surgery after a preoperative evaluation with ^{18}F-fluorodeoxyglucose (FDG) positron emission tomography/computerized tomography (PET/CT) and diffusion-weighted magnetic resonance imaging (DW-MRI) were included in a prospective case-series study with planned data collection. Multiple linear regression analysis was used to determine the correlations between the study variables.

Results: The mean ADC_{min} and SUV_{max} values were determined as 0.72±0.22 and 16.54±8.73, respectively. A univariate analysis identified age, myometrial invasion (MI) and lymphovascular space involvement (LVSI) as the potential factors associated with ADC_{min} while it identified age, stage, tumor size, MI, LVSI and number of metastatic lymph nodes as the potential variables correlated to SUV_{max}. In multivariate analysis, on the other hand, MI was the only significant variable that correlated with ADC_{min} (p=0.007) and SUV_{max} (p=0.024). Deep MI was best predicted by an ADC_{min} cutoff value of ≤0.77 [93.7% sensitivity, 48.2% specificity, and 93.0% negative predictive value (NPV)] and SUV_{max} cutoff value of >20.5 (62.5% sensitivity, 86.2% specificity, and 81.0% NPV); however, the two diagnostic tests were not significantly different (p=0.266).

Conclusion: Among clinicopathologic features, only MI was independently correlated with SUV_{max} and ADC_{min}. However, the routine use of ^{18}F-FDG PET/CT or DW-MRI cannot be recommended at the moment due to less than ideal predictive performances of both parameters.

Keywords: Endometrial cancer, maximum standardized uptake value, minimum apparent diffusion coefficient

Address for Correspondence: Funda Aydın MD, Akdeniz University Faculty of Medicine, Department of Nuclear Medicine, Antalya, Turkey
Phone: +90 532 638 06 54 E-mail: afunda@akdeniz.edu.tr **Received:** 30.10.2016 **Accepted:** 09.01.2017

Öz

Amaç: Endometrium kanserinde (EK) primer tümörün maksimum standardize tutulum değeri (SUV_{maks}) ve minimum görünen difüzyon katsayısının (ADC_{min}) klinikopatolojik özellikler ile olan ilişkisini araştırmak ve bunların öngörü gücünü belirlemektir.

Yöntem: ^{18}F-fluorodeoksiglukoz (FDG) pozitron emisyon tomografisi/bilgisayarlı tomografi (PET/BT) ve difüzyon ağırlıklı-manyetik rezonans görüntüleme (DA-MRG) ile preoperatif değerlendirmeyi takiben evreleme cerrahisi yapılan toplamda 45 hasta, planlı veri toplama yapılan prospektif bir olgu serisine dahil edildiler. Çalışma verileri arasındaki ilişkiler çoklu doğrusal regresyon analizi ile araştırıldı.

Bulgular: Ortalama ADC_{min} ve SUV_{maks} sırasıyla 0,72±0,22 ve 16,54±8,73 olarak bulundu. Tek değişkenli analizde yaş, myometriyal invazyon (Mİ) ve lenfovasküler alan tutulumu (LVAT) ADC_{min} ile ilişkili potansiyel faktörler olarak bulunurken, yaş, evre, tümör büyüklüğü, LVAT ve metastatik lenf düğümlerinin sayısı SUV_{maks} ile ilişkili potansiyel değişkenler olarak tespit edildiler. Diğer taraftan, çok değişkenli analizde Mİ, ADC_{min} (p=0,007) ve SUV_{maks} (p=0,024) ile ilişkili tek anlamlı değişkendi. Derin Mİ en iyi, ≤0,77'lik [%93,7 duyarlılık, %48,2 özgüllük ve %93,0 negatif öngörü değeri (NPD)] bir ADC_{min} kesim değeri ve >20,5'lik (%62,5 duyarlılık, %86,2 özgüllük ve %81,0 NPD) bir SUV_{maks} kesim değeri ile öngörülebiliyordu. Ne var ki, her iki tanısal test birbirlerinden anlamlı şekilde farklı değildi (p=0,266).

Sonuç: Klinikopatolojik özelliklerden yalnızca Mİ bağımsız ve anlamlı şekilde SUV_{maks} ve ADC_{min} ile ilişkiliydi. Ne var ki, her iki parametrenin ideal olmayan öngörü performansları nedeniyle ^{18}F-FDG PET/BT veya DA-MRG'nin rutin kullanımı şu noktada önerilemez.

Anahtar kelimeler: Endometrium kanseri, maksimum standardize tutulum değeri, minimum görünen difüzyon katsayısı

Introduction

Endometrial cancer (EC) is the most common gynecologic malignancy in developed countries (1). The majority of patients present with disease limited to the uterus at the time of diagnosis, which leads to a generally high survival rate (2). Unfortunately, it has been reported that deaths from EC have increased over the past two decades, probably due to underestimation of actual tumor spread and increased rate of high-risk histology (3).

EC is staged surgically using the International Federation of Gynecology and Obstetrics (FIGO) and American Joint Committee on Cancer staging systems (4,5). While total hysterectomy and bilateral salpingo-oophorectomy (TH/BSO) is the mainstay treatment of uterine-confined disease, a comprehensive staging surgery including systematic lymphadenectomy allows for assessing the true extent of disease and the need for adjuvant therapy (6). Nevertheless, a systematic lymphadenectomy leads to a doubling of the complication rate (7). Besides, there are two randomized controlled trials demonstrating no survival benefit for lymphadenectomy especially in patients with presumed uterine-confined disease (8,9).

According to the widely agreed view, a systematic lymphadenectomy may be omitted in selected patients considered to be at low-risk for extrauterine spread, without an unfavorable impact on disease prognosis. The most used criteria for defining low-risk patients are based on preoperative and intraoperative pathologic findings including well or moderately differentiated histology, tumor size less than 2 cm, and myometrial invasion (MI) less than 50% (10). However, accurate identification of this group of patients may be somewhat problematic due to the variability in tumor grade and depth of MI on final pathologic examination (11).

The role of preoperative imaging for predicting tumor characteristics in patients with EC has been established by several studies, using different modalities (12,13,14). Diffusion-weighted magnetic resonance imaging (DW-MRI) and ^{18}F-fluorodeoxyglucose (FDG) positron emission tomography combined with computed tomography (PET/CT) are the two imaging techniques that stood out from the others with their capability to provide metabolic and functional information regarding tumor tissue properties, in addition to anatomic information. Minimum apparent diffusion coefficient value (ADC_{min}) derived from DW-MRI and maximum standardized uptake value (SUV_{max}) derived from ^{18}F-FDG PET/CT are semi-quantitative imaging biomarkers which have been suggested to be of value in estimation of tumor behavior, as well as disease prognosis (13,14). However, the clinical data regarding direct comparison of both biomarkers in preoperative evaluation of EC patients are sparse, and the routine use of them remains controversial.

In the current study, we aimed to investigate relationships of SUV_{max} and ADC_{min} of the primary tumor to clinicopathologic features, and to compare their predictive ability in patients with EC.

Materials and Methods

This prospective case-series with planned data collection enrolled consecutive patients with EC, who underwent primary staging surgery following a preoperative evaluation with ^{18}F-FDG PET/CT and DW-MRI between May 2012 and December 2014. All imaging studies were performed

within two weeks before the day of surgery, and all patients provided written informed consent.

Radiologic, pathologic and clinical data including age at surgery, ADC_{min} and SUV_{max} of the primary tumor, date and extent of the surgical procedure, number of lymph nodes (LNs) removed, stage of the disease, tumor histotype, tumor grade, tumor size, depth of myometrial invasion, lymphovascular space involvement (LVSI), cervical invasion, adnexal invasion, LN involvement, number of metastatic LNs, adjuvant therapy, disease status after primary therapy, disease recurrence, survival status, and the date of the last follow-up were recorded for all patients, following the The study were approved by the Akdeniz University of Local Ethics Committee (Protocol number: 23.12.2015; 386).

Patients with uterine sarcoma, primary synchronous malignancy, insufficient data, or that received radiotherapy, chemotherapy, or hormonal therapy as primary or neoadjuvant therapy were excluded.

Positron Emission Tomography/Computerized Tomography Technique and Image Analysis

Patients were requested to fast for at least six hours before imaging, and a venous blood glucose level below 200 mg/dL was ensured. An oral contrast agent was administered to all patients prior to scanning. In order to facilitate urinary excretion, they were asked to drink 500 ml of water and to void just before the acquisition. A whole body acquisition using integrated PET/CT scanner (Biograph 16 LSO; Siemens, Erlangen, Germany) was performed 45 to 60 minutes after intravenous administration of ^{18}F-FDG (0.16 mCi/kg). A CT scan (slice thickness, 3 mm; peak voltage, 120 kV; tube current, 110 mA/s) was performed, and used for anatomical localization and calculation of attenuation correction. The PET data were acquired from the vertex to the upper thigh, and the acquisition time for PET was three minutes per bed position. Attenuation-corrected PET, CT and fusion PET/CT images were interpreted by experienced nuclear medicine specialists. The SUV_{max} of the primary tumor was measured with a region of interest (ROI) technique. The measurements were performed in correlation with CT images while limiting the area of activity precisely and minimalizing the partial volume effect. Because of the close location to the bladder, it was important to separate the primary tumor and bladder activity in order to avoid incorrect measurements. From ROIs delineated on successive sections, the greatest SUV_{max} was noted. SUV_{max} values were automatically provided by a computer-assisted software program and they were calculated using the standard formula.

Diffusion-Weighted Magnetic Resonance Imaging Technique and Image Analysis

MRI examinations were performed using a 1.5 Tesla MRI scanner (Avanto; Siemens, Erlangen, Germany). The imaging protocol included: T2-weighted (T2W) fast-spin-echo (FSE) imaging in the sagittal and axial planes; FSE T1-weighted (T1W) imaging in the axial plane; fat-saturated FSE T2W imaging in the coronal plane; and DW imaging in the same sagittal plane (repetition time, 6100 msec; echo time, 88 msec; flip angle, 90°; field of view, 241x329 mm; slice thickness, 4 mm; interslice gap, 0.8 mm; matrix, 240x328; number of excitations, 5). The b-values of the diffusion sensitizing gradient were 50, 400 and 800 sec/mm^2. Post-contrast fat-saturated T1W sagittal and axial images were also obtained. Assessment of the images was performed by an experienced radiologist. The presence and the size of the endometrial lesion and its signal intensity relative to that of the adjacent myometrium were evaluated on T2W and DW images with a b-value of 800 sec/mm^2. ADC maps were generated automatically, and the measurements were performed by placing a ROI over the endometrial lesion with paying attention not to include areas of necrosis.

Surgical Procedures, Adjuvant Therapy and Follow-up

All patients underwent a staging surgery including at least TH/BSO, pelvic lymphadenectomy, omental biopsy, and peritoneal cytology. The pelvic lymphadenectomy consisted of complete removal of the LNs from the internal iliac, external iliac, obturatory and common iliac regions. A paraaortic LN dissection up to the renal vessels was added to the staging procedure in the presence of any of the followings:

1) Non-endometrioid or grade 2-3 endometrioid histology on preoperative biopsy,

2) MI greater than 50% on intraoperative frozen-section examination. All procedures were performed by two experienced gynecologic oncologists.

Tumor grading was conducted according to that of the World Health Organization (15), and staging was classified using the $FIGO_{2009}$ system (4). Non-endometrioid histotypes were considered grade 3 tumors. According to institutional practice, age (>50 yr), positive LVSI, tumor size (>2 cm) and lower uterine segment involvement were considered potential adverse risk factors. Adjuvant therapy strategy was as follows: Observation for stage 1A-grade 1 disease with no adverse risk factors; brachytherapy alone for stage 1A-grade 1 disease with one of the risk factors, stage 1A-grade 2-3 disease with no risk factors and stage 1B-grade 1-2 disease with no risk factors; external beam pelvic radiotherapy for stage 1A-grade 2-3 disease with one of the risk factors, stage 1B-grade 1-2 disease with one of the risk factors, stage 1B-grade 3 disease and stage 2 disease; chemotherapy plus external beam radiotherapy for stage 3 disease; and chemotherapy alone for stage 4B disease. The chemotherapy regimen included six cycles of paclitaxel 175 mg/m^2 plus carboplatin dosed at an area under the curve (AUC) of 5 to 6.

The surveillance practice was to follow-up patients who achieved a complete clinical remission after primary

therapy every three months for two years, every six months for the next three years, and then annually. Recurrence was defined as any documented relapse of the tumor, either systemically or locally, after a disease-free interval of more than three months.

Statistical Analysis

All analyses were performed using IBM SPSS Statistics 20 software (SPSS/IBM, Chicago, IL, USA). Binary variables were reported as counts and percentages; continuous variables were expressed as mean, standard deviation, median, and range. A multiple linear regression analysis was performed to demonstrate correlation among variables of interest. All variables were separately evaluated by a univariate analysis using the Mann-Whitney U test and Spearman's rank correlation coefficients (r value). Variables with a p value <0.05 in the univariate analysis were selected and included in the multivariate analysis.

To define the diagnostic threshold values of ADC_{min} and SUV_{max}, a receiver operating characteristic (ROC) curve analysis was performed by plotting every possible cutoff score's sensitivity on the y-axis against 1-specificity on the x-axis. The Youden index was calculated to choose the optimal cutoff values (16). For the ROC curve, the point with the largest sum of specificity and sensitivity was chosen as a threshold. In presenting the results, sensitivity, specificity, positive predictive value (PPV), and negative predictive value (NPV) were all reported. The AUCs of ROC curves and their 95% confidence intervals (CI) were compared using the method of DeLong et al. (17).

Results

A total of 45 patients were enrolled in the analysis. Table 1 presents the characteristics of patients. The mean age was 57.11±11.12 years. The mean ADC_{min} and SUV_{max} of the primary tumor were 0.72±0.22 and 16.54±8.73, respectively. The majority of patients (73.3%) had combined pelvic and paraaortic lymphadenectomy. The median number of pelvic LNs removed, paraaortic LNs removed, and total LNs removed (pelvic and paraaortic) were 28, 23, and 44, respectively. The distribution of the surgical stages of patients was as follows; stage 1A 21 patients (46.7%), stage 1B seven patients (15.6%), stage 2 six patients (13.3%), stage 3A three patients (6.7%), stage 3C six patients (13.3%), and stage 4B two patients (4.4%). Most of the patients (77.8%) had endometrioid histology. Deep MI (≥½) was observed in 35.5% of the patients, LVSI in 28.9%, cervical invasion in 31.1%, adnexal invasion in 13.3%, and LN metastasis in 17.8%. During the median follow-up period of 20 months (range, 7.5-30.5 months), six patients (13.3%) experienced disease recurrence with a median time to recurrence of 6 months (range, 4.5-15.5). Three examples of such cases are shown in Figure 1, 2, 3.

The results of multiple linear regression analysis were summarized in Table 2. In univariate analysis, while

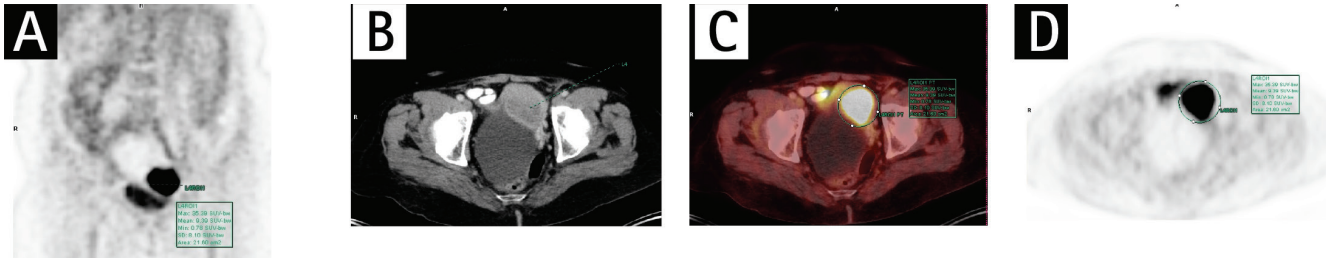

Figure 1. Maximum standardized uptake value of the primary tumor was measured 35,39. Endometrioid type endometrial carcinoma (grade 2, International Federation of Gynecology and Obstetrics stage 3A). A) Maximum intensity projection image. B) Transaxial computed tomography image. C) Transaxial positron emission tomography+computed tomography fusion image. D) Transaxial positron emission tomography image of the primary tumor

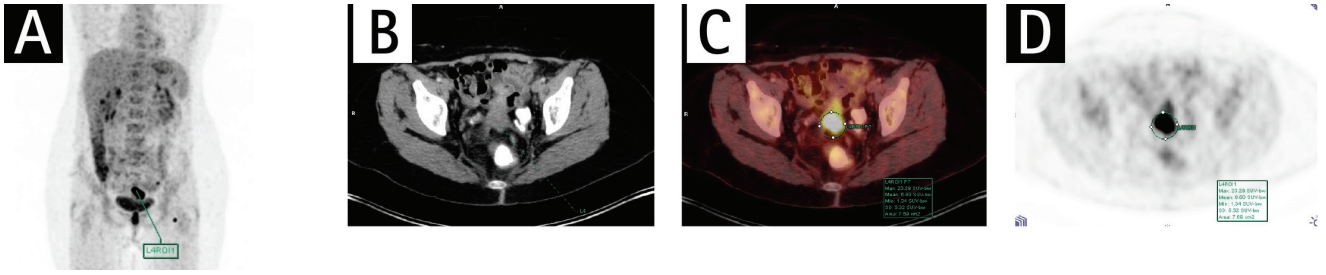

Figure 2. Maximum standardized uptake value of the primary tumor was measured 23,29. Non-endometrioid type (serous) endometrial carcinoma (grade 3, International Federation of Gynecology and Obstetrics stage 3C). A) Maximum intensity projection image. B) Transaxial computed tomography image. C) Transaxial positron emission tomography+computed tomography fusion image. D) Transaxial positron emission tomography image of the primary tumor

Table 1. Characteristics of patients

Variables	Values
Age at surgery, mean±SD, [median (range)], y	57.11±11.12, [56 (27-84)]
ADC_{min} of the primary tumor, mean±SD, [median (range)]	0.72±0.22, [0.65 (0.41-1.24)]
SUV_{max} of the primary tumor, mean±SD, [median (range)]	16.54±8.73, 15 [(5-35.39)]
Lymphadenectomy, n (%)	
Pelvic alone	12 (26.7)
Pelvic and paraaortic	33 (73.3)
No. of pelvic LNs removed, mean±SD, [median (range)]	27.25±7.74, [28 (11-49)]
No. of paraaortic LNs removed, mean±SD, [median (range)]	23.76±10.38, [23 (10-43)]
No. of total LNs removed, mean±SD, [median (range)]	44.98±16.25, [44 (16-79)]
FIGO stage, n (%)	
1A	21 (46.7)
1B	7 (15.6)
2	6 (13.3)
3A	3 (6.7)
3C	6 (13.3)
4B	2 (4.4)
Histological type, n (%)	
Endometrioid	35 (77.8)
Non-endometrioid	10 (22.2)
Grade, n (%)	
1	22 (48.9)
2	11 (24.4)
3	12 (26.7)
Tumor size, mean±SD, [median (range)], cm	3.54±1.92, [3 (0.35-8.30)]
Deep myometrial invasion (≥1/2), n (%)	16 (35.5)
Lymphovascular space invasion, n (%)	13 (28.9)
Cervical invasion, n (%)	14 (31.1)
Adnexal invasion, n (%)	6 (13.3)
LN metastasis, n (%)	8 (17.8)
No. of metastatic LNs, mean±SD, [median (range)]	1±2.61, [0 (0-11)]
Adjuvant therapy, n (%)	
No adjuvant	15 (33.3)
Brachytherapy alone	8 (17.8)
External beam radiotherapy +/- brachytherapy	11 (24.4)
Chemotherapy plus external beam radiotherapy +/- brachytherapy	9 (20.0)
Chemotherapy alone	2 (4.4)
Recurrence, n (%)	6 (13.3)
Median time to recurrence (95% CI), months	6 (4.5-15.5)
Survival status, n (%)	
Alive with no evidence of disease	39 (86.6)
Alive with disease	3 (6.7)
Dead of disease	3 (6.7)
Median follow-up time (95 %CI), months	20.5 (7.5-30.5)

SD: Standard deviation, ADC_{min}: Minimum apparent diffusion coefficient, SUV_{max}: Maximum standardized uptake value, LN: Lymph node, FIGO: International Federation of Gynecology and Obstetrics, CI: Confidential interval

Table 2. Univariate and multivariate linear regression analysis of factors associated with minimum apparent diffusion coefficient and maximum standardized uptake value of the primary tumor

Variables	Univariate analysis		Multiple linear regression analysis		
	r/U	p	Coefficients	95% CI	p
Age					
ADC_{min}	-0.405	**0.006**	-0.105	-0.361 to 0.152	0.416
SUV_{max}	0.340	**0.022**	0.136	0.122 to 0.394	0.293
FIGO stage					
ADC_{min}	-0.257	0.088	-	-	-
SUV_{max}	0.436	**0.003**	2.479	2.217 to 3.176	0.721
Non-endometrioid histology					
ADC_{min}	103.5	0.051	-	-	-
SUV_{max}	129.0	0.209	-	-	-
Grade					
ADC_{min}	-0.224	0.139	-	-	-
SUV_{max}	0.272	0.071	-	-	-
Tumor size					
ADC_{min}	-0.230	0.128	-	-	-
SUV_{max}	0.488	**0.001**	1.269	-0.226 to 2.765	0.094
Deep myoinvasion					
ADC_{min}	134.5	**0.021**	9.457	2.693 to 16.221	**0.007**
SUV_{max}	87.0	**0.001**	8.494	1.178 to 15.810	**0.024**
Lymphovascular space invasion					
ADC_{min}	110.5	**0.015**	2.758	-3.254 to 8.769	0.360
SUV_{max}	101.0	**0.007**	2.056	-4.515 to 8.628	0.530
Cervical invasion					
ADC_{min}	193.0	0.556	-	-	-
SUV_{max}	153.5	0.119	-	-	-
Adnexal invasion					
ADC_{min}	108.5	0.776	-	-	-
SUV_{max}	55.5	0.040	-	-	-
Lymph node metastasis					
ADC_{min}	109.0	0.247	-	-	-
SUV_{max}	84.0	0.057	-	-	-
No. of metastatic lymph nodes					
ADC_{min}	-0.171	0.262	-	-	-
SUV_{max}	0.295	**0.049**	0.502	-0.868 to 1.871	0.463
Recurrence					
ADC_{min}	90.5	0.376	-	-	-
SUV_{max}	87.0	0.316	-	-	-
Survival					
ADC_{min}	41.0	0.392	-	-	-
SUV_{max}	49.0	0.643	-	-	-

ADC_{min}: Minimum apparent diffusion coefficient, SUV_{max}: Maximum standardized uptake value, r; Spearman's rho correlation coefficient, U; Mann Whitney U test statistic, CI: Confidential interval, FIGO: International Federation of Gynecology and Obstetrics. Boldface indicates statistical significance ($p<0.05$)

the potential factors associated with ADC_{min} were age (p=0.006), deep MI (p=0.021), and LVSI (p=0.015); the potential factors associated with SUV_{max} were age (p=0.022), stage (p=0.003), tumor size (p=0.001), deep MI (p=0.001), LVSI (p=0.007) and number of metastatic LNs (p=0.049). However, only the deep myometrial invasion remained to be an independent variable associated with ADC_{min} (p=0.007) as well as SUV_{max} (p=0.024) after adjustment for other confounders in multivariate analysis. There was a significant but moderate and negative correlation between the ADC_{min} and SUV_{max} (r=-0.518, p<0.001).

Optimal cutoff values of ADC_{min} and SUV_{max} for predicting deep MI were found to be ≤0.77 (93.7% sensitivity, 48.2% specificity, 50.0% PPV, and 93.0% NPV) and >20.5 (62.5% sensitivity, 86.2% specificity, 71.0% PPV, and 81.0% NPV), respectively; although the comparison of two diagnostic tests revealed no statistical significance [AUC-ADC_{min}=0.812 (95% CI: 0.668-0.913), AUC-SUV_{max}=0.710 (95% CI: 0.556-0.836); p=0.266], (Figure 4). Moreover, the combination of two biomarkers (ADC_{min} ≤0.77 and SUV_{max} >20.5) failed to improve the diagnostic accuracy (56% sensitivity, 86.2% specificity, 69.2% PPV, and 78.1% NPV).

Discussion

In the current study, we investigated the correlation between various clinicopathologic features and SUV_{max} and ADC_{min} of the primary tumor in patients with EC. The study provides evidence that the depth of MI is the sole clinicopathologic feature independently associated with SUV_{max} as well as ADC_{min}. The combination of one of these biomarkers with intraoperative frozen-section examination may offer better prediction of deep myometrial invasion, and thereby selection of patients for an extensive surgery.

Several studies have evaluated the predictors of extrauterine tumor spread in EC patients, and most studies reported age, tumor grade, myometrial invasion, LVSI, and tumor histology as potential risk factors (6). With respect to these factors, there are various suggested risk assessment models in the current literature (10,18,19,20); however, the majority of these models are based on the results of preoperative biopsy and intraoperative frozen-section examination, which have been shown to be prone to underestimation of tumor grade and MI in 15% to 20% of patients (11,21). Although a comprehensive staging surgery still remains the most reliable approach for determining extrauterine tumor spread, it is evident that there is a need to develop novel preoperative risk assessment strategies to avoid systematic overtreatment in patients with EC.

Emerging data indicates that ADC_{min} value derived from DW-MRI and SUV_{max} derived from ^{18}F-FDG PET/CT may have a potential role in preoperative assessment of patients with EC (14). DW-MRI can visualize the microscopic movement of extracellular water protons, which allows discrimination of tissues according to their cellularity and fluid diffusivity (22). The diffusivity can be quantified by calculating the ADC_{min} value. SUV_{max} is a measure of glucose metabolism rate, which is also correlated with the cellularity of the tissue. When compared to benign lesions, malignant tumors show higher cellularity, and thereby lower ADC_{min} and higher SUV_{max} values (23,24). Although various studies suggested a possible relationship between the SUV_{max} and ADC_{min} of the primary tumor and tumor characteristics such as grade, myometrial invasion, stage, recurrence, and survival (13,14,25,26,27), uncertainty remains regarding the true magnitude and structure of these relationships as there are limited data that compare both parameters in the same study group.

In the single study investigating the relationships of SUV_{max} and ADC_{min} obtained from a preoperative evaluation with ^{18}F-FDG PET/CT and DW-MRI to clinicopathologic characteristics in patients with EC, Nakamura et al. (14) reported the data of 131 patients, with a median time to follow-up of ~20 months. The authors found that low ADC_{min} values were associated with stage 3 to 4 disease (p<0.001), grade 3 tumor (p<0.001), deep MI (p=0.002), cervical involvement (p=0.001), LN metastasis (p=0.018), LVSI (p<0.001), and large tumor size (p<0.001). Although there was a significant and inverse correlation with ADC_{min} and SUV_{max} (r=-0.677, p<0.001), the SUV_{max} of the primary tumor was associated with disease-free and

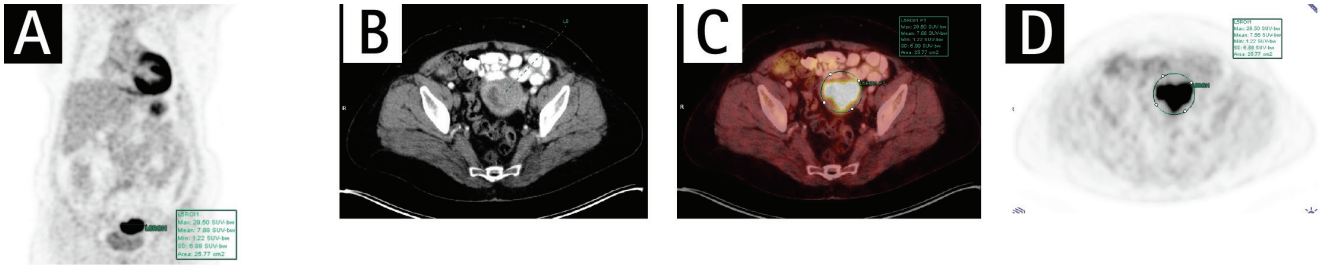

Figure 3. Maximum standardized uptake value of the primary tumor was measured 29,50. Endometrioid type endometrial carcinoma (grade 1, International Federation of Gynecology and Obstetrics stage 2). A) Maximum intensity projection image. B) Transaxial computed tomography image. C) Transaxial positron emission tomography+computed tomography fusion image. D) Transaxial positron emission tomography image of the primary tumor

overall survival rates while ADC_{min} was not. The other study of interest relating to this issue in the literature was reported by Shih et al. (28). Although the authors used the data obtained from an integrated PET/MRI system, they similarly found a significant inverse correlation between the SUV_{max} and ADC_{min} of the primary tumor in 36 patients with EC (r=-0.53, p=0.001). In that study, both SUV_{max} and ADC_{min} were significantly associated with many prognostic factors; however, unlike the study by Nakamura et al. (14), the authors found no significant association between SUV_{max} and tumor grade, as well as between ADC_{min} and myometrial invasion, LVSI, and LN metastasis.

A significant inverse correlation between SUV_{max} and ADC_{min} was also evident in our study. Contrary to previous studies, we observed that the SUV_{max} and ADC_{min} values were only associated with the depth of MI among all clinicopathologic factors. Both imaging biomarkers were comparable in their abilities to estimate deep myometrial invasion. However, combining these two biomarkers resulted in a decrease in the specificity rate and NPV. It is possible that the discrepancy between our findings and those of other researchers may be due to the differences in statistics used and sample size. While the previous studies assessed the relationships between variables by using correlational statistics only, we applied a multiple linear regression analysis to determine the independent effect of each variable. This method provided controlling for the potential confounding variables.

As with all studies, the analyses presented in this paper are not without limitations. Single-institutional cohort studies, such as this one, are inherently susceptible to referral and selection bias affecting the generalizability of findings. The small sample size of our study might have caused a sampling error, limiting the power in detecting associations. A relatively short median follow-up time and lack of analysis of other potential confounders, such as comorbidities, anthropometric measurements, smoking, and biochemical markers could also be considered potential limitations.

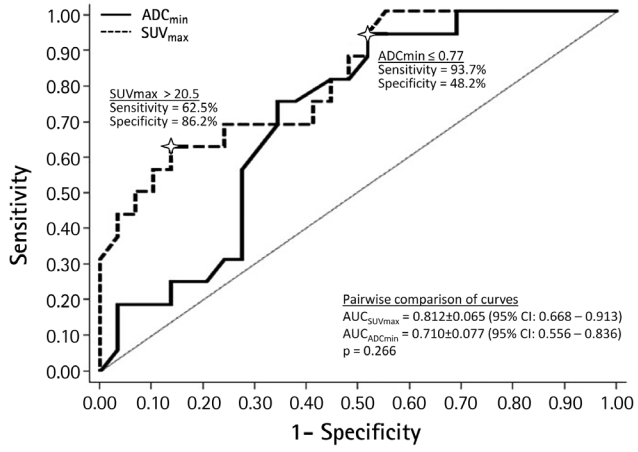

Figure 4. Receiver operating characteristic curve analysis for the diagnostic value of minimum apparent diffusion coefficient and maximum standardized uptake value of the primary tumor in predicting deep myometrial invasion

ADC_{min}: Minimum apparent diffusion coefficient, SUV_{max}: Maximum standardized uptake value, CI: Confidential interval

Conclusion

In conclusion, based on our results, SUV_{max} of the primary tumor derived from ^{18}F-FDG PET/CT and ADC_{min} of the primary tumor derived from DW-MRI may have a role in predicting deep MI with similar diagnostic accuracies. However, the predictive performances of both imaging biomarkers do not seem high enough to support their routine use. Furthermore, the combined use of the two tests may lead to worsening of the predictive accuracies of each biomarker. Trials with a larger cohort of patients and longer follow-up data are needed for further validation of these biomarkers.

Acknowledgments

The authors received no financial support for the research, authorship, and/or publication of this article.

The authors declare that they have no potential conflicts of interest with respect to the research, authorship, and/or publication of this article.

Ethics

Ethics Committee Approval: The study were approved by the Akdeniz University of Local Ethics Committee (Protocol number: 23.12.2015; 386), Informed Consent: Consent form was filled out by all participants.

Peer-review: Externally peer-reviewed.

Authorship Contributions

Surgical and Medical Practices: Tayfun Toptaş, Tayup Şimşek, Concept: Funda Aydın, Evrim Sürer Budak, Tayfun Toptaş, Ali Ozan Öner, Design: Funda Aydın, Evrim Sürer Budak, Tayfun Toptaş, Data Collection or Processing: Evrim Sürer Budak, Tayfun Toptaş, Ali Ozan Öner, Analysis or Interpretation: Evrim Sürer Budak, Tayfun Toptaş, Funda Aydın, Can Çevikol, Literature Search: Funda Aydın, Evrim Sürer Budak, Tayfun Toptaş, Writing: Funda Aydın, Evrim Sürer Budak, Tayfun Toptaş.

Conflict of Interest: No conflict of interest was declared by the authors.

Financial Disclosure: The authors declared that this study received no financial support.

References

1. GLOBOCAN 2012: Estimated cancer incidence, mortality and prevalence worldwide in 2012: International Agency for Research on Cancer. Available at: http://globocan.iarc.fr. Accessed 02.02.2016.
2. Siegel R, Ma J, Zou Z, Jemal A. Cancer statistics, 2014. CA Cancer J Clin 2014;64:9-29.

3. Ueda SM, Kapp DS, Cheung MK, Shin JY, Osann K, Husain A, Teng NN, Berek JS, Chan JK. Trends in demographic and clinical characteristics in women diagnosed with corpus cancer and their potential impact on the increasing number of deaths. Am J Obstet Gynecol 2008;198:218.
4. Creasman W. Revised FIGO staging for carcinoma of the endometrium. Int J Gynaecol Obstet 2009;105:109.
5. Edge SB, Byrd DR, Compton CC. AJCC Cancer staging manual, 7th ed. New York, Springer 2010.
6. NCCN Clinical Practice Guidelines in Oncology (NCCN Guidelines). Uterine Neoplasms, Version II. 2016. Available at: http://www.nccn.org. Accessed 02.02.2016.
7. Dowdy SC, Borah BJ, Bakkum-Gamez JN, Kumar S, Weaver AL, McGree ME, Haas LR, Cliby WA, Podratz KC. Factors predictive of postoperative morbidity and cost in patients with endometrial cancer. Obstet Gynecol 2012;120:1419-1427.
8. Benedetti Panici P, Basile S, Maneschi F, Alberto Lissoni A, Signorelli M, Scambia G, Angioli R, Tateo S, Mangili G, Katsaros D, Garozzo G, Campagnutta E, Donadello N, Greggi S, Melpignano M, Raspagliesi F, Ragni N, Cormio G, Grassi R, Franchi M, Giannarelli D, Fossati R, Torri V, Amoroso M, Crocè C, Mangioni C. Systematic pelvic lymphadenectomy vs. no lymphadenectomy in early-stage endometrial carcinoma: randomized clinical trial. J Natl Cancer Inst 2008;100:1707-1716.
9. ASTEC study group, Kitchener H, Swart AM, Qian Q, Amos C, Parmar MK. Efficacy of systematic pelvic lymphadenectomy in endometrial cancer (MRC ASTEC trial): a randomised study. Lancet 2009;373:125-136.
10. Milam MR, Java J, Walker JL, Metzinger DS, Parker LP, Coleman RL; Gynecologic Oncology Group. Nodal metastasis risk in endometrioid endometrial cancer. Obstet Gynecol 2012;119:286-292.
11. Frumovitz M, Singh DK, Meyer L, Smith DH, Wertheim I, Resnik E, Bodurka DC. Predictors of final histology in patients with endometrial cancer. Gynecol Oncol 2004;95:463-468.
12. Antonsen SL, Jensen LN, Loft A, Berthelsen AK, Costa J, Tabor A, Qvist I, Hansen MR, Fisker R, Andersen ES, Sperling L, Nielsen AL, Asmussen J, Høgdall E, Fagö-Olsen CL, Christensen IJ, Nedergaard L, Jochumsen K, Høgdall C. MRI, PET/CT and ultrasound in the preoperative staging of endometrial cancer - a multicenter prospective comparative study. Gynecol Oncol 2013;128:300-308.
13. Ghooshkhanei H, Treglia G, Sabouri G, Davoodi R, Sadeghi R. Risk stratification and prognosis determination using (18)F-FDG PET imaging in endometrial cancer patients: a systematic review and meta-analysis. Gynecol Oncol 2014;132:669-676.
14. Nakamura K, Joja I, Fukushima C, Haruma T, Hayashi C, Kusumoto T, Seki N, Hongo A, Hiramatsu Y. The preoperative SUVmax is superior to ADCmin of the primary tumour as a predictor of disease recurrence and survival in patients with endometrial cancer. Eur J Nucl Med Mol Imaging 2013;40:52-60.
15. Silverberg SG, Kurman RJ, Nogales F, Mutter GL, Kubik-Huch RA, Tavassoli FA. Tumours of the uterine corpus. In: Tavassolli FA, Devilee P (eds). World Health Organization Classification of Tumours, Pathology & Genetics, Tumours of the Breast and Female Genital Organs by The International Agency for Research on Cancer (IARC). 3th ed. Geneva, Switzerland, World Health Organization/IARC, 2003;222-223.
16. Hughes G. Youden's index and the weight of evidence. Methods Inf Med 2015;54:198-199.
17. DeLong ER, DeLong DM, Clarke-Pearson DL. Comparing the areas under two or more correlated receiver operating characteristic curves: a nonparametric approach. Biometrics 1988;44:837-845.
18. Mariani A, Webb MJ, Keeney GL, Haddock MG, Calori G, Podratz KC. Low-risk corpus cancer: is lymphadenectomy or radiotherapy necessary? Am J Obstet Gynecol 2000;182:1506-1519.
19. Vargas R, Rauh-Hain JA, Clemmer J, Clark RM, Goodman A, Growdon WB, Schorge JO, Del Carmen MG, Horowitz NS, Boruta DM. Tumor size, depth of invasion, and histologic grade as prognostic factors of lymph node involvement in endometrial cancer: a SEER analysis. Gynecol Oncol 2014;133:216-220.
20. Todo Y, Sakuragi N, Nishida R, Yamada T, Ebina Y, Yamamoto R, Fujimoto S. Combined use of magnetic resonance imaging, CA 125 assay, histologic type, and histologic grade in the prediction of lymph node metastasis in endometrial carcinoma. Am J Obstet Gynecol 2003;188:1265-1272.
21. Daniel AG, Peters WA. Accuracy of office and operating room curettage in the grading of endometrial carcinoma. Obstet Gynecol 1988;71:612-614.
22. Bammer R. Basic principles of diffusion-weighted imaging. Eur J Radiol 2003;45:169-184.
23. Takeuchi M, Matsuzaki K, Nishitani H. Diffusion-weighted magnetic resonance imaging of endometrial cancer: differentiation from benign endometrial lesions and preoperative assessment of myometrial invasion. Acta Radiol 2009;50:947-953.
24. Hickeson M, Yun M, Matthies A, Zhuang H, Adam LE, Lacorte L, Alavi A. Use of a corrected standardized uptake value based on the lesion size on CT permits accurate characterization of lung nodules on FDG-PET. Eur J Nucl Med Mol Imaging 2002;29:1639-1647.
25. Nakamura K, Imafuku N, Nishida T, Niwa I, Joja I, Hongo A, Kodama J, Hiramatsu Y. Measurement of the minimum apparent diffusion coefficient (ADCmin) of the primary tumor and CA125 are predictive of disease recurrence for patients with endometrial cancer. Gynecol Oncol 2012;124:335-339.
26. Inoue C, Fujii S, Kaneda S, Fukunaga T, Kaminou T, Kigawa J, Harada T, Ogawa T. Correlation of apparent diffusion coefficient value with prognostic parameters of endometrioid carcinoma. J Magn Reson Imaging 2015;41:213-219.
27. Woo S, Cho JY, Kim SY, Kim SH. Histogram analysis of apparent diffusion coefficient map of diffusion-weighted MRI in endometrial cancer: a preliminary correlation study with histological grade. Acta Radiol 2014;55:1270-1277.
28. Shih IL, Yen RF, Chen CA, Chen BB, Wei SY, Chang WC, Sheu BC, Cheng WF, Tseng YH, Chen XJ, Chen CH, Wei LH, Chiang YC, Torng PL, Yen ML, Shih TT. Standardized uptake value and apparent diffusion coefficient of endometrial cancer evaluated with integrated whole-body PET/MR: Correlation with pathological prognostic factors. J Magn Reson Imaging 2015;42:1723-1732.

Original Article
Mol Imaging Radionucl Ther 2017;26:33-37 DOI:10.4274/mirt.29484

The Efficacy of Yttrium-90 Radiosynovectomy in Patients with Camptodactyly-Arthropathy-Coxa Vara-Pericarditis Syndrome

Yttrium-90 Radyosinovektominin Kamptodaktili-Artropati-Koksa Vara-Perikardit Sendromlu Hastalarda Etkinliği

Sulaiman Mohammed Al-Mayouf[1], Nora Almutairi[1], Khalid Alismail[2]
[1]*King Faisal Specialist Hospital and Research Center, Clinic of Pediatric Rheumatology, Riyadh, Saudi Arabia*
[2]*King Faisal Specialist Hospital and Research Center, Clinic of Musculoskeletal Radiology, Riyadh, Saudi Arabia*

Abstract

Objective: Camptodactyly-arthropathy-coxa-vara-pericarditis (CACP) syndrome is an autosomal recessive disorder caused by mutations in *PRG4* gene that encodes for proteoglycan 4, the main lubricant for joints and tendon surfaces. It is a non-inflammatory arthropathy, characterized by joint effusions and synovial hypertrophy. So far, there is no effective treatment for this disorder. To evaluate the effectiveness of yttrium-90 radiosynovectomy in arthropathy of patients with CACP syndrome.

Methods: Consecutive patients with CACP syndrome were prospectively evaluated at the enrollment and 3 months after the right knee injection with yttrium-90. The outcome variables were patient/parent and physician's global assessment measured by a 3-point scale, right knee swelling and range of motion on a 3-point scale, in addition to magnetic resonance imaging (MRI) assessment of the right knee for bone, cartilage, fluid, synovial hypertrophy and soft tissue changes.

Results: Six (three boys, three girls) patients with a mean age of 12 years and mean follow-up duration of 8.5 years completed a single right knee intra-articular yttrium-90 injection with 5 mCi. The procedure was well tolerated without adverse events apart from mild and transient joint pain in two patients. There was a minimal radioisotope leakage to soft tissue in two patients. During the 3-month follow-up interval, there was no improvement in the outcome variables. Patients and parents did not notice favorable therapeutic effects and global physician assessment was unsatisfactory. There was no difference in knee joint swelling or range of motion. Furthermore, MRI findings were unchanged. However, there was a minimal increase in synovial fluid post injection.

Conclusion: Yttrium-90 radiosynovectomy seems to be a safe and well tolerated procedure, however, it did not show a beneficial therapeutic effect in arthropathy of CACP syndrome with the given dosage and interval. Studies including a larger number of patients and probably repeated injections are needed to derive satisfactory results about the effectiveness of yttrium-90 in CACP syndrome patients.

Keywords: Camptodactyly-arthropathy-coxa-vara-pericarditis, radiosynovectomy, yttrium-90

Address for Correspondence: Sulaiman Mohammed Al-Mayouf MD, King Faisal Specialist Hospital and Research Center, Clinic of Pediatric Rheumatology, Riyadh, Saudi Arabia
Phone: +996114427761 E-mail: mayouf@kfshrc.edu.sa **Received:** 26.12.2016 **Accepted:** 14.02.2017

Öz

Amaç: Kamptodaktili-artropati-koksa vara-perikardit (CACP) sendromu eklem ve tendon yüzeylerinin ana lubrikanı olan proteoglikan 4'ü kodlayan *PRG4* genindeki mutasyonlara bağlı bir otozomal resesif hastalıktır. Eklemde efüzyon ve sinovyal hipertrofi ile karakterize non-enflamatuvar bir artropatidir. Henüz bu hastalığın etkin bir tedavisi yoktur. Amacımız CACP sendromlu hastaların artropatisinde yttrium-90 radyosinovektominin etkinliğini araştırmaktır.

Yöntem: CACP sendromu tanısı alan ardışık hastalar tanı anında ve sağ dize yttrium-90 enjeksiyonu uygulanmasından 3 ay sonra prospektif olarak değerlendirildiler. Sonuç değişkenleri 3-puanlı skala üzerinden hasta/ebeveyn ve doktor genel değerlendirmesi, 3-puanlı skala üzerinden sağ diz ödemi ve hareket aralığı ve kemik, kıkırdak, sıvı, sinovyal hipertrofi ve yumuşak doku değişiklikleri açısından sağ diz manyetik rezonans görüntülemesi (MRG) idi.

Bulgular: Ortalama yaşı 12, ortalama takip süreleri 8,5 yıl olan altı hastaya (üç erkek, üç kız) tek sefer sağ dize 5 mCi intra-artiküler yttrium-90 enjeksiyonu uygulandı. İşlem iki hastada hafif ve geçici eklem ağrısı dışında herhangi bir komplikasyon olmadan iyi tolere edildi. İki hastada yumuşak dokuya minimal radyoizotop kaçağı oldu. Üç aylık takip süresince sonuç değerlerinde iyileşme olmadı. Hastalar ve ebeveynleri olumlu terapötik etki fark etmediler ve genel doktor değerlendirmesi tatmin edici değildi. Diz eklemi ödemi ve hareket aralığında değişiklik yoktu. MRG bulguları değişmedi, ancak enjeksiyon sonrası sinovyal sıvıda minimal artış saptandı.

Sonuç: Yttrium-90 radyosinovektomi güvenli ve iyi tolere edilen bir işlem olarak görülmektedir, ancak verilen doz ve sürede CACP sendromlu hastaların artropatisinde yararlı bir terapötik etki göstermemiştir. Daha fazla hasta içeren ve muhtemelen tekrarlayan enjeksiyonların uygulandığı çalışmalar yttrium-90'ın CACP sendromlu hastalardaki etkinliği ile ilgili gerekli sonuçları sağlayabilir.

Anahtar kelimeler: Kamptodaktili-artropati-koksa vara-perikardit, radyosinovektomi, yttrium-90

Introduction

Camptodactyly-arthropathy-coxa vara-pericarditis (CACP) syndrome is one of the autosomal recessive familial arthropathies (1,2,3,4). Typically, patients with CACP syndrome present with articular features mimicking most common rheumatic disorders, it is not unusual to mistake these disorders as juvenile idiopathic arthritis (JIA) (5). The locus of CACP syndrome was allocated to a 1.9-cm interval on human chromosome 1q25-31 by homozygosity mapping, and proteoglycan 4 (*PRG4*) was identified as the responsible gene (4,6). Furthermore, mutations in the gene encoding the secretion of *PRG4* lead to synovial hyperplasia and loss of its lubricating function, which is the principal pathological feature of this syndrome (7,8). Currently, there are 15 reported *PRG4* mutations (9,10,11).

CACP syndrome is a rare entity, and its worldwide frequency is yet unknown. Although, it has been described in different ethnicities, the diagnosis of CACP syndrome in Saudi families is relatively frequent (9,12,13,14). Unfortunately, there is no available effective treatment yet.

Medical synovectomy (radiosynovectomy) using radioactive isotope is considered as an alternative therapeutic option for different chronic inflammatory arthritis pathologies such rheumatoid arthritis, and osteoarthritis. Radiosynovectomy is also used as an adjuvant therapy in patients with pigmented villonodular synovitis and hemophilic arthropathy (15,16,17,18,19,20). It seems that radiosynovectomy was safe and highly beneficial to children with hemophilic arthropathy. To the best of our knowledge, radiosynovectomy has not been used in CACP syndrome patients. We conducted this study to assess the effectiveness of radiosynovectomy in the treatment of knee arthropathy, using yttrium-90 in patients with CACP syndrome.

Materials and Methods

Consecutive patients with CACP syndrome seen in pediatric Rheumatology clinic at King Faisal Specialist Hospital and Research Center, (KFSH-RC), Riyadh, between May 2015 and March 2016 were included. All involved patients had thorough history and physical examination and the basic blood tests, including complete blood counts, renal and hepatic profile, as well as magnetic resonance imaging (MRI) of both knees at enrollment and 3 months after the therapeutic intervention. The expert musculoskeletal radiologist performed yttrium-90 intra-articular injection of the right knee under fluoroscopy to ensure that the needle was correctly positioned under aseptic circumstances, and the dosage of yttrium-90 was 5 mCi (Figure 1). Following injection of yttrium-90, frontal and lateral scintigraphy was performed to check the distribution of the radioactive material in the joint. Long-acting glucocorticoids (kenalog 1 mg/ kg) was injected to reduce the risk of acute synovitis. Furthermore, following the procedure, the joint was immobilized by an elastic bandage and the patient was confined to bed for 3 days.

The outcome variables were the patient/parent and the physician's global assessment, range of motion, and swelling as well as MRI findings of the right knee. The parents/patients and the physician completed the global assessment as measured by a 3-point scale (improved, no change, worse). Right knee swelling and range of motion,

which was documented by a physical therapist, were assessed on a 3-point scale (improved, no change, worse) in addition to the right knee MRI findings including the bone, cartilage, fluid, synovial hypertrophy and soft tissue changes. Similar assessments were completed 3 months after yttrium-90 intra-articular injection.

All collected data were saved and the confidentiality of the patients protected. Personal identifying data were not collected for this research project. The Research Advisory Council and the Ethical Committee of the KFSH-RC approved the study (#2020023). Informed consent was obtained from each participant.

The results were expressed as mean + standard deviation for continuous variables and percentages for categorical variables. A p value <0.05 was considered as significant. The variables were compared using 2-sample t-tests, chi-square tests and Fisher's exact tests.

Results

Six (three boys, three girls) CACP syndrome patients with a mean age of 12 (7-20) years and a mean follow-up duration of 8.5 (3-11) years were included. The clinical and genetic findings of all patients were previously described (10,11,12). At the time of enrollment, all patients had bilateral flexion contracture and limited extension of knee joints. Additionally, they had significant swelling of the knee joint with large effusion and thickened rubbery synovium. There was no associated pain or tenderness on joint motion.

All patients had a normal complete blood count, renal and hepatic profile and acute phase reactants. MRI prior to yttrium-90 injection showed moderate to severe knee joint effusion with thickened enhanced synovium (Figure 2). The procedure was well tolerated without significant adverse events, gamma camera scans post yttrium-90 injection showed intra-articular homogenous distribution of the radioisotope. However, two patients had minimal leakage to soft tissue (Figure 3).

Outcome variables did not change significantly 3 months after post yttrium-90 injection. The patients and parents did not notice favorable therapeutic effects, there was no significant improvement in the global assessment of the parent/patients. Furthermore, the global physician assessment was unsatisfactory. Additionally, the range of motion of the right knee was almost the same and there

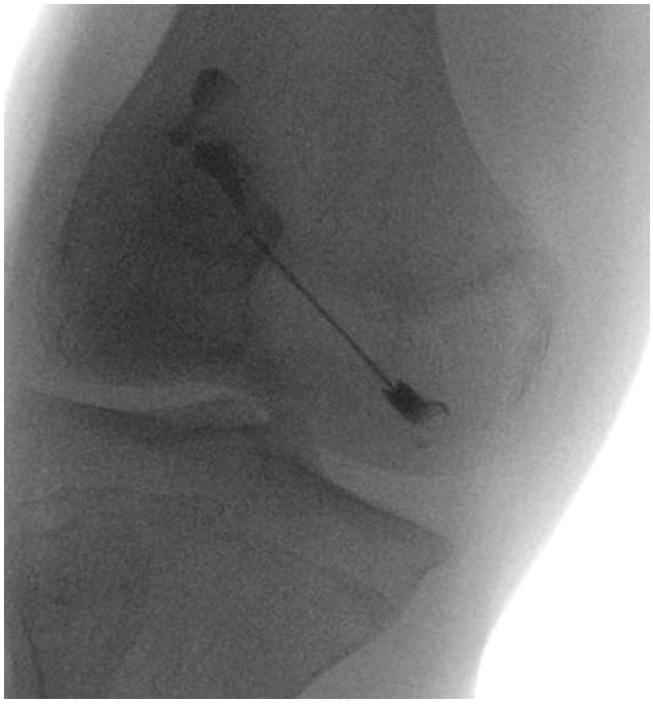

Figure 1. Anterior-posterior oblique projection shows the introduced needle from the medial side with the iodinated contrast

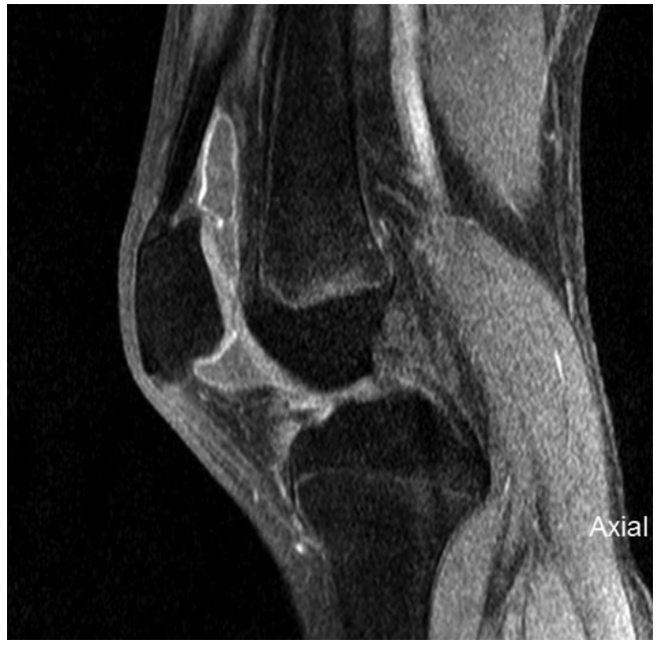

Figure 2. Sagittal T1 fat-saturated weighted magnetic resonance imaging images post contrast injection shows synovial hypertrophy and mild synovial enhancement. Note the amount of synovial fluid

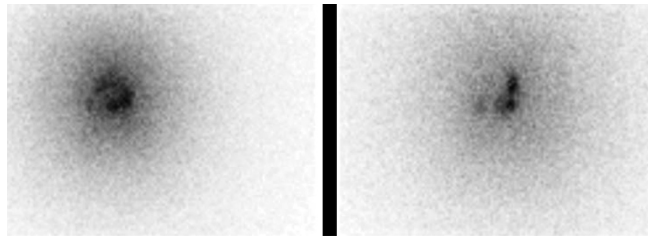

Figure 3. Gamma camera images showing the distribution of yttrium-90 within the joint

was no difference in knee joint swelling. Moreover, MRI findings remained unchanged. However, there was a minimal increase in synovial fluid post injection (Figure 4).

Discussion

CACP syndrome is a rare autosomal recessive non-inflammatory arthropathy with typical musculoskeletal manifestations, particularly coxa vara and multiple joint contractures.

Affected individuals usually suffer from limited range of motions, mainly the large joints, which might interfere with daily activities. Synovial hyperplasia and loss of the lubricating function is the pathological feature of this syndrome.

Taking the pathophysiology of the disease into consideration, it is predictable that CACP syndrome patients did not respond to anti-inflammatory medications. Actually, some patients with CACP syndrome were misdiagnosed as JIA and were treated with methotrexate and biologic therapy, but without beneficial therapeutic effects.

Despite the availability of effective medical treatment, including systemic anti-rheumatic and local articular treatment of inflammatory arthritis, other therapeutic interventions have been explored particularly in refractory cases. Historically, surgical synovectomy was one of the therapeutic options. However, such an intervention may induce further articular damage and complications.

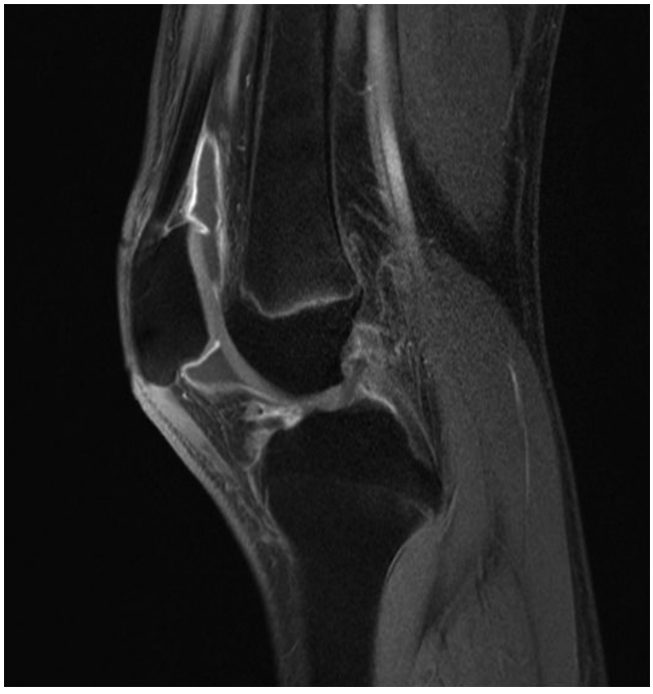

Figure 4. Sagittal T1 weighted fat-saturated magnetic resonance imaging images, post yttrium-90 therapy 2.8 mCi (millicurie)

Radiosynovectomy, which is a less invasive procedure is considered as an alternative therapeutic option for chronic inflammatory arthritis (15,16,17,18,19,20). Radiopharmaceutical excretion is not a concern since the application is local.

We have the privilege at KFSH-RC to follow the largest cohort of children with CACP syndrome (21). Typically, the synovial histopathology showed proliferating epithelium with moderate fibro-collagenous densities and multinucleated giant cells. The long-standing disease is mostly complicated by irreversible articular changes in the form of multiple joints stiffness and contractures, and bone dysplasia such as flattening of the femoral heads, widening of the femoral necks with osteophyte formations and secondary degenerative changes (22). We were hoping that the radioactivity concentrates in the synovium would induce a necrosis of the proliferating synoviocytes. Unfortunately, yttrium-90 radiosynovectomy did not show a beneficial therapeutic effect in our patients. Nonetheless, the procedure was safe and well tolerated. Previous studies of radiosynovectomy in children with hemophilic arthropathy showed encouraging results. However, it is worth mentioning that most patients with hemophilic arthropathy underwent more than one yttrium-90 intra-articular injections (23,24). It is advised to perform radiosynovectomy for hemophilic arthropathy without delay and before the synovitis becomes severe and chronic, otherwise the response to yttrium-90 injections would decrease. Interestingly, other studies revealed that the overall success rate for radiosynovectomy was related to the underlying disease: the treatment was more effective among patients with rheumatoid arthritis and less effective for patients with arthritis of unknown origin (25). Our results might be explained by the difference in the pathology of CACP syndrome. Furthermore, disease stage, particularly the severity of synovial hyperplasia and thickened synovium may be inversely related to the clinical response in addition to the applied dosage and interval of treatment.

Conclusions

Yttrium-90 radiosynovectomy seems to be a safe and well tolerated procedure, however, it did not show a beneficial therapeutic effect in arthropathy of CACP syndrome with the given dosage and interval. Studies including a larger number of patients and probably repeated injections are needed to derive satisfactory results about the effectiveness of yttrium-90 in patients with CACP syndrome.

Ethics

Ethics Committee Approval: King Faisal Specialist Hospital and Research Center Ethics Committee approved protocol (Research Advisory Council #2020023), Informed Consent: Obtained from each patient.

Peer-review: Externally peer-reviewed.

Authorship Contributions

Surgical and Medical Practices: Khalid Alismail, Concept: Sulaiman Mohammed Al-Mayouf, Design: Sulaiman Mohammed Al-Mayouf, Data Collection or Processing: Nora Almutairi, Analysis or Interpretation: Sulaiman Mohammed Al-Mayouf, Khalid Alismail, Nora Almutairi, Literature Search: Sulaiman Mohammed Al-Mayouf, Nora Almutairi, Writing: Sulaiman Mohammed Al-Mayouf.

Conflict of Interest: No conflict of interest was declared by the authors.

Financial Disclosure: The authors declared that this study received no financial support.

References

1. Chalom E, Ross J, Athreya B. Syndromes and arthritis. Rheum Dis Clin North Am 1997;23:709-727.
2. Al-Mayouf SM. Familial arthropathy in Saudi Arabian children: demographic, clinical,and biochemical features. Semin Arthritis Rheum 2007;36:256-261.
3. Bulutlar G, Yazici H, Ozdoğan H, Schreuder I. A familial syndrome of pericarditis,arthritis, camptodactyly, and coxa vara. Arthritis Rheum 1986;29:436-438.
4. Laxer RM, Cameron BJ, Chaisson D, Smith CR, Stein LD. The camptodactyly arthropathypericarditis syndrome: case report and literature review. Arthritis Rheum 1986;29:439-444.
5. Offiah AC, Woo P, Prieur AM, Hasson N, Hall CM. Camptodactyly-arthropathy-coxa varapericarditis syndrome versus juvenile idiopathic arthropathy. AJR Am J Roentgenol 2005;185:522-529.
6. Bahabri SA, Suwairi WM, Laxer RM, Polinkovsky A, Dalaan AA, Warman ML. The camptodactyly-arthropathy-coxa vara-pericarditis syndrome: clinical features and genetic mapping to human chromosome 1. Arthritis Rheum 1998;41:730-735.
7. Marcelino J, Carpten JD, Suwairi WM, Gutierrez OM, Schwartz S, Robbins C, Sood R, Makalowska I, Baxevanis A, Johnstone B, Laxer RM, Zemel L, Kim CA, Herd JK, Ihle J, Williams C, Johnson M, Raman V, Alonso LG, Brunoni D, Gerstein A, Papadopoulos N, Bahabri SA, Trent JM, Warman ML. CACP, encoding a secreted proteoglycan, is mutated in camptodactyly-arthropathy-coxa varapericarditis syndrome. Nat Genet 1999;23:319-322.
8. Rhee DK, Marcelino J, Al-Mayouf S, Schelling DK, Bartels CF, Cui Y, Laxer R, Goldbach-Mansky R, Warman ML. Consequences of disease-causing mutations on lubricin protein synthesis, secretion, and post-translational processing. J Biol Chem 2005;280:31325-31332.
9. Basit S, Iqbal Z, Umicevic-Mirkov M, Kamran Ul-Hassan Naqvi S, Coenen M, Ansar M, van Bokhoven H, Ahmad W. A novel deletion mutation in proteoglycan-4 underlies camptodactyly-arthropathycoxa-vara pericarditis syndrome in a consanguineous pakistani family. Arch Med Res 2011;42:110-114.
10. Alazami AM, Al-Mayouf SM, Wyngaard CA, Meyer B. Novel PRG4 mutations underlie CACP in Saudi families. Hum Mutat 2006;27:213.
11. Akawi N, Ali B, Al-Gazali L. A novel mutation in PRG4 gene underlying camptodactyly-arthropathy-coxa vara-pericarditis syndrome with the possible expansion of the phenotype to include congenital cataract. Birth Defects Res A Clin Mol Teratol 2012;94:553-556.
12. Bahabri S, Sakati N, Hugosson C, Hainau B, Al-Balla SR, Al-Mazyed A, Al-Dalaan A. Syndrome of camptodactyly, arthropathy and coxa vara (CAC syndrome). Ann Saudi Med 1994;14:479-482.
13. El-Garf A, Mahmoud G, Gheith R, Abd El-Aaty G, Abd El-Aaty H. Camptodactyly, arthropathy, coxa vara, and pericarditis syndrome among egyptians. J Rheumatol 2003;30:1081-1086.
14. Choi BR, Lim YH, Joo KB, Paik SS, Kim NS, Lee JK, Yoo DH. Camptodactyly, arthropathy, coxa vara, pericarditis (CACP) syndrome: a case report. J Korean Med Sci 2004;19:907-910.
15. Zwolak R, Majdan M, Skorski M, Chrapko B. Efficacy of radiosynoviorthesis and impact on chosen inflammatory markers. Rheumatol Int 2012;32:2339-2344.
16. Liepe K. Efficacy of radiosynovectomy in rheumatoid arthritis. Rheumatol Int 2012;32:3219-3224.
17. Chatzopoulos D, Moralidis E, Markou P, Makris V. Yttrium-90 radiation synovectomy in knee osteoarthritis: a prosective assessment at 6 and 12 months. Nucl Med Commun 2009;30:472-479.
18. Chrapko B, Zwolak R, Nocu A, Gołebiewska R, Majdan M. Radiation synovectomy with 90Y colloid in the therapy of recurrent knee joint effusions in patients with inflammatory joint diseases. Rheumatol Int 2007;27:729-734.
19. Rampersad A, Shapiro A, Rodriguez-Merchan E, Maahs J, Akins S, Jimenez-Yuste V. Radiosynovectomy: review of the literature and report from two haemophilia treatment centers. Blood Coagul Fibrinolysis 2013;24:465-470.
20. Van Kasteren M, Novakova I, Boerbooms A, Lemmens J. Long term follow up of radiosynovectomy with yttrium-90 silicate in haemophilic haemarthrosis. Ann Rheum Dis 1993;52:548-550.
21. Albuhairan I, Al-Mayouf SM. Camptodactyly-arthropathy-coxavara-pericarditis syndrome in Saudi Arabia: Clinical and molecular genetic findings in 22 patients. Semin Arthritis Rheum 2013;43:292-296.
22. Murphy JM, Vanderhave KL, Urquhart AG. Total hip arthroplasty in adolescents with severe hip arthropathy and dysplasia associated with camptodactyly-arthropathy-coxa vara-pericarditis syndrome. J Arthroplasty 2012;27:1581.e5-8.
23. Kavakli K, Aydoğdu S, Omay SB, Duman Y, Taner M, Capaci K, Memiş A, Balkan C, Karapinar D. Long-term evaluation of radioisotope synovectomy with Yttrium 90 for chronic synovitis in Trukish haemophilics: Ismir experience. Haemophilia 2006;12:28-35.
24. Ozulker T, Ozulker F, Derin E, Altun M, Aydogan G, Turkkan E, Adaş M, Tonbul M, Ozpaçacı T, Sezgin F, Değirmenci H. The efficacy of 315 magnetic resonance imaging and x-ray in the evaluation of response to radiosynovectomy in patients with hemophilic arthropathy. Mol Imaging Radionucl Ther 2011;20:38-44.
25. Jahangier Z, Moolenburgh J, Jacobs J, Serdijn H, Bijlsma J. The effect of radiation synovectomy in patients with persistent arthritis: a prospective study. Clin Exp Rheumatol 2001;19:417-424.

Case Report
Mol Imaging Radionucl Ther 2017;26:38-42 DOI:10.4274/mirt.70894

A Family with Von Hippel-Lindau Syndrome: The Findings of Indium-111 Somatostatin Receptor Scintigraphy, Iodine-123 Metaiodobenzylguanidine Scintigraphy and Single Photon Emission Computerized Tomography

Von Hippel-Lindau Sendromlu Aile: İndiyum-111 Somatostatin Reseptör Sintigrafisi, İyot-123 Metaiyodobenzilguanidin Sintigrafisi ve Bilgisayarlı Tek Foton Emisyonlu Tomografisi Bulguları

Pelin Arıcan[1], Berna Okudan Tekin[1], Seniha Naldöken[1], Rıza Şefizade[1], Dilek Berker[2]
[1]*Ankara Numune Training and Research Hospital, Clinic of Nuclear Medicine, Ankara, Turkey*
[2]*Ankara Numune Training and Research Hospital, Clinic of Endocrinology and Metabolism, Ankara, Turkey*

Abstract

Von Hippel-Lindau syndrome (VHLS) is an autosomal dominant hereditary familial disorder characterized by development of malignant and benign neoplasms. Differential diagnosis of the adrenal and pancreatic masses are difficult in patients with VHLS. Iodine-123 metaiodobenzylguanidine (I-123 MIBG) and indium-111 somatostatin receptor scintigraphies (In-111 SRS) have important roles in the differential diagnosis of adrenal and pancreatic masses in those patients. In this case report, we present the findings of I-123 MIBG single-photon emission computerized tomography (SPECT/CT) and In-111 SRS SPECT/CT in three members of a family with VHLS. In case 1, a residual neuroendocrine tumor (NET) was detected in the head of pancreas on In-111 SRS SPECT/CT images. In case 2 and 3, I-123 MIBG SPECT/CT confirmed the adrenal masses as pheochromocytoma, and the extra-adrenal mass as NET, before surgery. We thought that In-111 SRS and I-123 MIBG scan might be helpful in the routine work up of VHLS patients for diagnostic and therapeutic purposes. Hybrid SPECT/CT system may improve diagnostic accuracy of planar images since it assesses morphologic and functional information together.

Keywords: Von Hippel-Lindau disease, neuroendocrine tumors, scintigraphy, single-photon emission computerized tomography

Öz

Von Hippel-Lindau sendromu (VHLS) malign ve benign tümörler ile karakterize otozomal dominant herediter ailesel bir hastalıktır. VHLS'li hastalarda adrenal ve pankreatik kitlelerin ayırıcı tanısı zordur. Bu hastalarda iyot-123 metaiyodobenzilguanidin (I-123 MIBG) ve indiyum-111 somatostatin reseptör sintigrafileri (In-111 SRS) adrenal ve pankreatik kitlelerin ayırıcı tanısında önemli rol oynar. Bu olgu sunumunda VHLS'li ailenin üç üyesinin I-123 MIBG bilgisayarlı tek foton emisyonlu tomografisi (SPECT/BT) ve In-111 SRS SPECT/BT bulgularını sunuyoruz. Olgu 1'de, In-111 SRS SPECT/BT görüntülerinde pankreas başında rezidü nöroendokrin tümör (NET) saptandı. Olgu 2 ve 3'de, I-123 MIBG SPECT/BT cerrahi öncesi adrenal bezdeki kitleleri feokromositoma ve adrenal dışı kitleyi NET olarak onayladı. In-111 SRS ve I-123 MIBG sintigrafilerinin VHLS'li hastaların tanı ve tedavisi için rutin kullanımda yararlı olabileceğini düşündük. Hibrid SPECT/BT morfolojik ve fonksiyonel bilgileri birlikte değerlendirdiği için, planar görüntülerin tanısal doğruluğunu artırır.

Anahtar kelimeler: Von Hippel-Lindau hastalığı, nöroendokrin tümörler, sintigrafi, bilgisayarlı tek foton emisyonlu tomografi

Address for Correspondence: Pelin Arıcan MD, Ankara Numune Training and Research Hospital, Clinic of Nuclear Medicine, Ankara, Turkey
Phone: +90 542 286 75 75 E-mail: psarican@yahoo.com **Received:** 01.09.2015 **Accepted:** 21.01.2016

Introduction

Von Hippel-Lindau syndrome (VHLS) is an autosomal dominant hereditary familial neoplastic disorder characterized by retinal, cerebellar and spinal hemangioblastomas, liver, and kidney hemangiomas, clear cell renal carcinoma (RCC), pheochromocytoma, pancreatic tumors, pancreatic, renal, and epididymal cysts (1). The gene responsible for the disease is identified with direct gene mutation analysis (2). Clinic examination and imaging modalities are important in the diagnosis of VHLS (3). Nuclear medicine imaging modalities such as iodine-123 metaiodobenzylguanidine (I-123 MIBG) and Indium-111 somatostatin receptor scintigraphy (In-111 SRS) have important roles in the differential diagnosis of adrenal and pancreatic masses in those patients.

Here in, we present the findings of I-123 MIBG single photon emission computerized tomography (SPECT/CT) and In-111 SRS SPECT/CT in three members of a family with VHLS.

Case Reports

Case 1

A 39-year-old man with VHLS who had had adrenalectomy for pheochromocytoma 27 years ago, partial pancreatectomy for neuroendocrine tumor (NET) 6 years ago, and partial nephrectomy for RCC 5 years ago was referred to our department for evaluation of a residual mass in his pancreas. The contrast-enhanced abdominal CT revealed a 30-mm mass at the head of the pancreas. In-111 SRS imaging was performed after injection of 185 MBq In-111 octreotide (Octreoscan, Mallinckrodt, Netherlands). Whole body and static images were obtained 4 and 24 hours later. Focal radiotracer accumulation was seen in the right upper quadrant of the abdomen on planar images. Therefore, abdominal SPECT/CT was performed following planar imaging to the abdominal region (Millennium Hawkeye 4, GE Medical Systems, Wilwaukee, WI). SPECT/CT confined this pathologic uptake to the pancreatic region (Figure 1). The patient had revision surgery. Histolopathologic examination revealed a recurrent NET.

Case 2

The cousin of case 1, a 20-year-old woman was diagnosed with VHLS on gene mutation analysis. Hypertension and increased metanephrine levels were detected on psychical examination and laboratory tests. Magnetic resonance imaging (MRI) detected a hemangioma in the liver and masses in bilateral adrenal glands (right side: 28x22 mm, and left side: 20x18 mm). I-123 MIBG scintigraphy was performed before surgery to confirm adrenal masses as

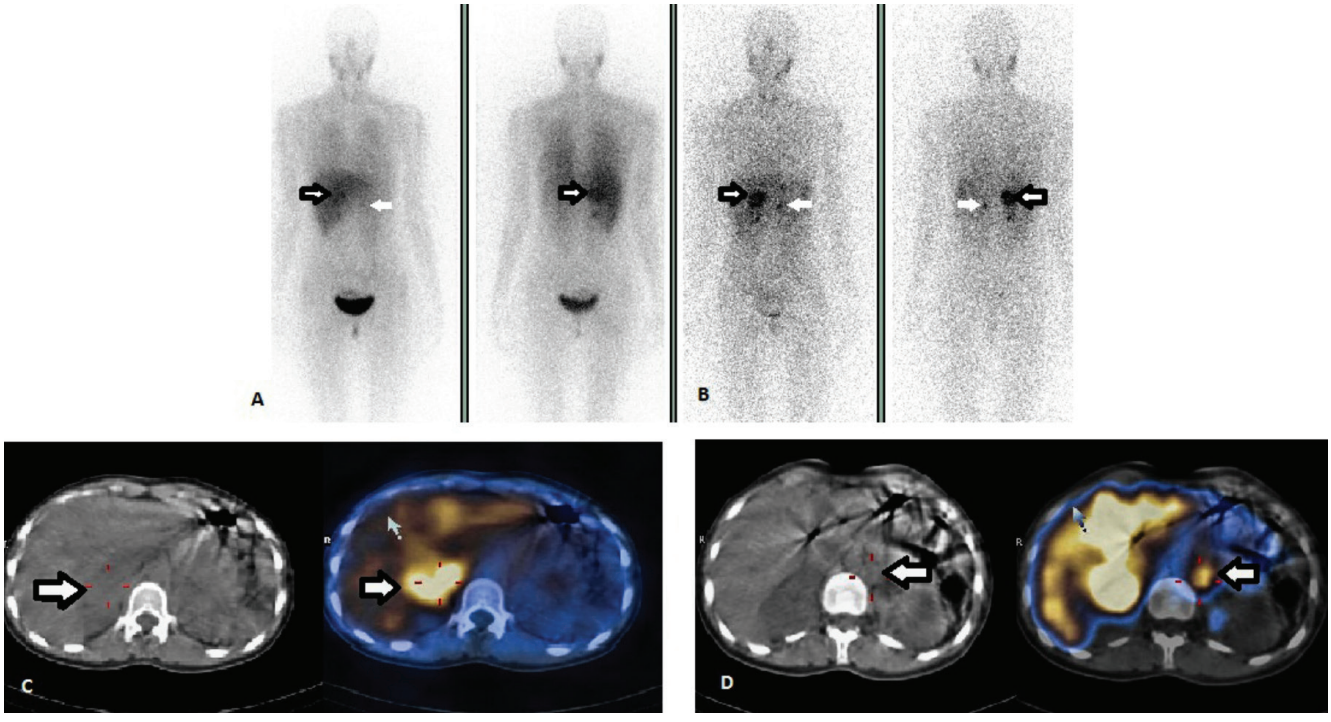

Figure 1. In-111 somatostatin receptor scintigraphies findings of case 1. Anterior-posterior whole body images show focal radiotracer accumulation medial to the right kidney (A) at 4, and (B) 24 hours (arrows). Axial (C) and coronal (D) computed tomography (CT), single photon emission computerized tomography (SPECT), and SPECT/CT images show that this accumulation is localized to the head of the pancreas (arrows). The diagnosis of residual neuroendocrine tumor was confirmed by histopathologic examination

pheochromocytoma. Whole body and static images were obtained 4 and 24 hours after injection of 370 MBq I-123 MIBG (I-123, Mallinckrodt, Netherlands). Planar images showed an abnormal radiotracer uptake bilaterally superior to kidneys. SPECT/CT fusion images demonstrated that those radiotracer accumulations were localized to the adrenal glands (Figure 2). Bilateral adrenalectomy was performed. Histopathologic examination revealed that the removed adrenal tumors were pheochromocytoma. Four years later, abdominal MRI revealed a mass between the liver and right adrenal gland (33x30x36 mm) and another one in the pancreatic tail (13x15x17 mm). I-123 MIBG SPECT/CT was performed with suspicion of local recurrence. Fusion images showed an abnormal accumulation in the right adrenal gland. There was no radiotracer accumulation in the pancreas, a Ga-68 DOTATOC positron emission tomography (PET/CT) was performed. Pathologic radiotracer uptake was demonstrated in the pancreas. The patient is planned to undergo surgery.

Case 3

Case 3 was a 38-year-old woman who is the cousin of both case 1 and 2. She had no complaints, and her parameters were in normal limits. She was diagnosed with VHLS on gene mutation analysis. An abdominal MRI was performed for screening purposes. MRI revealed masses with intensive contrast enhancement between the liver and right kidney (40x36x36 mm), and inferior to the left adrenal gland (14x15x15 mm). Those findings were suspicious for bilateral pheochromocytoma. I-123 MIBG was performed to characterize those tumors. Whole body and static images were obtained 4 and 24 hours after injection of 370 MBq I-123 MIBG. Whole body-scan and static planar images showed an abnormal radiotracer uptake infero-medial to the liver, and supero-medial to the left kidney. Following planar imaging, an abdominal SPECT/CT was performed. SPECT/CT images showed radiotracer uptake in the right adrenal gland region. The activity on the left side was localized to the extra-adrenal region (Figure 3). Right adrenalectomy and resection of the extra-adrenal lesion were performed following MIBG scan. Histopathologic examination confirmed the diagnosis of pheochromocytoma in the right adrenal gland, and paraganglioma in the extra-adrenal tumor.

Three members of this family with VHLS are still being followed up in the endocrinology department.

Literature Review and Discussion

VHLS is an autosomal dominant disorder characterized by presence of malignant and benign neoplasms. Clinical

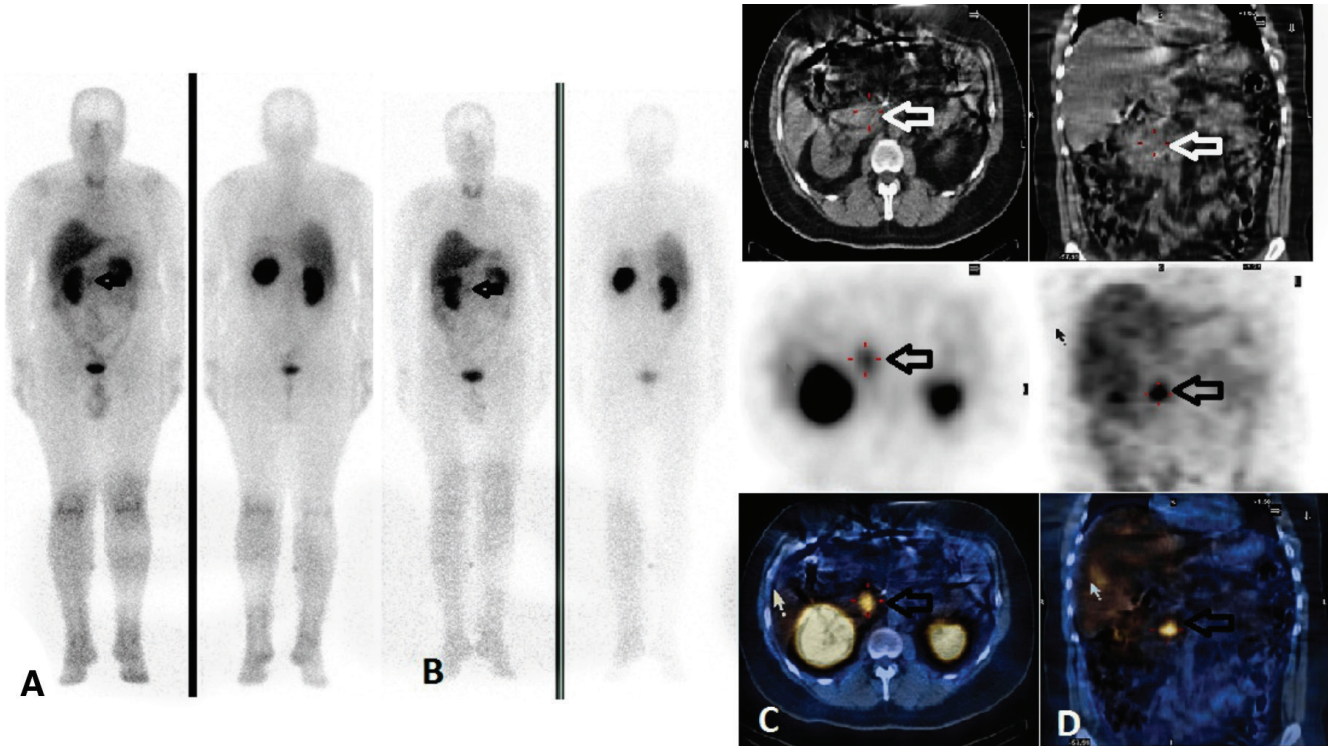

Figure 2. Iodine-123 metaiyodobenzilguanidin scintigraphy findings of case 2. Anterior-posterior whole body images show focal tracer uptake superior to the kidneys bilaterally (A) at 4, and (B) 24 hours, before surgery (arrows), (C) axial (D) coronal computed tomography (CT), single photon emission computerized tomography (SPECT), and SPECT/CT images reveal that those radiotracer accumulations are localized to the adrenal glands bilaterally (arrows). Histopathologic examination of the masses were reported as pheochromocytoma after surgery

diagnosis of VHLS is usually challenging due to involvement of various organs. Early detection of neoplasms is important to reduce morbidity. Adrenal glands and pancreas are usually involved in those patients. Clinical and laboratory findings facilitate the diagnosis. CT and MRI can localize adrenal, extra-adrenal, and pancreatic tumors. However, those imaging modalities can not characterize the functional status of the tumors. In-111 SRS is very useful for both the diagnosis and staging of pancreatic NET, and management of patients (4). Pancreatic tumors are detected in 5-10% of the cases with VHLS. In case 1, In-111 SRS SPECT/CT fusion images confirmed residual NET in the head of pancreas, which was previously detected with abdominal CT. The findings assisted to plan the treatment. The patient had a revision surgery. He was re-operated. Pulcrano et al. (5) reported the findings of In-111-DTPA0-octreotide scintigraphy in three members of a family with VHLS. The authors concluded that scintigraphy might be useful in the management plan of those patients. Recently, PET/CT performed using Ga-68 labelled peptides has been proven to be very useful for imaging of NET. Sharma et al. (3) reported the findings of Ga-68 DOTA-NOC PET/CT in a patient with VHLS. They demonstrated uptake of Ga-68 DOTA-NOC in all central nervous system and visceral tumors. In addition, Ga-68 DOTA-NOC PET/CT assisted the decision of treating the patient with Lu-177 DOTA-TATE. The authors suggested that Ga-68 DOTA-NOC PET/CT played an important role in the management and diagnosis of patients with VHLS, and that it should be used routinely in those patients.

I-123 MIBG scintigraphy is the imaging modality of choice in pheochromocytoma owing to its high sensitivity and specificity. I-123 MIBG is performed prior to surgery both to confirm the lesions as pheochromocytoma, and to determine metastatic, residual or recurrent disease (4). In case 2, I-123 MIBG SPECT/CT confirmed bilateral adrenal masses as pheochromocytoma before bilateral adrenalectomy was performed. Four years after surgery, I-123 MIBG SPECT/CT showed local recurrence in bilateral adrenal glands. Fujita et al. (6) reported a similar case with VHLS. Recurrence of bilateral pheochromocytoma was determined with I-123 MIBG scan in that case. Thoren et al. (7) reported a case with multiple pheochromocytomas and VHLS. They performed I-123 MIBG before surgery to confirm that the lesions were indeed pheochromocytoma and to rule out any metastatic disease. Arao et al. (8) confirmed the diagnosis of bilateral pheochromocytoma with MIBG scintigraphy in a case with VHLS. In our report, case 3 had no symptoms or history of hypertension. Her laboratory parameters were within

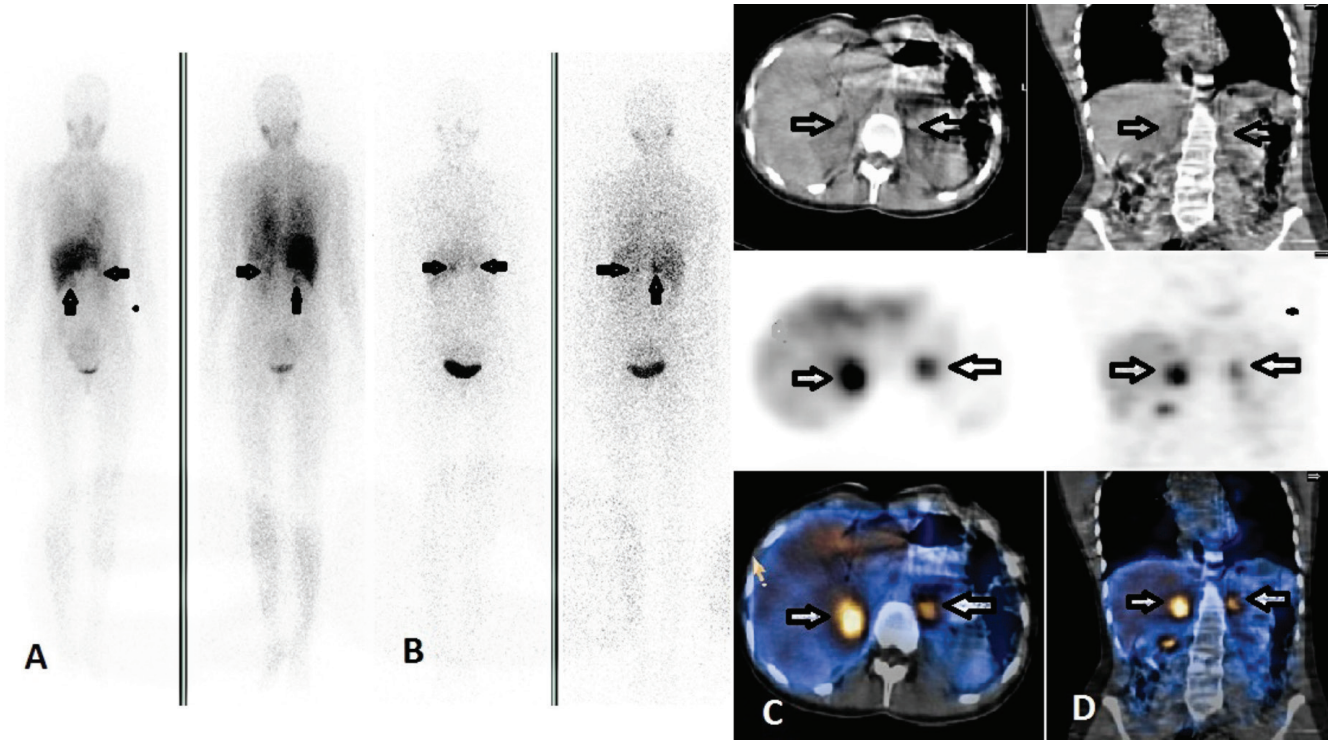

Figure 3. Iodine-123 metaiyodobenzilguanidin scintigraphy findings of case 3. Anterior-posterior whole body images show a large focal tracer uptake medial to the liver (arrows with black contours) and small focal activity superior to the left kidney (white arrows) (A) at 4, and (B) 24 hours, before surgery. Axial computed tomography (C), and single photon emission computerized tomography slices show the intense abnormal radiotracer accumulation in the right adrenal gland (arrows), and (D) a smaller activity in the extra adrenal and prevertebral region (arrows). After surgery, the histopathologic examination confirmed the mass in the right adrenal as pheochromocytoma, and the mass on the left side as paraganglioma

normal limits. Abdominal MRI revealed bilateral adrenal masses with significant I-123 MIBG accumulation. Fusion images confirmed the diagnosis of pheochromocytoma before surgery. I-123 MIBG SPECT/CT was helpful in the early diagnosis of this asymptomatic case. Otsuka et al. (9) described a similar case with VHLS who did not have any symptoms and had significant accumulation of I-131 MIBG in bilateral pheochromocytoma.

In conclusion, the data we obtained from our patients suggested that In-111 SRS and I-123 MIBG scan might be helpful in the routine work up of VHLS patients for diagnostic and therapeutic purposes. Hybrid SPECT/CT system can improve the diagnostic accuracy of In-111 SRS and I-123 MIBG images, since it evaluates morphologic and functional information together. SPECT/CT increases sensitivity and specificity of planar images.

Ethics

Informed Consent: Consent form was filled out by all participants.

Peer-review: Externally peer-reviewed.

Authorship Contributions

Surgical and Medical Practices: Pelin Arıcan, Berna Okudan Tekin, Dilek Berker, Concept: Pelin Arıcan, Berna Okudan Tekin, Design: Pelin Arıcan, Berna Okudan Tekin, Data Collection or Processing: Pelin Arıcan, Berna Okudan Tekin, Analysis or Interpretation: Pelin Arıcan, Berna Okudan Tekin, Literature Search: Pelin Arıcan, Rıza Şefizade, Seniha Naldöken, Writing: Pelin Arıcan.

Financial Disclosure: The authors declared that this study received no financial support.

Conflict of Interest: No conflict of interest was declared by the authors.

References

1. Richard S, Graff J, Lindau J, Resche F. Von Hippel-Lindau disease. Lancet 2004;363:1231-1234.
2. Crossey PA, Richards FM, Foster K, Green JS, Prowse A, Latif F, Lerman MI, Zbar B, Affara NA, Ferguson-Smith MA, et al. Identification of intragenic mutations in the von Hippel-Lindau disease tumour suppressor gene and correlation with disease phenotype. Hum Mol Genet 1994;3:1303-1308.
3. Sharma P, Dhull VS, Bal C, Malhotra A, Kumar R. Von Hippel-Lindau syndrome: demonstration of entire disease spectrum with (68)Ga-DOTANOC PET-CT. Korean J Radiol 2014;15:169-172.
4. Rufini V, Calcagni ML, Baum RP. Imaging of neuroendocrine tumors. Semin Nucl Med 2006;36:228-247.
5. Pulcrano M, Camera L, Pagano L, Del Vecchio S, Ferone D, Bodei L, Murgia A, Pace L, Storto G, Paganelli G, Colao A, Salvatore M, Lombardi G, Biondi B. Usefulness of [111In-DTPA0] octreotide scintigraphy in a family with von Hippel-Lindau disease. J Endocrinol Invest 2008;31:352-359.
6. Fujita N, Mikami J, Murasawa H, Okamoto A, Imai A, Hatakeyama S, Ishimura H, Yoneyama T, Koie T, Kamimura N, Ohyama C, Morohashi S, Kijima H. [Local recurrence of pheochromocytoma associated with von Hippel-Lindau disease 26 years after bilateral adrenalectomy: a case report]. Hinyokika Kiyo 2013;59:427-430.
7. Thoren KL, Balingit AG, Billingsley J. Multiple pheochromocytomas in a patient with blurred vision. Clin Nucl Med 2008;33:597-601.
8. Arao T, Okada Y, Tanikawa T, Inatomi H, Shuin T, Fujihira T, Yamashita H, Tanaka Y. A case of von Hippel-Lindau disease with bilateral pheochromocytoma, renal cell carcinoma, pelvic tumor, spinal hemangioblastoma and primary hyperparathyroidism. Endocr J 2002;49:181-188.
9. Otsuka F, Ogura T, Nakagawa M, Hayakawa N, Kataoka H, Oishi T, Makino H. Normotensive bilateral pheochromocytoma with Lindau disease: case report. Endocr J 1996;43:719-723.

Case Report
Mol Imaging Radionucl Ther 2017;26:43-46 DOI:10.4274/mirt.75436

Ectopic Pelvic Kidney Mimicking Sacral Metastasis on Post-Therapy Iodine-131 Scan of a Thyroid Cancer Patient

Tiroid Kanserli Bir Hastada İyot-131 Tedavisi Sonrası Taramada Sakral Metastazı Taklit Eden Ektopik Pelvik Böbrek

Selin Soyluoğlu Demir[1], Gül Ege Aktaş[1], Ahmet Polat[2], Ali Sarıkaya[1]
[1]*Trakya University Faculty of Medicine, Department of Nuclear Medicine, Edirne, Turkey*
[2]*Sultan 1. Murat State Hospital, Clinic of Radiology, Edirne, Turkey*

Abstract

A 25-year-old woman had total thyroidectomy and iodine-131 ablation therapy for papillary thyroid carcinoma. Whole body imaging on the 7th day of therapeutic activity demonstrated radioiodine uptake in the remnant tissue and intense heterogeneous uptake at the sacral region prominently in the posterior image. Initial interpretation was suspicious for sacral metastasis. Technetium-99m-methylene diphosphonate bone scan demonstrated normal bone uptake and the absence of left kidney. On blood-pool phase of bone scan, the absence of left renal activity and an extra area of uptake in the sacral region suggestive of pelvic kidney were noticed. Magnetic resonance imaging scan confirmed the ectopic pelvic kidney overlying the sacrum.

Keywords: Thyroid cancer, ectopic kidney, iodine-131, bone scan, false-positive

Öz

Papiller tiroid karsinomu tanısı alan 25 yaşında kadın hastaya total tiroidektomi ve sonrasında iyot-131 ablasyon tedavisi uygulandı. Terapötik aktivite sonrası 7. gün yapılan tüm vücut görüntülemede tiroid lojunda bakiye dokuya ait yoğun aktivite tutulumu ile sakral bölgede posterior imajlarda daha belirgin olmak üzere yoğun, heterojen bir aktivite tutulum alanı saptandı. Görünüm sakral metastaz şüphesi uyandırmaktaydı. Teknesyum-99m-metilendifosfonat kemik sintigrafisinde kemiklerde normal dağılım izlenirken, sol böbreğin normal lokalizasyonunda bulunmadığı görüldü. Kemik sintigrafisi kan havuzu fazı incelendiğinde, sol böbrek aktivitesi yerinde izlenmezken, sakral bölgede pelvik böbreğe ait olabilecek ekstra bir aktivite tutulum alanı saptandı. Yapılan manyetik resonans görüntüleme ile sakrum önünde lokalize ektopik pelvik böbrek doğrulandı.

Anahtar kelimeler: Tiroid kanseri, ektopik böbrek, iyot-131, kemik sintigrafisi, yanlış-pozitif

Introduction

Differentiated thyroid cancer is a possibly curable cancer that is associated with low mortality rates. It is usually managed by total thyroidectomy followed by iodine-131 (I-131) ablation of remnant thyroid tissue. Nevertheless, 1-3% of patients may have distant metastases at initial diagnosis, and another 7-23% may develop distant metastases during disease course. The distant metastases, particularly bone metastases, increase mortality rate and decrease quality of life. Radioiodine has been used for decades for the diagnosis and treatment of patients with papillary or follicular thyroid carcinoma, and patients are mainly followed-up with whole-body I-131 scintigraphy (WBS) and thyroglobulin levels. However, it is important

Address for Correspondence: Selin Soyluoğlu Demir MD, Trakya University Faculty of Medicine, Department of Nuclear Medicine, Edirne, Turkey
Phone: +90 284 235 76 41/1042 E-mail: dr.selina@gmail.com **Received:** 25.01.2016 **Accepted:** 11.05.2016

to identify false-positive sites to avoid unnecessary ablation therapy. Herein we report a case of a demonstrative example of pelvic kidney mimicking sacral metastasis on I-131 WBS.

Case Report

A 25-year-old woman underwent total thyroidectomy and central neck lymph node dissection with histopathologic diagnosis of papillary thyroid carcinoma. Three months after surgery, 5550 MBq (150 mCi) of I-131 was administered for thyroid remnant ablation. Post treatment WBS on the 7th day of treatment demonstrated intense uptake corresponding to thyroid remnant tissue and a heterogeneous radioiodine uptake in the sacral region, prominently in the posterior image (Figure 1). Initial interpretation was suspicious for sacral metastasis. No other abnormal focus was determined elsewhere in the whole body. The serum thyroglobulin level was 13.6 ng/ml and anti-thyroglobulin was 196.4 U/ml, while thyroid stimulating hormone value was 123.9 mIU/ml. Because of the patient's pelvic pain complaint and intermediate-high risk according to thyroglobulin level, a technetium-99m-methylene diphosphonate (MDP) bone scan was also performed. The osteoblastic phase of the bone scan demonstrated normal bone uptake and absence of the left kidney (Figure 2). We routinely perform 2-5-minute whole-body blood-pool imaging in our department, especially in case of whole-body tumor and metastasis evaluation with MDP bone scan. In some cases, the normal kidneys and urinary system can be cleared thoroughly in MDP bone scan and ectopic kidneys can be confusing. When the blood-pool phase was analyzed, absence of the left renal activity and an extra focus of uptake in the sacral region due to pelvic kidney was noticed (Figure 3). Magnetic resonance imaging (MRI) of patient confirmed the ectopic kidney located in the left posterior pelvic region overlying the sacrum with an anteriorly rotated renal pelvis (Figure 4).

Literature Review and Discussion

Radioiodine is a sensitive marker for diagnosing metastases of differentiated papillary or follicular thyroid carcinoma; however, is not specific for thyroid tissue. It can also be seen in normal tissue, including salivary glands, thymus, breast, liver, and gastrointestinal tract, or in benign or malignant

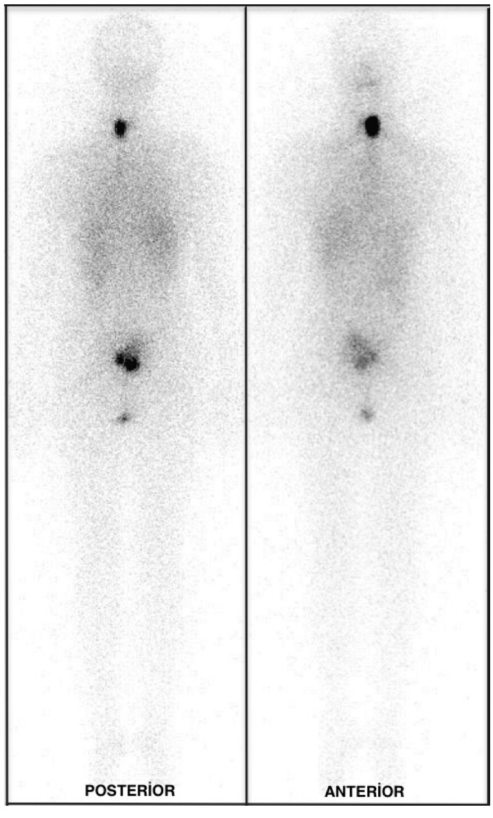

Figure 1. A whole-body scintigraphy performed 7 days after administration of iodine-131 showed intense uptake corresponding to thyroid remnant tissue and a heterogeneous radioiodine uptake in the sacral region, prominently in the posterior image

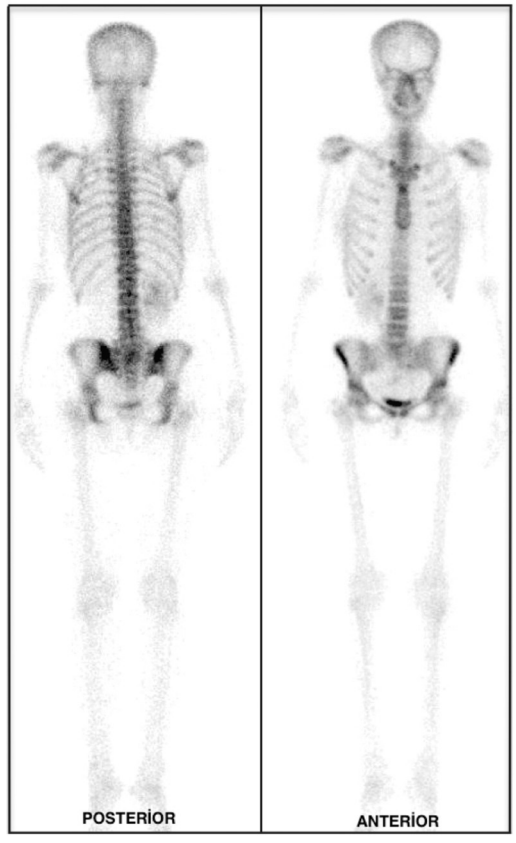

Figure 2. Osteoblastic phase of methylene diphosphonate bone scan demonstrated normal bone uptake and absence of the left kidney

non-thyroidal diseases, such as sinusitis, esophagus and gastric pathologies, pulmonary diseases, cysts and traumatic lesions, which could be mistaken for thyroid cancer metastases (1) and lead to unsuitable therapy, such as unnecessary reoperations and/or administration of repeated doses of I-131.

More than 90% of iodide is excreted from the body by the kidneys. As a result, physiologic urine activity or urine retention in dilated renal collecting systems can be seen on I-131 WBS. Ureteral or bladder diverticulum and renal cysts have been reported to cause false-positive findings mimicking abdominal and pelvic region metastases (2,3,4). Ectopic kidneys can also be a cause of false-positive WBS.

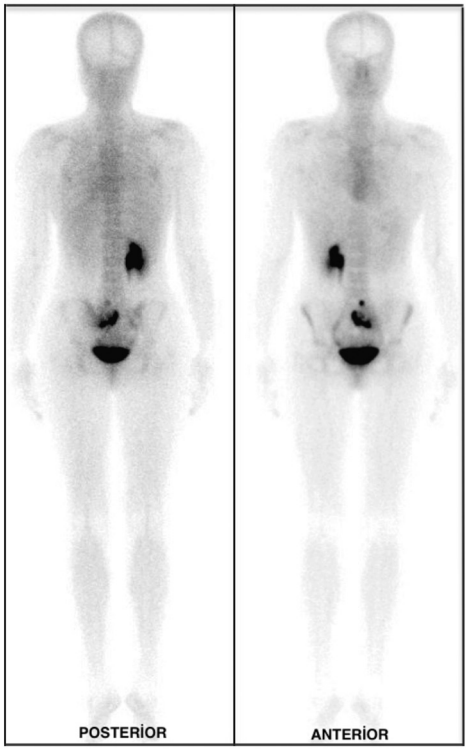

Figure 3. The absence of left renal activity and an extra focus of uptake in the sacral region due to pelvic kidney was seen on blood-pool phase

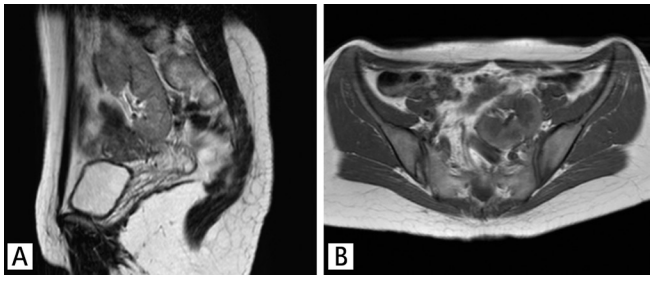

Figure 4. Axial T1-weighted (A) and coronal T2-weighted (B) magnetic resonance imaging demonstrated an ectopic kidney located in the left posterior pelvic region overlying the sacrum with an anteriorly rotated renal pelvis

Ectopic kidneys are due to developmental anomalies and may be located at the pelvic, iliac fossa or lumbar region, anywhere along the path of their usual ascent. If the kidney stays in the pelvic fossa during the ascending process, it is called a pelvic kidney. This anomaly can be unilateral or bilateral. The incidence of ectopic pelvic kidney is reported as 1:2100-1:3000 in autopsy series (5).

Ectopic kidneys are mostly asymptomatic. Hydronephrosis is seen in half of the patients, due to malrotation of the kidney and anteriorly placed renal pelvis leading to impaired urinary drainage (6). In our case, the pelvic kidney was located in the left posterior pelvic region overlying the sacrum with an anteriorly rotated renal pelvis (Figure 4, A axial; B sagittal).

As an additional finding, MRI reported that the pelvic kidney was adjacent to the left ovary. Because of the hydronephrosis seen quite often in pelvic kidneys, retention of high dose I-131 activity in this region may increase dosimetry of the ovarian tissue. Therefore, in case of an ectopic kidney detected prior to ablation treatment, precautions such as hydration and diuretic administration can be implemented.

Although ectopic kidney is a well-known finding, there are only few demonstrative cases showing ectopic kidney as a false-positive area for I-131 WBS (7,8), and few reports for MDP bone scan or other diagnostic modalities (9,10,11). Our case is a demonstrative example of pelvic kidney mimicking sacral metastases on I-131 WBS.

Ethics

Informed Consent: Consent form was filled out by all participants.

Peer-review: Externally peer-reviewed.

Authorship Contributions

Surgical and Medical Practices: Selin Soyluoğlu Demir, Ahmet Polat, Concept: Selin Soyluoğlu Demir, Gül Ege Aktaş, Design: Selin Soyluoğlu Demir, Gül Ege Aktaş, Data Collection or Processing: Selin Soyluoğlu Demir, Gül Ege Aktaş, Ahmet Polat, Analysis or Interpretation: Selin Soyluoğlu Demir, Ali Sarıkaya, Literature Search: Selin Soyluoğlu Demir, Ali Sarıkaya, Writing: Selin Soyluoğlu Demir

Conflict of Interest: No conflict of interest was declared by the authors.

Financial Disclosure: The authors declared that this study received no financial support.

References

1. Oh JR, Ahn BC. False-positive uptake on radioiodine whole-body scintigraphy: physiologic and pathologic variants unrelated to thyroid cancer. Am J Nucl Med Mol Imaging 2012;2:362-385.

2. Sutter CW, Masilungan BG, Stadalnik RC. False-positive results of I-131 whole-body scans in patients with thyroid cancer. Semin Nucl Med 1995;25:279-282.
3. Bakheet SM, Hammami MM, Powe J. False-positive radioiodine uptake in the abdomen and the pelvis: radioiodine retention in the kidneys and review of the literature. Clin Nucl Med 1996;21:932-937.
4. Letaief B, Boughattas S, Guezguez M, Hassine H, Essabbah H. Abdominal uptake of I-131 revealing a renal cyst. Clin Nucl Med 2001;26:255-256.
5. Bauer SB. Anomalies of the upper urinary tract. In: Walsh PC (eds). Campbell's urology. Philadelphia, WB Saunders, 2002;1894.
6. Cinman NM, Okeke Z, Smith AD. Pelvic kidney: associated diseases and treatment. J Endourol 2007;21:836-842.
7. Bakheet SM, Hammami MM. False-positive radioiodine whole-body scan in thyroid cancer patients due to unrelated pathology. Clin Nucl Med 1994;19:325-329.
8. Attard M, Marozzi P, Gambino L, Janni F, Salice P, Ficola U, Giuffrida D. False-positive results of an iodine-131 whole-body scan caused by an ectopic kidney. Clin Nucl Med 2001;26:271-273.
9. Pryma DA, Akhurst T. Hydronephrotic ectopic pelvic kidney simulates sacral metastasis from breast cancer. Clin Nucl Med 2005;30:244-245.
10. Valliappan S, Joyce JM, Myers DT. Possible false-positive metastatic prostate cancer on an In-111 capromab pendetide scan as a result of a pelvic kidney. Clin Nucl Med 1999;24:984-985.
11. Bader AA, Tamussino KF, Winter R. Ectopic (pelvic) kidney mimicking bulky lymph nodes at pelvic lymphadenectomy. Gynecol Oncol 2005;96:873-875.